AD-A036 088 DURHAM UNIV (ENGLAND) DEPT OF PHYSICS F/G 4/1
PHYSICAL CHARACTERISTICS OF THE NATURAL ATMOSPHERIC AEROSOL.(U)
OCT 76 S G JENNINGS DAJA37-75-C-1913
NL

UNCLASSIFIED

1 OF 2
AD A036088

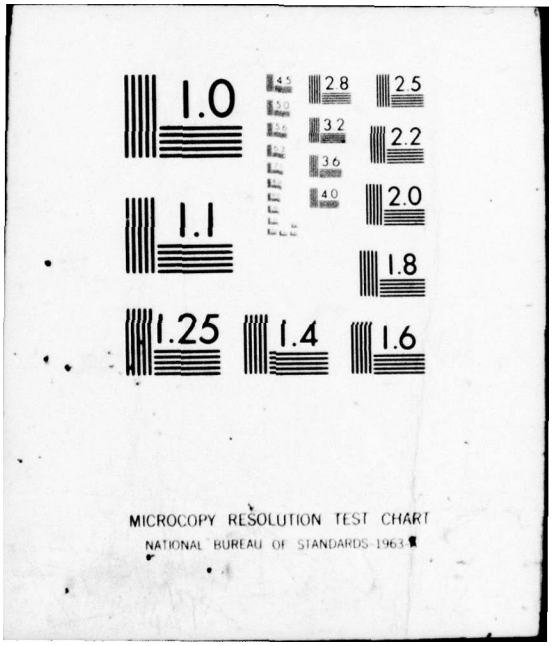
1.0
2.8
2.5
3.2
2.2
3.6
2.0
4.0
1.1
1.8
1.25
1.4
1.6
MICROCOPY RESOLUTION TEST CHART
NATIONAL BUREAU OF STANDARDS-1963-A

AD

PHYSICAL CHARACTERISTICS OF THE NATURAL ATMOSPHERIC AEROSOL

FINAL TECHNICAL REPORT

by

S. Gerard Jennings

October 1976

EUROPEAN RESEARCH OFFICE
United States Army
London, W.1., England

Contract Number DA-ERO-75-G-073
University of Durham

UNCLASSIFIED
SECURITY CLASSIFICATION OF THIS PAGE (When Data Entered)

REPORT DOCUMENTATION PAGE	READ INSTRUCTIONS BEFORE COMPLETING FORM
1. REPORT NUMBER	2. GOVT ACCESSION NO. / 3. RECIPIENT'S CATALOG NUMBER
4. TITLE (and Subtitle) (6) PHYSICAL CHARACTERISTICS OF THE NATURAL ATMOSPHERIC AEROSOL.	5. TYPE OF REPORT & PERIOD COVERED (9) FINAL TECHNICAL REPORT, MAR 75 - SEP 76, / 6. PERFORMING ORG. REPORT NUMBER
7. AUTHOR(s) (10) S. GERARD JENNINGS	8. CONTRACT OR GRANT NUMBER(s) (15) DAJA37-75-C-1913
9. PERFORMING ORGANIZATION NAME AND ADDRESS DEPT. OF PHYSICS, ~~SCIENCE LABORATORIES~~ UNIVERSITY OF DURHAM, SOUTH ROAD DURHAM DHI 3LE	10. PROGRAM ELEMENT, PROJECT, TASK AREA & WORK UNIT NUMBERS 6.11.02A 1T161102B53B 00 505 (17) (16)
11. CONTROLLING OFFICE NAME AND ADDRESS U.S. Army R&S Gp (EUR) Box 65 FPO NEW YORK 09510	12. REPORT DATE (11) Oct 76 / 13. NUMBER OF PAGES 107
14. MONITORING AGENCY NAME & ADDRESS(if different from Controlling Office) (12) 198 P.	15. SECURITY CLASS. (of this report) UNCLASSIFIED / 15a. DECLASSIFICATION/DOWNGRADING SCHEDULE

16. DISTRIBUTION STATEMENT (of this Report)

APPROVED FOR PUBLIC RELEASE

DISTRIBUTION UNLIMITED

17. DISTRIBUTION STATEMENT (of the abstract entered in Block 20, if different from Report)

18. SUPPLEMENTARY NOTES

19. KEY WORDS (Continue on reverse side if necessary and identify by block number)

(U) Atmospheric Aerosols
(U) Submicron Particles
(U) Air Quality

20. ABSTRACT (Continue on reverse side if necessary and identify by block number)

SEE OVER

DD FORM 1 JAN 73 1473 EDITION OF 1 NOV 65 IS OBSOLETE

UNCLASSIFIED 400 601
SECURITY CLASSIFICATION OF THIS PAGE (When Data Entered)

20 Abstract

In this report an analysis is made of continuous measurements of the number and size distribution of submicrometre and large aerosol particles up to 5 micrometres in radius. An automated ~~Royco~~ optical particle counter was used to take measurements at a 10 minute sampling frequency over a 49 day period at Durham Observatory, near Durham City, North East of England. Additional measurements were made at a remote mountain station at Great Dun Fell, 842 m msl and at an isolated maritime site. The averaged diurnal variation shows a maximum in particle number concentration from about 0200-0800 local time and a distinctive minimum over the period 1400-2000 hours. The particle number concentration follows a log-normal distribution. An analysis of the sampling grequency shows that the measurements could be made less frequently by factors up to 20, without loss of significant information.

A study is made of the theoretical growth of soluble aerosol particles with humidity. Novel approximations are incorporated in the application of the growth-equation to particles of sodium chloride and ammonium sulphate, which show good agreement with previous results. Experimental measurements of the growth of sodium chloride and ammonium sulphate particles, of initial radii of between 2 and 3 x 10^{-6}cm, with relative humidity agree well with the theoretical growth curves.

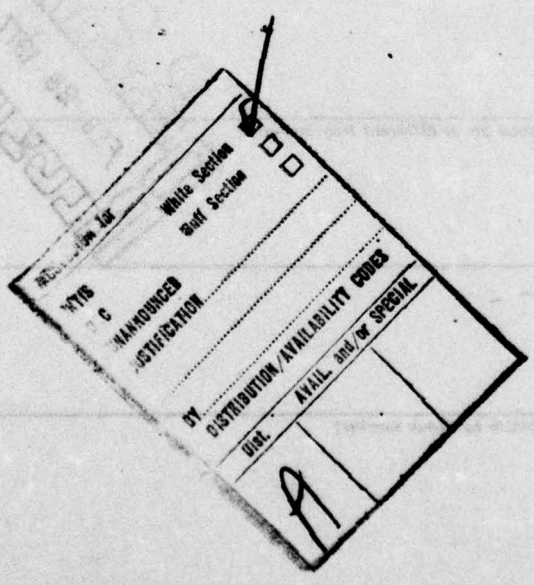

AD_____

PHYSICAL CHARACTERISTICS OF THE NATURAL ATMOSPHERIC AEROSOL

FINAL TECHNICAL REPORT

by

S. Gerard Jennings

October 1976

EUROPEAN RESEARCH OFFICE

United States Army
London, W.1., England

Contract Number DA JA 37-75-C-1913

University of Durham

ABSTRACT

An analysis is made of continuous measurements of the number and size distribution of submicrometre and large aerosol particles up to 5 micrometres in radius. An automated Royco optical particle counter was used to take measurements at a 10 minute sampling frequency over a 49 day period at Durham Observatory, near Durham City, North East of England. Additional measurements were made at a remote mountain station at Great Dun Fell, 842 m msl and at an isolated maritime site. The averaged diurnal variation shows a maximum in particle number concentration from about 0200-0800 local time and a distinctive minimum over the period 1400-2000 hours. The particle number concentration follows a log-normal distribution. An analysis of the sampling frequency shows that the measurements could be made less frequently by factors up to 20, without loss of significant information.

A study is made of the theoretical growth of soluble aerosol particles with humidity. Novel approximations are incorporated in the application of the growth-equation to particles of sodium chloride and ammonium sulphate, which show good agreement with previous results. Experimental measurements of the growth of sodium chloride and ammonium sulphate particles, of initial radii of between 2 and 3×10^{-6}cm, with relative humidity agree well with the theoretical growth curves.

Approximations to Mie's light scattering theory are used to calculate the extinction coefficient for four model particle size distributions of sodium chloride and ammonium sulphate as a function of humidity, solute dry mass particle and dry particle radius. The results indicate that sodium chloride particles are more efficient in reducing atmospheric transmission than ammonium sulphate particles by factors ranging between about 1.3 and 5.5 over a range of solute mass per particle from 3×10^{-17}g to 3×10^{-11}g. Calculations also show that a non-homogenous Junge type particle size distribution is the most effective in increasing the extinction coefficient at values greater than about 94 per cent relative humidity.

TABLE OF CONTENTS

CAPTIONS TO FIGURES

Figure 2.1 The sites for the measurement of the natural aerosol.

Figure 2.2 The diurnal variation of submicrometre particle number concentration averaged over 49 days during the Summer at Durham Observatory.

Figure 2.3 A comparison of the frequency distribution of sub-micrometre particles in the transient mode at three sites.

Figure 2.4 Cumulative frequency distributions of Aitken particle number concentration for three measurement periods.

Figure 2.5 Short term fluctuations in the particle number concentration at Great Dun Fell.

Figure 2.6 A cumulative percentage of measurements of particle concentration less than selected values of the percentage deviation from the arithmetic mean.

Figure 2.7 Position of Durham Observatory marked with X, in relation to built up areas, towns and industrial sites.

Figure 2.8 The diurnal variation for the natural atmospheric aerosol over the radius range categories 0.25-0.35, 0.35-0.7, 0.7-1.5, 1.5-2.5 and 2.5 to 5.0 micrometres averaged over 49 consecutive days from July 21st - September 8th 1975 at Durham Observatory.

Figure 2.9 A computer plot of the hourly variation of the natural aerosol particle concentration for the radius intervals 0.25-0.35, 1.5-2.5 and 2.5-5.0 micrometres from July 21st to September 8th 1975 at Durham Observatory.

Figure 2.10 Cumulative frequency distributions of the natural aerosol concentration from 49 measurement days at Durham Observatory over five radius intervals of 0.25-0.35, 0.35-0.7, 0.7-1.4, 1.4-3.0 and 3.0-5.0 micrometres.

Figure 2.20 A cumulative percentage plot of particle concentration in the radius range 0.25-0.35 micrometre, sampled continuously from July 15th-July 21st, 1975 at Durham Observatory.

Solid line: 1 minute sampling frequency

Δ : 10 minute sampling frequency

0 : 20 minute sampling frequency

Coincident points are shown by one symbol, Δ .

Figure 2.21 Cumulative percentage plots of particle concentration for the radius intervals of 0.25-0.35 and 2.5-5.0 micrometres, measured at Durham Observatory from July 21st-September 8th, 1975.

Solid lines: Measurements for a 50 minute sampling interval

0 : Measurements for a 150 minute sampling interval

Δ : Measurements for a 250 minute sampling interval

Coincident points are represented by the symbol Δ .

Figure 2.22 A comparison of the average number concentration of the atmospheric aerosol in the radius range 0.25-0.35 micrometres sampled at Great Dun Fell for the following periods:

(a) December 15th-January 6th, 1976

(b) December 25th-December 26th, 1975.

Figure 2.23 A scatterplot of natural particle concentration in the radius range 0.25-0.35 micrometres with wind speed in knots, sampled at Durham Observatory from July 21st-September 8th, 1975.

CAPTIONS TO TABLES

PHYSICAL CHARACTERISTICS OF THE NATURAL ATMOSPHERIC AEROSOL

1. GENERAL INTRODUCTION

1.1 Historical Background

The need for more research into the particle size distribution and physical characteristics of the natural atmospheric aerosol is adequately described by Wagman (1967) in a review prepared for the O.E.C.D. The fine-particle aerosol content of the atmosphere is largely composed of Aitken type or condensation nuclei, possessing radii of the order of 0.01 micrometres. Sources of particulate matter in the atmosphere are both natural and anthropogenic, although the atmospheric aerosol is mainly produced by human activity and so study of its properties must be closely related to pollution problems. Yet, it is only quite recently that serious study within this context has been carried out, for example, by Peterson and Paulus (1967). The need for more measurements of particle concentration and size distribution over wide areas was recommended by a working group at the 7th International Conference on Condensation and Ice Nuclei, 1969, whilst it has been more recently emphasized by Junge and Jaenicke (1971) that the determination of the background levels for atmospheric aerosol particles is an urgent problem, since man's activity is continually changing the conditions in the atmosphere.

The atmospheric particle distribution for the size range between about 0.1 and a few microns is one of the most significant parameters which controls the transmission properties of the atmosphere. Although a theoretical basis exists for the reduction in atmospheric visibility by aerosols (Middleton, 1963), more experimental work and theoretical data is urgently required to elucidate more fully the relationship between optical characteristics of atmospheric aerosols, such as the extinction coefficient due to light scattering by the large particles, and physical characteristics, for example, aerosol mass concentration, particle size distribution and refractive index of the constituent particles.
In addition, although many series of observations have indicated that visibility decreases with increasing relative humidity, more computational work is required to assess more fully the relative efficiency of aerosol particle constituents in reducing the transmission efficiency in the atmosphere. More computational work on the effect of relative humidity on the extinction coefficient of ammonium sulphate, which is one of the main

constituents of the natural aerosol, is required.

1.2 The Number and Size Distribution of the Natural Atmospheric Aerosol

The natural aerosol size distribution is now established as being bimodal in surface and volume. The particle size mode in the 0.1 to 1 micrometre range is usually named the 'accumulation mode' because aerosol particles which grow into the range from smaller sizes by coagulation or condensation tend to remain in this size range. They also have the longest lifetime of any particle size range. The 'transient mode' generally refers to the aerosol particles in the range 0.01 micrometres since fresh combustion or anthropogenic nuclei sources tend to dominate the particle size regime. The 'coarse particle mode' for particle radii larger than about 1 micrometre originates mainly from mechanical processes such as dust, fly-ash, sea spray etc.

The size and concentration of atmospheric aerosol particles influences the rate of growth of fog droplets and also affects visibility. A considerable amount of experimental work has been carried out in an attempt to understand variations in particle concentration and size distribution, particularly for the large and giant nuclei. Junge (1953) used a two stage konimeter to determine the size distribution of the aerosol at Frankfurt, in the Zugspitze and on Mount Taurus. He found that particles of radius $r > 0.1$ micrometres obeyed a size distribution law of the form

$$n(r) = \frac{dN}{d(\log r)} \qquad (1.1)$$

where dN is the number of particles in the radius interval d(log r). Equation 1.1 means that the particles in each logarithmic interval of radius contribute equally to the mass concentration of the aerosol.

Cartwright et al. (1956) used an electron microscope to size particles, collected by a thermal precipitator, in the radius range 0.03 to 0.9 micrometres. Twomey and Severynse (1964) determined the size distribution of the natural aerosol by means of a diffusion battery in conjunction with a photoelectric nucleus counter at various stages of diffusional decay. Friedlander and Pasceri (1965) measured the size distribution in the radius range 0.4 to 20 micrometres using a four stage Casella impactor. They found good agreement with the Junge form of the size distribution curve.

At the International Workshop on Condensation and Ice Nuclei (1971), Whitby and Husar found that the natural aerosol measured at Fort Collins, Colorado was similar to that obtained by Junge in the South Atlantic. Whitby and Husar used the Minnesota Aerosol Analysing System (MAAS) to make their measurements. This system consists of an optical particle counter operating in the radius range from 0.6 to 12 micrometres, an electrical aerosol analyser operating over the range 0.0075 to 0.6 micrometres and a condensation nucleus counter for the Aitken nuclei range.

Junge and Jaenicke (1971) have presented background aerosol particle size distribution data collected during the Atlantic Expedition of the R.V. Meteor over 24 days from April 13th, 1969. As stated by the authors, further details in addition to the total concentration measured by each instrument would have overcrowded their diagram (Figure 4). They found two maxima in the particle size distribution curve, one above 0.1 micrometre and the other at the small particle end. The distribution above 0.3 micrometres radius shows a steady decrease uninterrupted by secondary maxima. Whitby et al. (1975) presented particle size distribution data for a 24 hour period on 19th and 20th September, 1972 of aerosol sampled along the Harbor Freeway in Los Angeles, California.

Although particle size distributions in the 'accumulation mode' have now been made by some of the above workers for some years, few continuous measurements extending over periods of days or longer have been published. In the following report, measurements made continuously over a 49 day and 22 day period are presented of the natural atmospheric aerosol size distribution in the radius range 0.25 up to 5 micrometres using a calibrated Royco optical counter.

1.3 The Growth of Aerosol Particle Size with Humidity

If a droplet is formed on a wholly or partially soluble nucleus, the equilibrium vapour pressure at the surface of the drop is reduced by an amount which depends on the chemical nature and concentration of the solution. Condensation will occur at a lower supersaturation than on an insoluble nucleus of the same size.

For a pure droplet the critical radius r_c that an aggregate of molecules must attain in order to be in equilibrium with the surrounding vapour was first deduced by Kelvin (1870) and is given by the relation

$$r_c = 2M\sigma/\rho RT \ln(P/P_\infty) \qquad (1.2)$$

where P is the pressure of the supersaturated vapour, P_∞ is the equilibrium vapour pressure at temperature T over a plane surface of the liquid, σ is the surface tension of the droplet, ρ is the density of the liquid, R is the universal gas constant and M is the molecular weight of the liquid. Equation 1.2 was modified, first by Kohler (1921) and later by Wright (1936), to yield an expression for the equilibrium vapour pressure at the surface of a solution droplet. Wright's expression for the vapour pressure P_r, of a solution droplet of radius r' is given by the equation

$$\frac{P_r}{P_\infty} = \exp \frac{2\sigma M}{\rho' R T r'} - \frac{3 i m_o M}{4\pi r^3 \rho' W} \qquad (1.3)$$

where P is the equilibrium vapour pressure over a plane water surface, m_o is the mass of the solute in grammes, M is the molecular weight of water, ρ' is the density of the solution droplet, W is the molecular weight of the solute and i is the van't Hoff factor which allows for the modification of Raoult's Law to include electrolytic solutions. The van't Hoff factor varies with the chemical nature and concentration of the solution. Wright assumed i to be constant for all concentrations.

Mason (1971) derives a new form for the equilibrium vapour pressure over a solution droplet. This is discussed in more detail in Section 2.2. Using experimentally derived values of the van't Hoff factor, i, from McDonald (1953), Mason found that the numerical difference between his expression and that of Wright was never more than a few per cent except for small highly concentrated droplets. Values of i for eight electrolytes over a range of molality from 0.0001 have been tabulated by Low (1969) and these values are used in the calculations described in sections 3 and 4 of this report.

Dessens (1949) was one of the first workers to study the growth of salt particles. He used large particles of sodium chloride and zinc chloride suspended from very fine spiders' webs in an unsaturated environment of controlled humidity. Similar results were obtained by Junge (1952a) who measured the equilibrium radii of artificial nuclei of calcium chloride and sodium chloride. He demonstrated (1952b) that the growth of atmospheric aerosol particles in continential air masses showed deviations from the theoretical predictions. The growth curves of individual particles showed considerable variation but the average values were rather uniform with little growth below about 70% relative

humidity and a smaller growth above 70% than theory predicted for pure salts. This behaviour was explained at the time by a mixture of soluble and insoluble matter in each particle thus introducing the now generally accepted concept of "mixed nuclei".

Using mobility measurements to determine particle size Orr, Hurd and Corbett (1956) obtained reasonable agreement with the then available growth equations for particles of sodium chloride and calcium chloride and other salts with initial radius between 2×10^{-6}cm and 3×10^{-6}cm. More recently, Winkler and Junge (1972) have described a gravimetric method for determining the growth of atmospheric aerosol particles as a function of relative humidity. They found that the continental aerosol has a growth curve which indicates considerably less water absorption than for pure salts. In addition they found that the presence of insoluble matter in the particles has the effect of reducing total growth and of smoothing the growth curve.

Since sodium chloride in the form of sea salt constitutes the largest single component of particulate matter in the atmosphere it was decided to study the growth of sodium chloride in the laboratory with increasing relative humidity. The recent work of Eggleton (1969) and Heard and Wiffen (1969) has shown ammonium sulphate to be another important constituent particularly in continental atmospheric aerosols. Heard and Wiffen have shown that on many occasions most of the particles in haze conditions are nearly pure ammonium sulphate. Twomey (1971) is of the opinion that most of the cloud nuclei over the sea are composed of ammonium sulphate, formed by gaseous reactions in the atmosphere over the continents. However, in spite of the importance of ammonium sulphate nuclei in the atmospheric aerosol few calculations of particle growth have been published. Both theoretical and experimental work on the growth of sodium chloride and ammonium sulphate particles with relative humidity are described in Section 3 of the report.

1.4 The Effect of Atmospheric Particles on Transmission

Solid and liquid aerosol particles in the atmosphere reduce the visibility. An important contribution to the lowering of visibility is made by the condensation of water vapour on particles at the higher values of relative humidity. In the most general case both scattering and absorption of light contribute to the extinction of light between object and observer. The general expression for light extinction is

$$I = I_o \exp(-\sigma x) \qquad (1.4)$$

where I_o is the initial light intensity, I is the intensity after its passage along a distance x and σ is the extinction coefficient and is the sum of two terms,

$$\sigma = \sigma_{abs} + \sigma_{scatt} \tag{1.5}$$

Here σ_{abs} is due to absorption by gases and particles but is considered small compared with σ_{scatt} (Middleton , 1963). The scattering coefficient, σ_{scatt} is the dominant factor causing changes in visibility in the atmosphere. The extinction coefficient, σ, is related to the visibility by the Koschmieder relationship,

$$\text{Visual range} = \frac{3.91}{\sigma} \tag{1.6}$$

as derived by Middleton (1963, p. 105), Middleton also shows that the extinction coefficient for a monodisperse aerosol of particle radius a and concentration N is given by

$$\sigma = NK\pi a^2 \tag{1.7}$$

where K is the scattering area ratio or the ratio of the area of the wavefront affected by the particle to the cross-sectional area of the particle itself. K is a function of the particle radius to the wavelength, λ, of the incident radiation and of the refractive index of the particle. It is usually tabulated against the parameter $\alpha = 2\pi a/\lambda$ for specific values of the refractive index.

Interest in the relationship between relative humidity and visual range dates back at least to the studies of Wright (1939) on the atmospheric opacity at Valentia. His results showed that, in maritime air, the atmospheric opacity varied with relative humidity in much the same way as theory would suggest for a sodium chloride aerosol. More recently, Garland (1969) has made a study of the effect of ammonium sulphate particles on visibility. This work will be discussed in more detail in Section 4. Hanel (1972) has computed extinction coefficients of atmospheric aerosol particles with relative humidity. His calculations are based on measurements of the density, refractive index and coefficient of mass increase with humidity of atmospheric aerosol. His results agree to within a few per cent with those obtained by Mie theory, which is the complete rigorous theory for the scattering of light by isotropic, spherical particles developed by Mie (1908).

Covert, Charlson and Ahlquist (1972) have measured the light

scattering coefficient of artificially produced nuclei in the laboratory over a wide range of humidity, with an integrating nephelometer. However, their results have not been compared with predicted values of the extinction coefficient.

The effect of particle mass on the extinction coefficient for monodisperse aerosols of sodium chloride and ammonium sulphate is studied in Section 4 of the report. In addition, the influence of a range of particle size distributions on the extinction coefficient as the relative humidity is varied is examined.

1.5 Objectives of the Research Programme

In order to calculate the effect of relative humidity on the growth of atmospheric particles it is desireable to know the shape of the aerosol size distribution. In addition, knowledge of the particle size distribution is essential in order to predict accurately the effect of particle growth in the extinction coefficient. Consequently one of the first objectives of the research programme was to carry out an extensive series of measurements of the number and size distribution of the natural atmospheric aerosol, mainly in the radius range from about 0.3 up to 5 micrometres. The effect of meteorological parameters on the distributions is assessed. In addition, knowledge of the 'transient mode' particle number spectrum was thought desirable since (a) the growth of the aerosol particle size with relative humidity is most sensitive and rapid at the lower end of the particle size range and ultimately controls the final size of the particle and (b) it is considered important to establish the influence of geographical locations and anthropogenic sources on the variation of the number concentration of the transient mode particles. This work is described in Section 2.

The second objective of the research work is to calculate the growth of aerosol particle size over a wide range, with relative humidity. Laboratory measurements of the growth of sodium chloride and ammonium sulphate aerosol particles will be presented and compared with the theoretical growth curves. The effect on model particle size distributions is also considered. Two important atmospheric particle constituents of sodium chloride and ammonium sulphate are chosen in this study. New procedures and approximations are used in the application of the humidity growth equations to the predictions of the increase of particle size with humidity as described in Section 3.

The third objective of the research programme is to estimate the effect of particle growth on the extinction coefficient due to light scattering using approximations to Mie's theory. Results of extinction coefficients for monodisperse and model particle size distributions of sodium chloride and ammonium sulphate aerosol particles are presented In addition, calculations on the reductions in visibility due to measured aerosol particle size distributions will be presented and discussed in Section 4.

2. NATURAL AEROSOL NUMBER AND SIZE DISTRIBUTIONS

2.1 Number Concentration of the Submicrometre Natural Aerosol

A study of the number concentration of submicrometre aerosol particles in the 'transient mode' was carried out at Durham Observatory 2 km SSW of Durham City with a population of 27,500 inhabitants in the North East of England, at Great Dun Fell, 842 m msl on the Northern Pennine mountain range, Westmorland, England and at Lanehead, Weardale, altitude 432 m msl situated 16 km NE of Great Dun Fell. The locations of the three sites is shown in figure 2.1.

Using an automated version of the Nolan-Pollak (1946) photoelectric nucleus counter, measurement of the Aitken nucleus number concentration was made at the three locations over periods which varied from three hours up to forty nine days at varying sampling frequencies. Further details of the particle counting system is given by Jennings (1975). The diurnal variation of the particle concentration taken at twenty minute intervals and averaged over 49 continuous days of measurement at Durham Observatory during the summer months are shown in Figure 2.2. The pattern is similar to that obtained by Hogan (1966) in the United States with the daily peak occurring at about mid afternoon and being preceded by a district minimum during the early hours of the morning when the production of anthropogenic particles is predictably at its lowest.

An investigation of the frequency distribution of the individual observations were calculated using suitable class intervals. The cumulative frequency distribution which expresses the percentage of observation less than a selected value of particle concentration, Z, as a function of the logarithm of the concentration was calculated and plotted on probability paper. A line of best fit using the weighted least squares method, which also allow for the exaggerations of the deviation close to the probability scale is drawn for each set of measurements. This procedure is followed in figure 2.3 where a comparison of the cumulative distribution curves are drawn for the three respective sites (a) Great Dun Fell which is remote, exposed and far removed from population, (b) Lanehead, which is sparsely populated and

(c) Durham Observatory. The values of the number concentration made at the two elevated sites were increased due to a pressure effect of about 0.7 and 0.3 per cent respectively for a one per cent pressure change in the operation of the particle counter. A comparison of the cumulative distribution curves for the three sites indicates quite clearly the effective use of this form of the frequency distribution in order to compare the median and extremes of aerosol particle concentration for different sites, as indicated by Hogan (1966). It can also be seen that the distribution of number concentration for the three sites is approximately log-normal.

Specimen results of particle concentration, Z, sampled at two minute intervals for a three, four and twenty hour measurement on different dates at Great Dun Fell are shown in figure 2.4. The measurements indicate that the particle number concentrations follow closely a log normal distribution in each case. The maximum value for the median of April 14th is probably due to the averaged lower value of wind speed on that day (table 2.1).

The calculation of the geometric mean, Zg, and the geometric standard deviation σ_g is simplified considerably when the cumulative distributions are plotted on logarithmic probably paper as done in figure 2.3. The geometric standard deviation, σ_g, is obtained from the relations

$$\sigma_g = \frac{84.13\% \text{ number concentration}}{50\% \text{ number concentration}} = \frac{50\% \text{ number concentration}}{15.87\% \text{ number concentration}} \qquad (2.1)$$

Values of Zg and σ_g are estimated for a number of observational periods at the three sites and are given in Table 2.1.

A typical short term fluctuation in particle number concentration measured at the remote site of Great Dun Fell is shown in figure 2.5 for two three hourly runs from 0000-0300 and from 0800 to 1100 GMT respectively. An example of a large perturbation above the background particle count, due to some extraneous source can be seen in the upper curve. This illustrates the sensitivity of the apparatus in detecting minute changes of the order of fractions of a picogram in the aerosol mass and indicates that the detection of the onset of localized sources of particles is particularly effective in areas of low particle levels. The lower curve of figure 2.5 is characteristic of the site at Great Dun Fell in that the variation in particle concentration, Z, is generally smooth, which is probably due to the site location, being far removed from the large short-term fluctuations usually associated with artificially produced aerosol. In this specimen result, fifty per cent of the observations lie within about fifteen per cent of the average concentration

TABLE 2.1

Values of geometric mean, geometric deviation, arithmetic mean and median of Aitken nuclei observations at three sites

Site	Date(s)	Average wind speed (knots)	Geometric mean Z_g	Geometric standard deviation σ_g	Arithmetic mean $\bar{Z}$	$\frac{\bar{Z}}{Z_g}$ calculated	$\frac{\bar{Z}}{Z_m}$ measured
Durham Observatory	August 21st-26th	6.5	11,100	1.59	11,701	1.11	1.08
Lanehead	June 3rd-7th	19	4,050	2.11	5,811	1.32	1.22
Great Dun Fell	April 14th	9	3,000	1.18	3,007	1.01	1.03
—	March 12th	16	2,300	1.38	2,391	1.05	1.15
—	March 2nd	35	2,020	1.21	1,943	1.02	1.01
—	March 22nd-23rd	34	1,450	1.50	1,584	1.09	1.14
—	April 4-6th	36.5	1,020	1.97	1,285	1.26	1.07
—	August 22nd	17	980	1.16	965	1.01	1.05

for the three hour period.

A study of the effect of sampling frequency on the distribution of Aitken particle number concentration was also made. The cumulative percentage of measurements of particle concentration which were less than selected values of the percentage deviation from the average of the total number of two minute measurements is shown in figure 2.6 for the twenty hour run of March 22nd - March 23rd. The solid line represents the two minute sampling measurements. The close proximity of the measured values for the ten and twenty minute sampling intervals indicates clearly that the frequency of sampling of number concentration can be increased by at least an order of magnitude from a two minute sampling frequency without significant loss in generality or applicability of the results. This is important since the operating time of the automated system can be increased before servicing is required and in addition the volume of data required for analysis can be substantially reduced.

A summary of the values of the geometric mean, Zg, (equal to the median for a log normal distribution), the geometric standard duration, σ_g, and the arithmetic mean, $\bar{Z}$, of Aitken particle number concentration measured at the three sites of Durham Observatory, Lanehead and Great Dun Fell are given in Table 2.1. The results are arranged in order of decreas- number concentration. A comparison is made between the theoretical ratio between $\bar{Z}$ and Zg as derived from the formula

$$\ln\left(\frac{\bar{Z}}{Zg}\right) = 0.5\ (\ln\ \sigma_g)^2 \qquad (2.2)$$

with the measured values of $\bar{Z}$ and the median Z_m. Although the greatest difference in the ratios was about 15 per cent (for April 4th-6th data) the mean difference reduces to only about 1 per cent which gives an overall indication that the Aitken particle number concentration is log-normally distributed at these sites. The relatively low values of σ_g for the majority of the particle distributions at Great Dun Fell indicates the small dispersion of the measurements about their average value which appears to be characteristic of this remote site. The average value of the geometric mean of the number concentration of Aitken nuclei at Great Dun Fell was about 1800 for all the sampling intervals which is in reasonable agreement with data taken at sparsely populated mountain sites, for example, the Whiteface S mountain site of Hogan (1966). Frequency distribution curves follow closely a log-normal distribution for each measurement period. It is shown that a two minute sampling frequency of particle monitoring can be increased by about an order of magnitude without causing a significant change in the particle number distribution. This enables the extension of automatic running of the instrumentation for larger periods without recourse to reservicing. It has been found that the particle counter assembly operates satisfactorily over long periods under field conditions.

2.2 Natural Aerosol Size Distributions in the 0.25 to 5.0 Micrometre Radius Range

2.2.1 Instrumentation and measurement procedure

The acquisition of an optical particle counter, a Royco model 225 with autoscan digital display facility together with a digital printer in the early part of the contract period has permitted the investigation

of the size distribution of aerosol particles in the significantly important optical range of particle radius from 0.25 up to 5.0 micrometres and greater. The Royco optical counter allowed the aerosol particle size range to be classified into five radius categories. 0.25-0.35, 0.35-0.7, 0.7-1.4, 1.4-3.0 and 3.0-5.0 micrometres respectively. The particle counter was precalibrated with homogeneous sources of Latex particles over the five ranges. Measurements were made at three distinctive sites, (a) at Durham Observatory which represents a semi-rural site, adjacent to Durham City with a population of 27,500 people, (b) at Great Dun Fell which is an exposed remote elevated mountain site (842 m above sea level) and (c) at a remote maritime site at Ardnamurchan Lighthouse off the West Coast of Scotland, the most westerly point of the British Isles. Continuous meteorological records of wind speed, wind direction, temperature and humidity were available at Durham Observatory. The location of the site, marked X, is shown in figure 2.7 in relation to surrounding towns, industrial zones and built up areas. The measuring equipment was easily transportable and could be put into operation shortly after arrival at any of the field stations.

Air was drawn in at a height of 2.5 m above ground level at Great Dun Fell and at a height of 4 m above ground level at Durham Observatory and at Ardnamurchan. An oil-free Diaphragm pump operating at a flow rate of 70 l min^{-1} was used to draw the air through a mixing vessel from which the air sample was drawn to the optical counter sensor head via a short piece of anti-static tubing at a constant flow rate of 2.83 l min^{-1} Calculations showed, using the fractional loss formula for particles settling in a horizontal tube, (Thomas, 1958), that negligible loss of particles occurred. The number concentration for each size category was printed onto an automatically operating digital line printer and subsequent analysis of the measurements was facilitated by means of an IBM 360/168 computer.

2.2.2 Experimental results of particle size distributions in the 0.25 to 5 micrometre radius range

Results are described of continuous measurements over 49 days from 21st July to September 8th 1976, of the particle size distribution in the radius range 0.25 to 5 micrometre at Durham Observatory In addition, continuous measurements over a 11 and 21 day period from 4th to 14th July 1975 and from 15th December to January 6th 1976 respectively, made at the remote station at Great Dun Fell 832 m, msl on the Northern Pennine Range are also discussed. An analysis is also

made of aerosol particle measurements taken continuously every minute over a 6 day period from 15th July to 21st July 1975 at Durham Observatory. Maritime measurements of the particle size distributions made continuously over the period from 28th March to 4th April 1976 at Ardnamurchan Lighthouse are also presented.

Measurements of the particle radius categories 0.25-0.35, 0.35-0.7, 0.7-1.5, 1.5-2.5 and 2.5-5.0 micrometres were taken successively over a period of ten minutes, so that a fifty minute time interval existed between identical size category sampling times. The diurnal variation of the individual particle size categories averaged over the 49 continuous observational days is shown in figure 2.8. Each experimental point represents the arithmetic mean of approximately 50 readings. It clearly shows maximum number concentration occurring for all size categories, with the exception of the largest category, at the approximate period from 0200 to 0800 BST (British Standard Time). The afternoon period from 1400 up to about 2000 hours BST is characterized by a distinct minimum in particle concentration for the lower particle size categories. This general trend in the variation of particle concentration is also reflected in the measurements made at Great Dun Fell.

The hourly variations of particle concentration in the radius ranges 0.25-0.35, 1.5-2.5 and 2.5-5.0 micrometres is shown in figure 2.9 over the total period of measurement. The increase in particle numbers at night followed by an afternoon decrease can also be observed here. A general increase in the number concentration can be seen to occur from about 3rd to 15th August which corresponds to a significant increase in the daily average temperature for the period. This is also reflected in the positive correlation coefficient values of Table 2.3. This indicates that photochemical reactions are making an important contribution to particle production.

A frequency distribution of the individual observations over the 49 days sampling was calculated using suitable class intervals. The cumulative frequency distribution, which expresses the percentage of observations less than a selected value of particle concentration N, was calculated and plotted on probability paper. The results of the cumulative distribution of the five selected particle size ranges are shown in figure 2.10. A line of best fit using the weighted least squares procedure which also allows for the exaggerations of the deviations due to the probability scale following the procedure of Kottler (1950), is drawn for each particle size range. It can be seen from figure 2.10 that the particle concentration follows closely a log-normal distribution in each case. A log-normal distribution was also found for the other sizes.

One advantage of displaying aerosol particle distribution on logarithmic probability paper is that the geometric mean, Z_g, and the geometric standard deviation, σ_g, can be obtained directly from the graph since Z_g corresponds to the 50% probability value and σ_g can be derived from the plot using equation (2.1). The values of Z_g and σ_g obtained from the curves of figure 2.10 are shown in Table 2.2 and compare well with the computed values. The median of the measurements, which corresponds to the geometric mean for a log normal distribution, is also given in Table 2.2.

TABLE 2.2

A comparison between the values of the geometric mean Z_g and the geometric standard duration σ_g for the atmospheric aerosol sampled at Durham Observatory.

Particle Radius Range (micrometres)	0.25-0.35	0.35-0.7	0.7-1.5	1.5-2.5	2.5-5.0
Geometric mean Z_g of particle concentration cm^{-3} (from Fig. 2.10)	3.75	0.98	0.48	0.035	0.004
Computed value of Z_g from all measurements	3.85	1.08	0.52	0.036	0.0039
Computed value of the median	3.65	0.96	0.48	0.035	0.0039
Geometric Standard Deviation σ_g, of particle concentration (from Fig. 2.10)	3.13	3.19	2.52	2.11	2.37
Computed value of σ_g	2.84	3.05	2.67	2.21	2.44

The diurnal variation of the aerosol particle distribution over the four radius categories of 0.25-0.35, 0.35-0.7, 0.7-1.4 and 1.5-2.5 micrometres averaged over 22 days of continuous measurements at Great Dun Fell from December 15th to January 6th, 1976 are shown in figure 2.11. It can be seen that the diurnal variation of particle concentration over the size categories follows approximately the same trend as the Durham results, i.e. a peak in the early morning. Runs with a minimum appearing in the afternoon period. A comparison between the values of number concentration for the particle radius categories 0.25-0.35 and 1.5-3.0 micrometres measured at Great Dun Fell during the 22 day period with the averaged values over a 49 day continuous measurement period at Durham Observatory is shown in figure 2.12. The comparison shows that the aerosol particle concentration is about an order of magnitude lower for the mountain site, for the two size categories. This is mainly due to the effect of altitude and the remoteness of the Great Dun Fell site.

The site at Great Dun Fell offers the opportunity of examining the variation of particle concentration at quiescent periods, for example on Sundays, when anthropogenic influences are close to minimum. The gradual decay of particle concentration for a Sunday (July 6th, 1975) at Great Dun Fell is shown in figure 2.13. This is particularly noteworthy for the three upper size categories. The plot also illustrates the sensitivity of the particle counter at remote locations in detecting the onset of local sources of particulate matter at about 0700 and 1700 hours BST. The observed lag is mainly due to the difference in sampling times of the individual size categories. A significant difference in the particle size distribution shape for the measurements made on Friday and Saturday compared with the lower values measured on Sunday (13th July) at Great Dun Fell as seen in figure 2.14. This illustrates the effect of anthropogenic sources at this remote site site since the mean wind speed and direction was approximately the same for the three days.

Evidence of a bimodal structure for the aerosol particle size distribution at Durham Observatory over 25 days of measurements is shown in figure 2.15. It is interesting to note that the particle range from 0.7-1.5 micron radius constitute the greatest volume percentage of particles present in the aerosol. The bimodal structure is also evidenced in figure 2.16, where the distribution is fitted by two log-normal components similar to the treatment of Davies (1974). A correction for the overestimation of number concentration for the tails of the two component curves was made by plotting a cumulative curve of the measured distribution on logarithmic probability paper. The interpretation of particle size distribution curves is facilitated by the use of this fitting procedure.

The particle size distribution is presented in figure 2.17 as a

log-radius number distribution following Junge (1963).

$$\frac{dN}{d \log r} = cr^{-\beta} \qquad (2.3)$$

where dN is the number of particles per cm^3 in the range d log r, and c is a constant depending on the total number, N, of particles per cm^3. The log-radius distribution averaged over the 49 days of continuous measurements at Durham Observatory is shown in figure 2.17. A weighted line of best fit yields a slope β of value 3.04, which shows good agreement with values obtained by several workers for continental aerosols. The results for the remote location at Great Dun Fell over 21 days continuous run from December 15th-January 6th, 1976 are also shown. For this distribution, the line of best fit gives a slope β of 2.74. The curves also show that the particle number concentration at Great Dun Fell is approximately an order of magnitude lower than the corresponding values at Durham Observatory.

The diurnal variation of the particle size distribution in the maritime atmosphere off the west coast of Scotland at Ardnamurchan point is shown in figure 2.18. Although the site is very remote, the average particle concentration assumed values comparable with the Durham Observatory location. This is most probably due to the generation of particles from sea-spray and from air-bubbles bursting at the air-sea-water interface as discussed extensively by Blanchard (1963). Further evidence for this particle production mechanism is furnished by the mean logarithmic radius distribution of the maritime aerosol at Ardnamurchan shown in Figure 2.19 which indicates an enhanced production of sea-salt particles in the radius region of around one micrometre which is characteristic of the size produced both by sea-spray and bubble-bursting mechanisms.

A study of the effect of sampling frequency on the distribution of particle number concentration was made. Measurements of the particle size category 0.25-0.35 micrometre radius was taken every minute for a 6 day period from July 15th to July 21st giving a total of 7600 counts. There is an interval of sixty seven seconds between successive measurements since the interval of seven seconds is used for print out and resetting procedures. The cumulative percentage of readings of particle number concentration which were less than selected values of the percentage deviation from the mean of all the measurements is shown in figure 2.20. The solid line represents the one minute sampling measurements. The close proximity of the measured values for the ten and twenty minute intervals indicates clearly that the sampling frequency can be increased by at least twenty-fold from a one minute sampling frequency without significant loss of information.

This finding is reinforced by a similar analysis carried out on the measurements of particle concentration over the 49 days at Durham Observatory. In figure 2.21 the solid lines represent the fifty-minute sampling measurements for the smallest and largest radius intervals. The relatively close proximity of the values for 150 and 250 minute sampling frequencies compared to the 50 minute solid curve illustrates that sampling frequency can be extended to these large values particularly over long measurement periods. One can see that about 30 per cent of the total number of measurements are within $\pm$ 50 per cent of the overall mean concentration value for the lowest sized category, whilst about 50 per cent of the measurements are within one standard deviation of the mean. Higher cumulative percentage values apply to the large particle sized categories.

A rare opportunity of obtaining the background level of aerosol particle production at a period of minimum anthropogenic activity was achieved by monitoring the particle concentration over a 21 day continuous sequence which included the Christmas period. The particle size distribution was continuously measured at the remote mountain station at Great Dun Fell from December 15th 1976. The period from 0000 hours on December 25th until 0000 hours on December 27th was considered to represent accurately the period of least activity during the year, when particle production from man-made sources such as vehicular traffic and industrial pollutants is at a minimum level. This predicted pattern is confirmed by the result in figure 2.22 where the average value of particle size concentration for the days December 25th and 26th is compared with the overall average for the 21 day period. This pattern is repeated also for the other size ranges, and it clearly shows a marked reduction in the particle concentration for the 2 day period.

A correlation analysis was carried out on the July-September measurements at Durham Observatory. The Pearson Product - moment correlation coefficient at a significance level of 0.1 per cent, unless otherwise stated, between the 5 particle size categories and the meteorological parameter of wind direction, wind speed, humidity and temperature is given in Table 2.3. There is a high correlation between the adjacent size categories. A relatively high negative correlation is obtained between the wind speed and the particle concentration with the exception of the largest size category. A scatter diagram of wind speed in knots versus the concentration of particle size in the range 0.25-0.35 micrometres is shown in figure 2.23. A line of regression of the parameter Y $\{\log_{10}$ (particle concentration)$\}$ on X $\{$wind speed$\}$, is

$Y = - 0.0588 X + 0.8953$. The decrease in particle concentration with increase in wind speed occurs for all size categories examined and may be attributed to increased vertical transportation of the particles due to an increase in atmospheric turbulence.

2.2.3 A discussion of the results

The presentation and analysis of the results was facilitated by means of an IBM/168 computer. For example, a typical computer output plot of the diurnal variation of particle size at Durham Observatory is shown in figure 2.24.

The diurnal variation of the natural aerosol particle size distribution in the size range from 0.25 up to 1.4 micrometres in radius is distinctive in that it assumes a shape which is approximately an inverse relation to that normally measured for the submicrometre Aitken particle distribution. This can be seen by comparing the shapes of the curves of figure 2.8 with that of figure 2.2. Few continuous measurements over long periods of time are available with which to compare the larger particle distribution results. Measurements of the particle number concentration in the size range 0.5 to 5 micrometre radius, made along the Harbor freeway in Los Angeles, California in 1972 were made available by Marple, Sverdrup and Whitby (1976). The measurements taken during the dates 19th, 20th, 21st, 27th, 28th and 29th September at 10 minute intervals, yielded on average 15 measurements per hourly interval. The mean values of total concentration in the radius range of 0.5-5.0 micrometres are shown in figure 2.25 (a) and the diurnal shape compares favourably with the diurnal variation of the total concentration of particle size in the radius range 0.7 to 5 micrometres averaged over 49 days at Durham Observatory plotted in figure 2.25 (b).

The general increase in particle concentration particularly for the lower size categories in the period 0000 to 0600 hours can probably be attributed to the increase in humidity, as also reflected in the positive correlation between the parameters, seen in Table 2.3. The diurnal variation is characterized by the occurrence of a distinct minimum in the period from about 1400-2000 hours. This may be partly due to coagulation of the larger size categories with the submicrometre Aitken particles (which possess high concentration values in this period seen in figure 2.2). This trend of minimum particle concentration occurring in mid afternoon is also reflected in the measurements made at Great Dun Fell.

TABLE 2.3

Values of the Pearson Product-moment correlation coefficient, between the particle number concentration in the five radius intervals, and the meteorological parameters

Particle Concentration	Radius Range 0.25-0.35μm	Radius Range 0.35-0.7μm	Radius Range 0.7-1.5μm	Radius Range 1.5-2.5μm	Radius Range 2.5-5.0μm	Wind Direction	Wind Speed	Humidity	Temperature
Radius Range 0.25-0.35μm	1	0.87	0.76	0.59	0.48	-0.33	-0.54	0.24	0.27
Radius Range 0.35-0.7μm		1	0.92	0.66	0.50	-0.36	-0.50	0.27	0.29
Radius Range 0.7-1.5μm			1	.73	0.51	-0.34	-0.44 (2.3%)	0.36	0.21
Radius Range 1.5-2.5μm				1	0.70	-0.36	-0.32	.16	.33
Radius Range 2.5-5.0μm					1	-0.30	-0.16	-0.04 (7.0%)	.45
Wind Direction						1	0.25	0.01	-0.25
Wind Speed							1	-0.26	-0.06
Humidity								1	-0.41
Temperature									1

The results from figures 2.20 and 2.21 indicate that particle size distribution measurements can be made less frequent, by as much as twenty-fold, without losing significant information. This is important since the operating time of the measurement system can be increased before servicing is required and in addition the volume of particle size data required for analysis can be substantially reduced. Part of the above work is also described by Jennings and Elleson (1976).

3. THE GROWTH OF HYGROSCOPIC PARTICLES WITH HUMIDITY

3.1 Introduction

The theory of the growth of water soluble aerosol particles has been considered by many workers, for example by Orr et al. (1958), Low (1969b), Hanel (1970) and Mason (1971). There have been at least three different approaches in the theoretical treatment of the growth of soluble particles with humidity.

Firstly, a growth equation was developed by Mason (1971) which used experimental values of the van't Hoff factor determined by McDonald (1953). Low (1969b) derives an analytical expression for the growth equation, using the mean ionic activity coefficient Υ as the fundamental parameter upon which the solution effect on particle growth depends. Abundant experiemntal data on Υ is available and possesses the advantage that important properties such as the lowering of vapour pressure in electrolytic solutions can be readily computed.

The third approach, used by Hanel (1970), is based on the measured values of the volume and mass increase of atmospheric aerosol particles and appears to be valid over the entire humidity range. Hanel's growth equations can only be applied to bulk atmospheric aerosol for which the variation of mass with humidity is known.

The theoretical growth of aerosol particles of sodium chloride and ammonium sulphate with humidity is outlined in the following sections. The fundamental growth equation is broadly based on the treatment by Mason (1971). Some new procedures and approximations are used in the application of the growth equation to the prediction of aerosol particle size with varying humidity. A comparison is made between the growth curves and those plotted by Mason. The effect of relative humidity on the mean size of aerosol particles of sodium chloride and ammonium sulphate is examined experimentally. A comparison is made between the

experimental growth curves and the theoretical models.

3.2 The Growth Curve Equation Relating Particle Radius to Humidity

The vapour pressure P_r over a droplet of pure water of radius r exceeds that over a plane water surface P_∞ at the same temperature in accordance with the expression

$$\frac{P_r}{P_\infty} = \exp\left\{\frac{2\sigma M}{RrT}\right\} \tag{3.1}$$

where σ is the surface tension of the droplet, M is the molecular weight of water, R is the universal gas constant and T is the absolute temperature.

The effect of a dissolved salt in a droplet is to reduce the vapour pressure over its surface. For a solution of constant concentration this can be described by the relation

$$\frac{P_{r'}}{P'_\infty} = \exp\left\{\frac{2\sigma' V'_w}{RTr'}\right\} = \delta \tag{3.2}$$

where the dashed quantities are defined as above but refer to the solution droplet. V_w' is the partial molar volume of water in the solution and δ is known as the curvature correction.

Since the solution concentration is a function of the droplet radius r' the vapour pressure over the plane solution also depends on r'. The vapour pressure $P_{r'}$ over the surface of solution droplet exceeds that over a plane surface of the solution according to the expression

$$\frac{P_{r'}}{P_\infty} = \frac{P'_\infty(r')}{P_\infty} \exp\left\{\frac{2\sigma V'_w}{RTr'}\right\} \tag{3.3}$$

The following approximation is used in the calculations:

$$V'_w \simeq V_w \simeq \frac{M}{\rho} \tag{3.4}$$

where ρ is the density of pure water and V_w is the molar volume of pure water. Use of this approximation, as shown by a close examination of the measured densities of aqueous solutions, has been made by Hanel (1970). On the other hand numerous authors including Orr (1958), Mason (1971), Low (1969) use M/ρ' in place of the partial molar volume of water in the solution, V_w', which leads to substantial error, particularly for small droplets, as indicated in Table 3.1 from Hanel (1970).

TABLE 3.1

$\frac{P_\infty'}{P_\infty}$	V_w' (cm^3/Mol)	$\frac{M_w}{\rho'}$ (cm^3/Mol)
0.76	17.80	15.04
0.80	17.84	15.36
0.85	17.89	15.79
0.90	17.95	16.35
0.95	18.01	17.05
1.00	18.05	18.05

The difference between the partial molar volume of water, V_w', and the ratio $\frac{M_w}{\rho'}$ as a function of the vapour pressure ratio $\frac{P_\infty'}{P_\infty}$ for aqueous NaCl at 18°C.

It can be seen from the table that V_w' differs from V_w the molar volume of pure water by less than 3% as the humidity is varied from 76 to 100 per cent.

Equation 3.3 can now be written as

$$\frac{P_{r'}}{P_\infty} = \frac{p'_\infty(r')}{P_\infty} \exp\left\{\frac{2\sigma' M}{\rho R T r'}\right\} \tag{3.5}$$

Mason (1971) has derived an expression for $\frac{P_{r'}}{P_\infty}$ which is of the form

$$\frac{P_{r'}}{P_\infty} = \left[1 + \frac{i m_o M}{W\left\{\frac{4}{3}\pi r^3 \rho' - m_o\right\}}\right]^{-\rho/\rho'} \cdot \exp\left\{\frac{2\sigma' M}{\rho' R T r'}\right\} \tag{3.6}$$

where m_o is the mass of the dry solute, W is the molecular weight of of the solute and i is the van't Hoff factor.

Direct comparison of equations 3.5 and 3.6 can be made, noting that a different approximation for V_w' has been made in each case. This yields the result

$$\frac{p'_\infty(r')}{P_\infty} = \left[1 + \frac{i m_o M}{W\left\{\frac{4}{3}\pi r'^3 \rho' - m_o\right\}}\right]^{-\rho/\rho'} \tag{3.7}$$

so equation 3.5 now becomes

$$\frac{P_{r'}}{P_\infty} = \left[1 + \frac{i m_o M}{W\left\{\frac{4}{3}\pi r'^3 \rho' - m_o\right\}}\right]^{-\rho/\rho'} \cdot \exp\left\{\frac{2\sigma' M}{\rho R T r'}\right\} \tag{3.8}$$

When the droplet is in equilibrium with the surrounding atmosphere the vapour pressure over its surface, $P_{r'}$, must equal the partial pressure of water in the air.

Hence

$$\frac{P_{r'}}{P_\infty} = \frac{H}{100}$$

where H is the relative humidity of the air.

Equation 3.8 now becomes

$$\frac{H_{r'}}{100} = \left[1 + \frac{i m_o M}{W\left\{\frac{4}{3}\pi r'^3 \rho' - m_o\right\}}\right]^{-\rho/\rho'} \cdot \exp\left\{\frac{2\sigma' M}{\rho R T r'}\right\} \qquad (3.9)$$

This equation can be used to calculate the radius of the solution droplet in equilibrium with the atmosphere at a specified relative humidity.

Using r_o as the equivalent radius of the dry particle we may write

$$m_o = \frac{4}{3}\pi r_o^3 \rho_o \qquad (3.10)$$

where ρ_o is the density of the dry particle.

From this we obtain the result

$$H_{r'} = \left[1 + \frac{iM}{W}\left\{\frac{1}{\frac{\rho'}{\rho}\left\{\frac{r'}{r_o}\right\}^3 - 1}\right\}\right]^{-\rho/\rho'} \cdot \exp\left\{\frac{2\sigma' M}{\rho R T r'}\right\} \cdot 100\% \qquad (3.11)$$

At a temperature T of 25°C ($T = 298K$), the parameters ρ, M and R possess the values 0.997g cm^{-3}, 18.02g and 8.317×10^7 erg $mole^{-1}K^{-1}$ respectively.

Therefore we can write equation (3.11)

$$H_{r'}[25°C] = \left[1 + \frac{18.02\, i}{W}\left\{\frac{1}{\frac{\rho'}{\rho}\left\{\frac{r'}{r_o}\right\}^3 - 1}\right\}\right]^{-\rho/\rho'} \cdot \exp\left\{1.459 \times 10^{-9} \frac{\sigma'}{r'}\right\} \cdot 100\% \qquad (3.12)$$

3.3 Use of the Particle Growth Equation

Equation 3.12 is the fundamental equation relating humidity to particle radius. The following procedures are used when the equation is applied since the surface tension, density and van't Hoff factor are all functions of solution concentration (and therefore droplet size).

Moreover the van't Hoff factor cannot be expressed in an analytical form.

Approximate relations based on known experimental values are used and extrapolated where necessary.

3.3.1 Molality of the solution

The molality, η , of a solution is defined by the equation

$$\eta = \frac{1000}{M} \cdot \frac{n_s}{n} \tag{3.13}$$

where n_s is the number of moles of solute and n the number of moles of solvent. M is the molecular weight of pure water.

For a droplet containing dissolved salt the dry mass of which is m_o,

$$n_s = \frac{m_o}{W} \tag{3.14}$$

where W is the molecular weight of the salt and,

$$n = \frac{m' - m_o}{M} \tag{3.15}$$

where m' is the mass of the solution droplet.

Therefore

$$\eta = \frac{1000}{W} \cdot \left(\frac{M}{W}\right) \cdot \frac{m_o}{m' - m_o} \tag{3.16}$$

$$= \frac{1000}{W} \cdot \frac{1}{\left\{\frac{m'}{m_o} - 1\right\}}$$

Using equation 3.10 and the relation

$$m' = \frac{4}{3}\pi \rho' r'^3 \tag{3.17}$$

we obtain the result

$$\eta = \left(\frac{1000}{W}\right) \cdot \frac{1}{\left[\frac{\rho}{\rho_o} \cdot \frac{r'}{r_o} - 1\right]} \qquad (3.18)$$

The percentage concentration, p, of the solution can be expressed as

$$p = 100 \cdot \frac{\rho_o}{\rho'} \left(\frac{r_o}{r'}\right)^3 \qquad (3.19)$$

3.3.2 The density of salt solution as a function of the percentage concentration

The density of various salt solutions is tabulated as a function of the percentage concentration (Handbook of Chemistry and Physics, 43rd. ed., 1961). The relationship is approximately linear with increasing concentration for sodium chloride and ammonium sulphate until the saturated solution level is reached. Values in the supersaturated region are not known but the density of the dry particle (p = 100%) does not lie on the extrapolated straight line but rather above it. In order to extrapolate the curve into the supersaturated region a quadratic function has been fitted to the data as shown in Figure 3.1 for sodium chloride. A similar curve was obtained for ammonium sulphate. The functions used are given by equations 3.20 and 3.21 for sodium chloride and ammonium sulphate respectively.

$$\rho' = 5.45 \times 10^{-5} p^2 + 6.20 \times 10^{-3} p + 0.999 \qquad (3.20)$$

$$\rho' = 4.08 \times 10^{-5} p^2 + 3.61 \times 10^{-3} p + 0.999 \qquad (3.21)$$

Given a quadratic fit of the form

$$\rho' = Ap^2 + Bp + C$$

Equation 3.19 assumes the form

$$\left[\frac{r'}{r_o}\right]^3 = \frac{100\,\rho_o}{Ap^3 + Bp^2 + Cp} \qquad (3.22)$$

or

$$Ap^3 + Bp^2 + Cp - 100\,\rho_o \cdot \left[\frac{r_o}{r'}\right]^3 = 0 \qquad (3.23)$$

Therefore, the solution concentration can be evaluated if the droplet radius, r', is known. The relationship between the solution concentration, p, and $(r'/r_o)^3$, where r_o is the radius of the dry particle, can easily be obtained for selected values of density ρ_o.

3.3.3 The surface tension as a function of molality

Linear equations of the form given below for sodium chloride (equation 3.24) and ammonium sulphate (equation 3.25) were found to fit the curves of the variation of surface tension with molality given by Low (1969a).

$$\sigma' = 1.623\,m + 72.78 \qquad (3.24)$$

$$\sigma' = 2.168\,m + 72.78 \qquad (3.25)$$

3.3.4 The van't Hoff factor, i

Low (1969a) has tabulated the van't Hoff factor, i, as a function of molality in the range 0.0001 to 6 for sodium chloride and 0.0001 to 5.5 for ammonium sulphate. At lower molalities i tends towards the value 2.0 for sodium chloride and 3.0 for ammonium sulphate.

The highest molality tabulated in both cases corresponds to the saturated solution. In order to attempt to describe the properties of the supersaturated solution it is necessary to assume that the experimental data can be extrapolated. Cubic equations of the form given below were found to be a good approximation to the data at the higher concentrations. It is assumed that they continue to describe the behaviour of the solutions up to molalities of the order of 20.

For sodium chloride the cubic equation, fitted to Low's data at molalities of 1, 2, 4 and 6 is

$$i = 1.81736 + 6.1336 \times 10^{-2} m + 2.61582 \times 10^{-2} m^2 - 9.33083 \times 10^{-4} m^3 \qquad (3.26)$$

The equation for ammonium sulphate, using molalities of 3, 4, 5 and 5.5 is

$$i = 1.74017 + 5.7799 \times 10^{-2} m + 1.1904 \times 10^{-2} m^2 - 5.25333 \times 10^{-4} m^3 \qquad (3.27)$$

A good fit for the larger values of molality was obtained using these equations as can be seen in Figures 3.2 and 3.3, where the van't Hoff factor, i, is plotted as a function of molality, m , for sodium chloride and ammonium sulphate respectively. The use of the extrapolated values obtained from Equations 3.26 and 3.27 is fully justified since the particle growth curve indicates a smooth variation as low as 40% relative humidity. The following procedure for solving the growth equation for a salt solution at a particular radius, r', for selected values of density, ρ_o, and initial dry particle radius, r_o, using the described interpolation equations, was adopted.

(i) The percentage concentration, p, of the solution was evaluated using the cubic equation 3.23.

(ii) The density of the salt solution was calculated from expressions 3.20 and 3.21.

(iii) The molality of the solution was calculated using equation 3.18.

(iv) The surface tension, σ', of the solution was obtained from equations 3.24 and 3.25.

(v) The values of the van't Hoff factor, i, were taken from Low (1969a) up to a molality of 6.0 for sodium chloride and 5.5 for ammonium sulphate. For higher molality values, i was obtained by the use of equations 3.26 and 3.27 as described above.

(vi) The above parameters were then substituted into equation 3.12 which gives the humidity at which a particle of radius r' is in equilibrium with the surrounding atmosphere. An IBM 370/168 computer was used in the numerical side of the equation.

No attempt has been made to predict the recrystallisation of the droplets with decreasing humidity. The transition from solid to solution droplets has been considered by Orr et al. (1958) but no satisfactory theory of the recrystallisation point has yet been evolved.

Good agreement was found to exist between the growth curves derived using the described procedure with those calculated by Mason (1971) for sodium chloride. The extent of the agreement can be seen in Table 3.2 which indicates a difference of less than 0.4% between Mason's formulation and the present analysis over the range of humidity shown. Good agreement was also found between the computed growth curves of ammonium sulphate and those derived by Garland (1969).

TABLE 3.2

Particle radius (μm)	Relative humidity (%)		Difference (%)
	Equation 3.12	Mason	
0.084	72.9	72.6	0.31
0.096	83.7	83.6	0.18
0.108	89.5	89.4	0.12
0.120	92.9	92.8	0.07
0.144	95.2	95.2	0.03

Comparison of the growth curve predictions using equation 3.12 with those due to Mason (1971). A solute mass of 10^{-15} gm has been used.

3.4 The Experimental Arrangement and Procedure in the Measurement of the Increase in Aerosol Particle Size with Humidity

3.4.1 The experimental apparatus

A schematic diagram of the apparatus is shown in figure 3.4. A collison nebulizer (May, 1973) is used to generate the particles. The atmomized spray leaves the nebulizer through a heated vertical tube in order to vapourise the water from the salt droplets. The particles then enter a variable volume storage vessel of maximum volume 1 m^3. The base of the storage vessel consisted of a standard glove box with the normal observation window and access to the interior of the vessel, which was lined with blotting paper. The humidity in the chamber could be varied by controlling the flow of water to the vessel, and was measured by means of a psychrometer. The particle number concentration was measured by means of a Nolan-Pollak photoelectric nucleus counter which is well described in the literature, for example, Nolan (1972). The sampling of the aerosol particles was automated using electrically operated solenoid values and an electric cam timer. Calibration tables (Metnieks and Pollak, 1959) were used to determine the number concentration of particles in the storage vessel.

A cocylindrical condenser was used to measure the mean particle radius as the humidity was altered. Particles entering the condenser are brought to electrical equilibrium by a weak radioactive alpha source (Americium 241 foil of strength 125 μC). The ratio of the concentration of uncharged particles, No, to the total concentration, Z, has been related to an equivalent size, r, by Keefe, Nolan and Rich (1959) who assumed that the charge distribution on the aerosol obeys a Boltzmann law when the aerosol is in electrical equilibrium. Values of aerosol radius as a function of No/Z have been tabulated (Metnieks and Pollak, 1961). Further detail of the experimental apparatus used is given by Elleson (1976).

3.4.2 The experimental procedure

The storage vessel was first filled with dry, filtered air by means of a compressor pump. The system was then tested for filtered air by means of the photoelectric counter through the observation of the "scintillation effect". When the storage vessel was free from nuclei, aerosol particles generated by the Collison atomizer were

introduced into the storage vessel continuously. The particle concentration was allowed to rise to about 5×10^4 particles cm^{-3} before generation was stopped. It was found that, at higher concentrations, rapid growth of the particles by coagulation occurred. Measurements of particle number concentration were taken every 2 minutes throughout each experiment, beginning as soon as the aerosol generator was switched on. The psychrometer fan was switched on at the start of an experimental run and the wet and dry bulb readings were taken throughout the experiment at 2 minute intervals. Equivalent size measurements were made, when the particle concentration became steady, using an ion tube as described in the last section. The size measurements were taken continuously throughout the experiment.

Once the initial size was established, the humidity in the chamber was raised by introducing water into the storage vessel. Selected parts of the walls were wetted in order to obtain size measurements at intermediate humidity values. It was found that the relative humidity remained quite stationary over a size measurement. The rate of rise of humidity could be increased by introducing additional water to the vessel. During a complete experimental run, at least five size measurements could be made at different humidity values. In general, the lowest humidity attained was about 50 per cent whilst the highest value was usually of the order of 92 per cent.

An analysis of the particle size distribution using a diffusion battery following Fuchs (1962) method indicated that the distribution was approximately log-normal. A typical experiment took approximately one and a half hours to perform during which time some coagulation is expected. Experimental measurements at almost constant humidity indicated that the contribution of coagulation to particle growth of about 2.3% could be regarded as negligible.

3.5 Comparison Between the Experimental Results of Particle Size Growth with Humidity, and Prediction

The measurements of particle size as the relative humidity was increased are shown in figures 3.5 and 3.6 for both ammonium sulphate and sodium chloride particles. The measurements for ammonium sulphate represent the growth for three initial dry radii of 2.8×10^{-6} cm, 2.9×10^{-6} cm and 3.1×10^{-6} cm. It can be seen that the smallest particle size grows to 4.0×10^{-6} cm as the humidity is increased from 61% to 89%, which represents a size increase of 43%. The largest

particle size of 3.1×10^{-6}cm is increased to a value of 5.0×10^{-6}cm which is an increase of 61%. The growth of sodium chloride particles of initial radius 2.5×10^{-6}cm, 2.7×10^{-6}cm and 2.8×10^{-6}cm as the humidity is increased from about 60% to about 92% is shown in figure 3.6. The smallest particles increase in size by a factor of two over this range. A summary of the fractional increase in particle size as the humidity is increased to the maximum value is given in Table 3.3 for both salts.

TABLE 3.3

	Initial Humidity (%)	Radius ($\times 10^{6}$cm)	Final Humidity (%)	Radius ($\times 10^{6}$cm)	Fractional Size Increase
ammonium sulphate	62	2.8	89	3.9	0.39
	63	2.9	92	4.7	0.62
	59	3.1	92	5.0	0.61
sodium chloride	56	2.5	90	5.1	1.04
	64	2.7	92	5.0	0.85
	67	2.8	89	4.4	0.57

A typical experimental growth of ammonium sulphate and sodium chloride particles

A comparison is made between the experimental growth curves and the theoretical predictions according to Equation 3.12. Two theoretical curves for ammonium sulphate, between which the experimental points are approximately bounded, are drawn for initial dry particle radii of 2.4×10^{-6}cm and 2.6×10^{-6}cm in figure 3.7. The comparison shows good agreement between the experimental values and the theoretical curves representing particle sizes of 3.1×10^{-6}cm and 3.3×10^{-6} at 60% relative humidity. Similar theoretical curves are drawn for sodium

chloride in figure 3.8 for initial dry particle radii of 1.8×10^{-6}cm and 2.0×10^{-6}cm. These yield values of the theoretical radii at 60% relative humidity of 2.8×10^{-6}cm and 3.1×10^{-6}cm which compare favourably with the initial experimental values.

The experimental points lie very close to the predicted lines with some variation which may be explained in terms of the particles going into solution and recrystallising before entering the humidity chamber. When the particles are generated by the nebulizer they are droplets of solution. Since they are dried to about 55% relative humidity a proportion will recrystallise but some will remain in a supersaturated solution form. This mixture of particles is then introduced to the storage chamber where the humidity is increased. The supersaturated droplets would be expected to follow a curve similar to the theoretical curve as shown by the curves in figures 3.7 and 3.8 but the dry particles, on reaching a critical humidity, will go into solution and grow significantly over a very small range of humidity. At this point some spreading of the points will start to occur. Work by Orr et al. (1956) indicates that particles tend to dissolve at a precise value of the humidity but recrystallisation can occur over a much wider range and cannot yet be satisfactorily predicted. The same work suggests that sodium chloride and ammonium sulphate particles with initial radii of the order of 0.01 micrometres would completely dissolve at about 70% and 63% relative humidity respectively.

A spread of results is indeed observable in the sodium chloride curve at a value of 73% to 74% relative humidity. There appears to be a lack of spread in the experimental values for ammonium sulphate which probably indicates that only a small percentage of particles recrystallised after generation. It can be seen that maximum particle growth occurs for the two salts at the higher values of relative humidity. Experimental measurements at constant humidity indicate that coagulation plays little part in the growth of the aerosol particles compared with the growth due to the condensation of water vapour.

4. THE EFFECT OF PARTICLE GROWTH AND HUMIDITY ON TRANSMISSION PROPERTIES OF AN AEROSOL

The effect of particle growth on visibility is examined using approximations to Mie's theory due to Diermendjian (1960) and Penndorf (1962). Extrapolation procedures similar to those described above are used to predict the variation of particle refractive index with solution concentration. The results are compared with work carried out by Garland (1969) and Hanel (1971). A study is also made of the effect of particle mass and both model and measured particle size distributions for sodium chloride and ammonium sulphate on the extinction coefficient σ.

4.1 The Effect of Particle Size and Refractive Index on the Extinction Coefficient

It is clear that the presence of suspended matter will affect the transmission of light through a medium. In the case of an aerosol, the nature of the effect depends on the particle size in relation to the wavelength of light. A convenient parameter is the size parameter $\alpha = 2\pi r/\lambda$ where r is the particle radius and λ is the wavelength of light. For $\alpha \approx 1$, it is necessary to consider the variation of the electromagnetic field inside and outside a small sphere and to solve the resulting differential equations. This was first solved by Mie (1908). In view of the complexity of the analytical treatment, approximations to Mie's results are used in the following treatment of light extinction.

Following the procedure outlined by Middleton (1963), the extinction coefficient, σ, can be expressed as

$$\sigma = N\pi r^2 K \tag{4.1}$$

for a monodisperse aerosol of particle radius r and N particles per unit volume. K is known as the scattering area ratio since it is the ratio of the area of the wavefront acted upon by the particle to the area of the particle itself. If the aerosol is polydisperse the extinction coefficients of all the monodisperse components can be added together with the result that the extinction coefficient is given by the relation

$$\sigma = \sum_{i=1}^{n} N_i \pi r_i^2 K_i \tag{4.2}$$

where n is the number of different particle sizes and N_i is the particle number concentration of particles of radius r_i.

If the extinction coefficient can be found, a value of the visibility can be obtained using the visual range, V, which is defined by Middleton (1963) as

$$V = \frac{3.912}{\sigma} \tag{4.3}$$

Solution of equation 4.2 is straightforward if K is known. Tabulated values of K as a function of α and the refractive indices of value 1.33, 1.44, 1.55 and 2.00 are known. Approximate equations for K have been derived by Penndorf (1962) and Diermendjian (1960) and are used in the following calculations.

If the refractive index, μ, of the material under consideration is expressed in the complex form

$$\mu = n + ik \tag{4.4}$$

then the approximation of Diermendjian can be written as

$$K_i = [1+D]\left\{2 - \frac{4\cos g}{\rho}\exp\{-\rho\tan g\}\sin\{\rho - g\} + 4\left[\frac{\cos g}{\rho}\right]^2\left\{\cos 2g - \exp\{-\rho\tan g\}\cos\{\rho - 2g\}\right\}\right\} \tag{4.5}$$

where

$$\rho = \frac{4\pi r_i}{\lambda}[n_i - 1] \quad , \quad g = \arctan\left\{\frac{k_i}{n_i - 1}\right\}$$

$$D = \frac{\{n_i-1\}^2}{1.632 n_i}[f(g)+1] + \frac{0.2\rho - \{n_i - 1\}}{f(g)\{n_i - 1\}} \quad \text{for } \rho \leq 5\{n_i - 1\}$$

$$D = \frac{\{n_i - 1\}}{8.16 n_i}[f(g)+1]\rho \quad \text{for } 5\{n_i-1\} \leq \rho \leq \frac{4.08}{1+3\tan g}$$

$$D = \frac{\{n_i - 1\}[f(g)+1]}{2n_i[1+3\tan g]} \quad \text{for } \frac{4.08}{1+3\tan g} \leq \rho \leq \frac{4.08}{1+\tan g}$$

$$D = \frac{2.04(n_i - 1)\{f(g)+1\}}{n_i \rho f(g)} \quad \text{for } \rho > \frac{4.08}{1+\tan g}$$

and

$$f(g) = 1 + 4\tan g + 3\tan^2 g$$

Penndorf's approximation, given below, is used when $\alpha_i = \frac{2\pi r_i}{\lambda} \leq 1$,

$$K_i = A\alpha_i + B\alpha_i^3 + C\alpha_i^4 \tag{4.6}$$

where

$$A = \frac{24\, n_i k_i}{Z_1}$$

$$B = \frac{4}{15} n_i k_i + \frac{20 n_i k_i}{3 Z_2} + \frac{24}{5} n_i k_i \frac{\left[7\left\{n_i^2+k_i^2\right\}^2 + \left\{4n_i^2 - k_i^2 - 5\right\}\right]}{Z_1^2}$$

$$C = \frac{\frac{8}{3}\left\{\left[\left\{n_i^2+k_i^2\right\}^2 + \left\{n_i^2 - k_i^2 - 2\right\}\right]^2 - 36\, n_i^2 k_i^2\right\}}{Z_1^2}$$

where

$$Z_1 = \left\{n_i^2+k_i^2\right\}^2 + 4\left\{n_i^2 - k_i^2\right\} + 4$$

$$Z_2 = 4\left\{n_i^2+k_i^2\right\}^2 + 12\left\{n_i^2 - k_i^2\right\} + 9$$

4.2 The Effect of Relative Humidity on the Extinction Coefficient for a Wide Range of Particle Size Distributions

The theoretical relation between aerosol size and relative humidity was treated in Sections 3.2 and 3.3, One can use this relation to study the effect of humidity on the shape of a selected particle size distribution. The influence of two humidity values of 75 and 95 per cent on a Junge type distribution with slope β of -3 is to displace the curve laterally as seen in figure 4.1.

The calculations on the variation of visibility with relative humidity were performed using a wavelength of 0.55 micrometres for light. This corresponds to an average wavelength in the range over which the human eye is sensitive. It was assumed that the imaginary part of the refractive index was zero which means that absorption of light by the particles is not accounted for. This assumption is justifield by the negligible or zero values of the imaginary part of the refractive index given by Hanel (1972) for bulk atmospheric aerosol. Linear approximations to the real part of the refractive indices for sodium chloride and ammonium sulphate respectively are given below as functions of the percentage concentration of the solutions

$$\mu = 0.00177p + 1.333 \tag{4.7}$$

$$\mu = 0.00158p + 1.333 \tag{4.8}$$

The approximation relations show good agreement with tabulated values given in the Handbook of Chemistry and Physics (1969). Values of the extinction coefficient, σ, were calculated as a function of relative humidity and particle mass by means of a computer programme. The particle number concentration was chosen to correspond to one microgram of salt per m^3.

The extinction coefficient, σ, of an atmosphere containing one microgram of ammonium sulphate per cubic metre is plotted in figure 4.2 for the following size distributions:

(a) A monodisperse aerosol at the mass median radius of 0.21 micrometres of a modified Junge type distribution shown in Figure 4.3.

(b) A monodisperse aerosol at the mass median radius of 0.3 micrometres of a distribution measured by Heard and Wiffen (1969).

(c) An atmospheric ammonium sulphate particle size distribution measured by Heard and Wiffen (1969) using electron microscope techniques. This distribution is shown in Table 4.1.

(d) A Junge type particle size distribution as shown in figure 4.3.

It can be seen that good agreement was obtained between the results using approximations to Mie's theory and the results of Garland (1969) who used an interpolation formula to calculate the scattering area ratio, K, for each particle size. Some of Garland's calculated points, identified by o, are shown in figure 4.2 to illustrate the agreement between the two sets of results.

TABLE 4.1

Radius (μm)	Dry particle mass (gm)	Percentage of the total number concentration
0.060 - 0.105	4.30×10^{-15}	22.9
0.105 - 0.145	1.45×10^{-14}	25.7
0.145 - 0.185	3.43×10^{-14}	13.5
0.185 - 0.230	6.70×10^{-14}	14.8
0.230 - 0.270	1.16×10^{-13}	7.67
0.270 - 0.310	1.84×10^{-13}	6.40
0.310 - 0.350	2.74×10^{-13}	5.14
0.350 - 0.395	3.90×10^{-13}	2.56
0.395 - 0.435	5.36×10^{-13}	1.28

The size distribution of ammonium sulphate particles in the atmosphere on 23.8.67 reported by Heard and Wiffen

Figure 4.4 shows the variation of the extinction coefficient with humidity and dry particle mass over a range from 3×10^{-17}gm to 3×10^{-11}gm for ammonium sulphate in an atmosphere containing one microgram of salt per cubic metre. It can be seen that maximum extinction occurs, at the selected value of 99% relative humidity, for a dry particle mass of 10^{-14}gm corresponding to a radius of 1.2×10^{-5}cm. It is also clear that visibility is reduced by approximately an order of magnitude over the whole range of particle mass as the humidity is increased from 80% to 99%.

The extinction coefficient, σ, for an atmosphere containing 1 microgramme of sodium chloride particulate per m^3 in figure 4.5 for selected particle size distributions. The distributions used are identical to distributions (a), (b) and (d) of figure 4.2, whilst distribution (c) is a model sea-spray distribution similar to that used by Hanel (1972), and shown in figure 4.6. It is clear by comparing the plots of extinction coefficient with relative humidity for sodium chloride and ammonium sulphate in figures 4.5 and 4.2 that the extinction coefficient is generally greater in the case of sodium chloride particles for the particle size distributions (a), (b) and (d).

The extinction coefficient, σ, is plotted against the dry particle mass over a range from 3×10^{-17}gm to 3×10^{-11}gm for sodium chloride in figure 4.7 for an atmosphere containing 1 µgm of salt per m^3. It can be seen from figure 4.7 that for a relative humidity of 99 per cent, maximum extinction occurs at a dry particle radius of 8.2×10^{-6}cm. The shapes of the curves are similar to those for ammonium sulphate, although important differences between the two sets of results will be discussed in the next section.

The change in extinction coefficient, σ, as the dry particle radius, r_o, is varied from 2×10^{-6}cm up to 1×10^{-3}cm is shown in figure 4.8 for the following values of relative humidity: 80, 95, 99 and 99.9 per cent. These calculations were performed for dry particles of sodium chloride. It can be calculated that for particle radius greater than 4×10^{-5}cm, the extinction coefficient, at 99.9, 99 and 95 per cent exceeds the values at 80 per cent by average factors of 30.7, 6.6 and 2.5 respectively. The average fractional increase in extinction coefficient at 99.9, 99 and 95 per cent above that at 80 per cent relative humidity possess values of 110, 28 and 4.6 respectively for dry particle sizes less than 4×10^{-5}cm. It can also be observed that the peak value of extinction coefficient is shifted towards smaller dry particle radius with increasing values of relative humidity.

A comparison was made between the extinction coefficient at selected values of humidity H, σ (H), with the extinction coefficient at a value of humidity k, σ (k), where k was chosen to be a humidity value at which it could be assumed that the particle was dry. The values used for k were taken as 48.4 and 53.7 per cent for ammonium sulphate and sodium chloride respectively which correspond to the lowest values of humidities calculated using the particle growth equation. A graph of the ratio $\sigma(H)/\sigma(k)$ is plotted against the relative humidity, H, in figures 4.9 and 4.10. The curves for both ammonium sulphate and sodium chloride are computed for a Junge distribution, shown in figure 4.3 and for a mono-

disperse aerosol of particle radius 0.21 micrometres, corresponding to the mass median radius of the Junge distribution.

It can be seen from the curves for the monodisperse aerosols of particle radius 0.21 micrometres that the ratio $\sigma(H)/\sigma(k)$ attains a value of 2.0 at a relative humidity of 86% and 6.0 at 97% for ammonium sulphate. In the case of the monodisperse aerosol of sodium chloride particles of radius 0.21 micrometres, the ratio $\sigma(H)/\sigma(k)$ is equal to 2.4 and 4.7 at 86% and 97% relative humidity respectively.

The curves of $\sigma(H)/\sigma(k)$ versus relative humidity, H, indicate that the Junge form of distribution is more effective at reducing visibility than the monodisperse aerosol. The ratio of $\sigma(H)/\sigma(k)$ attains a value of 2.0 at 77% and 6.0 at 92% relative humidity for the sodium chloride aerosol and the same values at 81% and 95% respectively for the ammonium sulphate particles.

4.3 A Discussion of the Results Related to Atmospheric Extinction

An expression has been derived for the extinction coefficient, σ, for both a homogeneous and a non-homogeneous source of aerosol particles This has involved the use of approximations for the scattering area ratio, K, based on the equations of Diermendjian (1960) and Penndorf (1962). K is a function of the particle radius, the wavelength of the incident light and the refractive index of the particle. The variation of refractive index with humidity was taken into account by means of a linear approximation equation relating the refractive index to the percentage concentration of the salt solution in the droplet. The two linear approximations for ammonium sulphate and sodium chloride give good agreement with tabulated values.

The effect of relative humidity on the extinction coefficient for a monodisperse aerosol of sodium chloride and ammonium sulphate over a range of particle mass of 3×10^{-17} to 3×10^{-11}gm is shown in figures 4.7 and 4.4 respectively. The particle number concentration was chosen to correspond to one microgram of salt per cubic metre. It can be seen that the shapes of the curves are quite similar for both sets of results. The smooth variation of the curves below a mass of about 10^{-15}gm indicates the region over which Rayleigh's scattering law, for particle size much less than the wavelength of light can be regarded as a good approximation to the more precise Mie theory. The undulations in the curves can be attributed to the oscillatory variation of the scattering area ratio with the particle radius. The oscillations are most pronounced for values of particle radius less than about 10 micrometres.

Values of the maximum extinction coefficient obtained for sodium chloride and ammonium sulphate at relative humidities of 80%, 95% and 99% are shown in Table 4.2. The sodium chloride aerosol yields a value of extinction coefficient greater than ammonium sulphate by a factor of about two for the three humidity values. Maximum contribution to the extinction coefficient is made by a dry particle of 1.90×10^{-5} and

TABLE 4.2

Relative Humidity (%)	Sodium Chloride		Ammonium Sulphate	
	Dry particle radius (cm)	σ (km^{-1})	Dry particle radius (cm)	σ (km^{-1})
80	1.90×10^{-5}	0.024	2.40×10^{-5}	0.013
95	1.30×10^{-5}	0.075	2.04×10^{-5}	0.034
99	7.90×10^{-6}	0.295	1.20×10^{-5}	0.150

Maximum values of the extinction coefficient, σ, for monodisperse aerosols with number concentration corresponding to 1 microgram per cubic metre

2.4×10^{-5}cm for sodium chloride and ammonium sulphate respectively when the relative humidity is 80%. These values are shifted to the lower values of 7.9×10^{-6}cm and 1.2×10^{-5}cm respectively as the humidity is increased to 99%.

Individual values of the extinction coefficient as a function of solute mass and relative humidity are shown in Table 4.3 for the two salts. The ratio of the extinction coefficient due to a monodisperse aerosol of sodium chloride to the corresponding values for a similar aerosol of ammonium sulphate at the selected values of dry particle mass from 10^{-16}gm to 10^{-11}gm for the values of relative humidity 80%, 95% and 99% are tabulated in Table 4.4. It can be seen that for the lower values of solute mass of 10^{-16}gm to 10^{-14}gm the sodium chloride particles are more efficient in reducing visibility by factors ranging from 1.7 to 5.5. The sodium chloride aerosol particles possess larger values of extinction coefficient by an average factor of 1.54 for the remaining three solute masses of 10^{-13}gm, 10^{-12}gm and 10^{-11}gm.

TABLE 4.3

	Dry Particle Radius (μm)	Solute Mass per Droplet (g)	Particle number concentration (cm^{-3})	Extinction Coefficient (km^{-1}) Relative Humidity (%)		
				80	95	99
ammonium sulphate	0.0238	10^{-15}	10,000	1.4×10^{-4}	7.0×10^{-4}	4.0×10^{-3}
	0.0513	10^{-15}	1,000	1.4×10^{-3}	6.2×10^{-3}	5.4×10^{-2}
	0.111	10^{-14}	100	7.0×10^{-3}	2.6×10^{-2}	1.5×10^{-1}
	0.238	10^{-13}	10	1.3×10^{-2}	3.3×10^{-2}	4.7×10^{-2}
	0.513	10^{-12}	1	3.5×10^{-3}	8.0×10^{-3}	3.1×10^{-2}
	1.11	10^{-11}	0.1	1.6×10^{-3}	4.0×10^{-3}	1.1×10^{-2}
sodium chloride	0.0223	10^{-15}	10,000	4.4×10^{-4}	3.0×10^{-3}	2.2×10^{-2}
	0.0480	10^{-15}	1,000	4.0×10^{-3}	2.2×10^{-2}	1.4×10^{-1}
	0.103	10^{-14}	100	1.6×10^{-2}	5.4×10^{-2}	2.5×10^{-1}
	0.223	10^{-13}	10	2.3×10^{-2}	4.3×10^{-2}	6.5×10^{-2}
	0.480	10^{-12}	1	5.4×10^{-3}	1.5×10^{-2}	3.3×10^{-2}
	1.03	10^{-11}	0.1	3.0×10^{-3}	6.3×10^{-3}	1.6×10^{-2}

Selected values of the extinction coefficient as a function of particle size and relative humidity

TABLE 4.4

Humidity (%)	Particle Mass(gm)					
	10^{-16}	10^{-15}	10^{-14}	10^{-13}	10^{-12}	10^{-11}
80	3.14	2.85	2.29	1.77	1.54	1.38
95	4.29	3.55	2.46	1.30	1.68	1.58
99	5.50	2.59	1.67	1.38	1.06	1.45

The ratios of extinction coefficients for sodium chloride to the corresponding values for ammonium sulphate

Results of the extinction coefficient due to selected particle size distributions for ammonium sulphate and sodium chloride as a function of relative humidity in the range 70 to 99% are presented in figures 4.2 and 4.5 respectively. It can be seen that the extinction coefficient for the two monodisperse aerosol particles of ammonium sulphate of radius 0.21 and 0.3 micrometres labelled curve (a), (b) respectively in figure 4.2 exceeds the values of extinction coefficient due to the distribution measured by Heard and Wiffen (1969) and a typical Junge distribution (Figure 4.3) represented by curve (d) in figure 4.2 for values of humidity less than about 92%. For values of humidity greater than 98.5% the contribution to the extinction coefficient is greater for the non-homogeneous Junge distribution. The values of the extinction coefficient are tabulated in Table 4.5 for the four particle size distributions of ammonium sulphate for values of relative humidity ranging from 70% to 99%.

The results of figure 4.5 indicate that the Junge type distribution causes the largest extinction for values of humidity greater than 94 per cent. The sea-spray aerosol (distribution (c)) has approximately the same effect on the extinction as the Junge distribution up to about 90 per cent relative humidity. The extinction coefficient for a Junge type distribution exceeds that due to the sea-spray distribution by an average value of 35 per cent for the relative humidity range between 90 and 99 per cent.

It can be seen from the computational results of figure 4.8 that the increase in extinction coefficient is most sensitive over the dry particle range from about 3×10^{-6} to 7×10^{-5}cm. Thus, changes in the shape of particle size distributions in this size band will cause the

TABLE 4.5

Distribution	Relative Humidity (%)				
	70	80	90	95	99
(a)	1.10×10^{-2}	1.30×10^{-2}	1.97×10^{-2}	3.35×10^{-2}	7.08×10^{-2}
(b)	1.00×10^{-2}	1.21×10^{-2}	1.70×10^{-2}	2.03×10^{-2}	3.16×10^{-2}
(c)	8.40×10^{-3}	9.31×10^{-3}	1.47×10^{-2}	2.59×10^{-2}	1.00×10^{-1}
(d)	4.64×10^{-3}	5.62×10^{-3}	9.72×10^{-3}	1.94×10^{-2}	1.22×10^{-1}

The extinction coefficient, km^{-1}, of an ammonium sulphate aerosol as a function of relative humidity for the following distributions:-

(a) A monodisperse aerosol of particle radius 0.21 micrometres

(b) A monodisperse aerosol of particle radius 0.30 micrometres

(c) A Heard and Wiffen distribution

(d) A Junge type distribution

greatest change in extinction coefficient. The occurrence of peaks in the particle size distribution, by sea-spray particles for example, in the coarse particle mode will have little influence on the total extinction coefficient due to the aerosol.

Selected values of the extinction coefficient from figure 4.5 for the four size distributions for a range of relative humidity from 70% to 99% are shown in Table 4.6. A comparison of the extinction coefficients shown in Tables 4.5 and 4.6 indicates that the extinction coefficient due to the sodium chloride particle distributions exceeds that due

to the ammonium sulphate distributions for all the distributions considered. Average values, over the relative humidity range from 70% to 99%, of the ratio of the extinction coefficients for sodium chloride and ammonium sulphate for the three distributions (a), (b) and (d) are equal to 1.60, 1.35 and 2.25 respectively.

TABLE 4.6

Distribution	Relative Humidity (%)				
	70	80	90	95	99
(a)	1.73×10^{-2}	2.24×10^{-2}	3.55×10^{-2}	5.01×10^{-2}	6.88×10^{-2}
(b)	1.30×10^{-2}	1.50×10^{-2}	1.78×10^{-2}	1.86×10^{-2}	7.94×10^{-2}
(c)	1.03×10^{-2}	1.41×10^{-2}	2.48×10^{-2}	4.21×10^{-2}	1.34×10^{-1}
(d)	8.66×10^{-3}	1.45×10^{-2}	2.55×10^{-2}	5.31×10^{-2}	2.37×10^{-1}

The extinction coefficient, km^{-1}, of a sodium chloride aerosol as a function of relative humidity for the following distributions:-

(a) A monodisperse aerosol of particle radius 0.21 micrometres

(b) A monodisperse aerosol of particle radius 0.30 micrometres

(c) A sea spray aerosol

(d) A Junge type distribution

The rate of increase of extinction coefficient at particular values of humidity, $\sigma(H)$, is compared to the extinction coefficient at a humidity, k, $\sigma(k)$ considered sufficiently low to assume that the salt nucleus is dry. Values of $\sigma(H)/\sigma(k)$ shown in figures 4.9 and 4.10 indicate that the extinction coefficient increases more rapidly for a sodium chloride monodisperse aerosol of particle radius 0.21 micrometres than for an ammonium sulphate aerosol source up to a value of about 95% relative humidity. The rate of rise of $\sigma(H)/\sigma(k)$ is greater for the two salts for a non-homogeneous Junge type distribution than for the monodisperse aerosol of particle size equivalent to the mass median radius of the Junge distribution. It can be seen from figure 4.10 that the extinction coefficient for a Junge distribution for both sodium chloride and ammonium sulphate approaches the same rate of increase with increasing values of humidity.

4.4 Overall Conclusions

A comprehensive analysis has been made of both number and size distributions of submicrometre and large aerosol particles over the size range from about 2×10^{-6}cm up to 5×10^{-4}cm radius. The measurement techniques adopted proved versatile and successful at both rural mountain and maritime field stations. It was shown that the diurnal pattern of aerosol size distributions in the radius range from 0.25 up to 5 micrometres showed a distinct maximum in the early morning hours followed by a minimum in mid afternoon. Sampling analysis indicates that measurements of the particle size distribution can be made less frequent by factors least as large as twenty-fold without loss in significant information of the data.

New procedures and approximations were made in calculating the growth of an aerosol particle with increase in relative humidity, which gave good agreement with calculated values of Mason (1971) and Garland (1969). Experimental growth measurements of both sodium chloride and ammonium sulphate particles with humidity gave reasonably good agreement with the theoretical growth predictions.

The effect of humidity (and hence particle growth) upon the extinction coefficient of an atmosphere containing sodium chloride and ammonium sulphate particles over a radius range from 2×10^{-6} up to 1×10^{-3}cm was examined. It was found that sodium chloride particles are more efficient in reducing visibility than ammonium sulphate particles for four different model distributions. In addition, a non-homogeneous Junge type particle size distribution results in the greatest values of extinction coefficient at greater than about 94% relative humidity.

REFERENCES

Blanchard, D.C. (1963). The Electrification of the Atmosphere by Particles from Bubbles in the Sea. Progress in Oceanography, 1, 71-202.

Cartwright, J., Nagelschmidt, G. and Skidmore, J.W. (1956). The Study of Air Pollution with the Electron Microscope. Q.J.R. Met. Soc., 82, 82-86.

Covert, D.S., Charlson, R.J. and Ahlquist, N.C. (1972). A Study of the Relationship of Chemical Composition and Humidity to Light Scattering by Aerosols. J. App. Met. 11, 968-976.

Davies, C.N., 1974. 'Size Distribution of Atmospheric Particles'. Aerosol Science, 5, 293-300.

Dessens, H. (1949). The Use of Spiders' Threads in the Study of Condensation Nuclei. Q.J.R. Met. Soc., 75, 23-26.

Diermendjian, D. (1960). Atmospheric Extinction of Infrared Radiation. Q.J.R. Met. Soc., 86, 371-381.

Eggleton, A.E.J. and Atkins, D.H.F. (1969). The Chemical Composition of Atmospheric Aerosols on Tees-side and its Relation to Visibility. Atmos. Environ., 3, 355-372.

Elleson, R.K. (1976). Studies of the Growth and Size Distribution of Aerosol Particles. M.Sc. Dissertation, University of Durham.

Friedlander, S.K. and Pasceri, R.E. (1965). Measurements of the Particle Size Distribution of the Atmospheric Aerosol: I. Introduction and Experimental Methods, "J. Atmospheric Sci., 22 (5), 571-576.

Fuchs, N.A., Stechkina, I.B. and Starosselskii, V.I. (1962). On the Determination of Particle Size Distribution in Polydisperse Aerosols by the Diffusion Method. Brit. J. Appl. Phys. 13, 280-281.

Garland, J.A. (1969). Condensation on Ammonium Sulphate Particles and its Effect on Visibility. Atmos. Environ., 3, 347-354.

Handbook of Chemistry and Physics (1969), 50th Edition. Chemical Rubber Company.

Hanel, G. (1970). The Size of Atmospheric Aerosol Particles as a Function of the Relative Humidity. Beitr. Phys. Atm., 43, 119-132.

Hanel, G. (1971). New Results Concerning the Dependence of Visibility on Relative Humidity and Their Significance as a Model for Visibility Forecast. Beitr. Phys. Atm., 44, 137-167.

Hanel, G. (1972). Computation of the Extinction of Visible Radiation by Atmospheric Aerosol Particles as a Function of the Relative Humidity, based on Measured Properties. Aerosol Science, 3, 377-386.

Heard, M.J. and Wiffen, R.D. (1969). Electron Microscopy of Natural Aerosols and the Identification of Particulate Ammonium Sulphate. Atmos. Environ., 3, 337-340.

Hogan, A.W. (1966). Some Characteristics of Aitken Nuclei Concentrations. J. Rech. Atmos., 2, 87-93.

Jennings, S.G. (1975). Measurements of the Number Concentration of Aitken Nuclei at Mountain and Rural Sites. Jnl. de Rech. Atmos., 11, 59-66.

Jennings, S.G. and Elleson, R.K. (1976). Natural Aerosol Size Distributions in the 0.25-5.0 micrometre Radius Range. Atmos. Environ. (in press).

Junge, C. (1952). The Constitution of Atmospheric Aerosols. Annln. Met., 5, supplement.

Junge, C. (1953). Die Rolle der Aerosole und der Gasformigen Beimengungen der Luft im Spurenstroffhaushalt der Troposphare. Tellus, 5, 1-26.

Junge, C. (1963). Air Chemistry and Radioactivity. Academic Press, New York.

Junge, C. and Jaenicke, R. (1971). New Results in Background Aerosol Studies from the Atlantic Expedition of the R.V. Meteor, Spring 1969. Aerosol Science, 2, 305-314.

Keefe, D., Nolan, P.J. and Rich., T.A. (1959). Charge Equilibrium in Aerosols According to the Boltzmann Law. Proc. R. Irish Acad., 60, 27-45.

Kelvin, Lord (1870). On the Equilibrium of Vapour at a Curved Surface of Liquid. Proc. R. Soc. Edin. 7, 63.

Kohler, H. (1921). Zur Kondensation des Wasserdampfes in der Atmosphare. Geophys. Publ., 2.

Kottler, F. (1950). The Distribution of Particle Sizes. J. Franklin Inst., 250, 419-441.

Low, R.D.H. (1969a). A Comprehensive Report on Nineteen Condensation Nuclei. ECOM-5249, White Sands Missile Range, New Mexico.

Low, R.D.H. (1969b). A Generalised Equation for the Solution Effect in Droplet Growth. J. Atmos. Sci.,26, 608-611.

McDonald, J.E. (1953). Erroneous Cloud-Physics Applications of Raoult's Law. J. Meteor., 10, 68-70.

Marple, V.A., Sverdrup, G.M. and Whitby, K.T. (1976). Private Communication.

Mason, B.J. (1971). The Physics of Clouds (2nd Ed.). Clarendon Press, Oxford.

May, K.R. (1973). The Collison Nebulizer: Description, Performance and Application. Aerosol Science, 4, 235-243.

Metnieks, A.L. and Pollak, L.W. (1961). Tables and Graphs for Use in Aerosol Physics. Number of Uncharged Particles in per cent total number of particles v. Radius and vice versa. Geophys. Bull. No., 20. Dub. Inst. Adv. Studies.

Middleton, W.E.K. (1963). Vision through the Atmosphere. University of Toronto Press.

Mie, G. (1908). Beitrage zur Optik truber Medien, speziell Kolloidaler Metallosungen. Ann. d. Physik, 25, 377.

Nolan, P.J. and Pollak, L.W. (1946). The Calibration of a Photoelectric Nucleus Counter. Proc. R. Irish Acad.,51, 9-31.

Nolan, J.P. (1972). The Photoelectric Nucleus Counter. Proc. Roy. Soc. Dublin, A4, 161-180.

Orr, C. Jr., Hurd, F.K., Hendrix, W.P. and Corbett, W.J. (1956). An Investigation into the Growth of Small Aerosol Particles with Humidity Change. Final Report Project No. A-162. Engineering Experiment Station of the Georgia Institute of Technology, Atlanta, Georgia.

Orr, C. Jr., Hurd, F.K. and Corbett, W.J. (1958). Aerosol Size and Relative Humidity. J. Colloid. Sci. 13, 472-482.

Penndorf, R.B. (1962). Scattering and Extinction Coefficients for Small Absorbing and Nonabsorbing Aerosols. J. Opt. Soc. Am., 52 896-904.

Peterson, C.M. and Paulus, H.J., 1967. Micrometeorological Variables Applied to the Analysis of Variation in Aerosol Concentration and Size. APCA Paper No. 67-133, Air Pollution Control Association Annual Meeting, Cleveland, Ohio.

Thomas, J.W. (1958). Gravity Settling of Particles in a Horizontal Tube. J. Air Poll. Control Ass., 8, 32.

Twomey, S. (1971). The Composition of Cloud Nuclei. J. Atmos. Sci., 28, 377-381.

Twomey, S. and Severynse, J. (1964). On the Relation Between Size of Particles and Their Ability to Nucleate Condensation of Natural Clouds. J. Rech. Atmos.,1, 81-85.

Wagman, J., 1966. Current Problems in Atmospheric Aerosol Research. Int. J. Air and Water Poll., 10, 777-782.

Whitby, K.T., Clark, W.E., Marples, V.A., Sverdrup, G.M., Sem, G.J., Willeke, K., Liu, B.Y.H. and Pui, D.Y.H. (1975). Characterisation of California Aerosols - 1. Size Distribution of Freeway Aerosol. Atmos. Environ. 9, 463-482.

Whitby, K.T. and Husar, R.B. (1971). Generation of Artificial Aerosols. The Second International Workshop on Condensation and Ice Nuclei, Dept. of Atmos. Sci., Colorado State University, 29-32.

Winkler, P. and Junge, C. (1972). The Growth of Atmospheric Aerosol Particles as a Function of the Relative Humidity. J. Rech. Atmos. 6, 617-638.

Wright, H.L. (1936). The Size of Atmospheric Nuclei: Some Deductions from Measurements of the Numbers of Charged and Uncharged Nuclei at Kew Observatory. Proc. Phys. Soc., 43, 675-689.

Wright, W.D. (1939). Atmospheric Opacity: A Study of Visibility Observations in the British Isles. Q.J.R. Met. Soc., 65, 411-442.

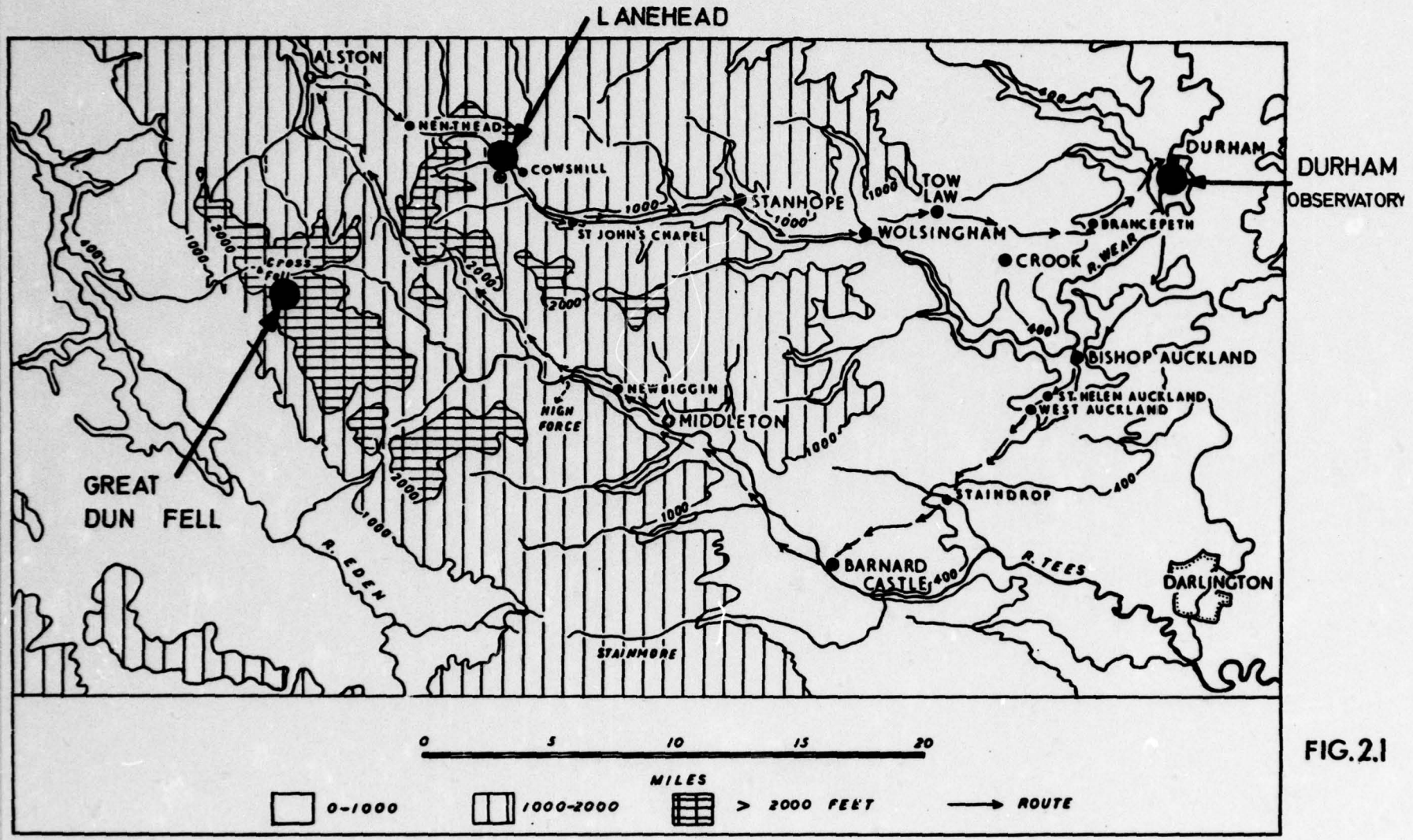
LANEHEAD
ALSTON
NENTHEAD
COWSHILL
STANHOPE
ST JOHN'S CHAPEL
WOLSINGHAM
TOW LAW
DURHAM
DURHAM OBSERVATORY
BRANCEPETH
CROOK
R. WEAR
BISHOP AUCKLAND
ST. HELEN AUCKLAND
WEST AUCKLAND
STAINDROP
BARNARD CASTLE
DARLINGTON
R. TEES
NEWBIGGIN
HIGH FORCE
MIDDLETON
GREAT DUN FELL
R. EDEN
STAINMORE
1000
2000
400
0 5 10 15 20
MILES
0-1000
1000-2000
> 2000 FEET
ROUTE

FIG. 2.1

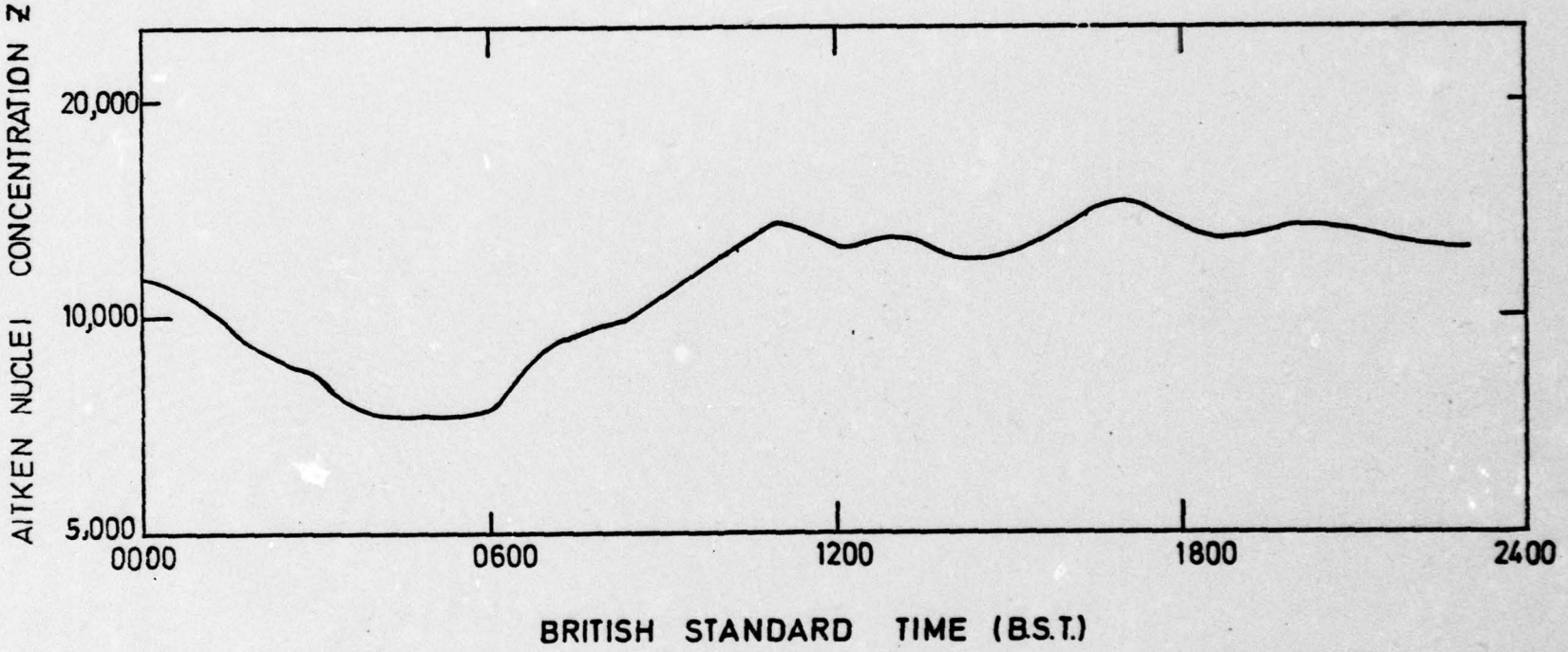
AITKEN NUCLEI CONCENTRATION N
20,000
10,000
5,000
0000
0600
1200
1800
2400
BRITISH STANDARD TIME (B.S.T.)

FIG. 22

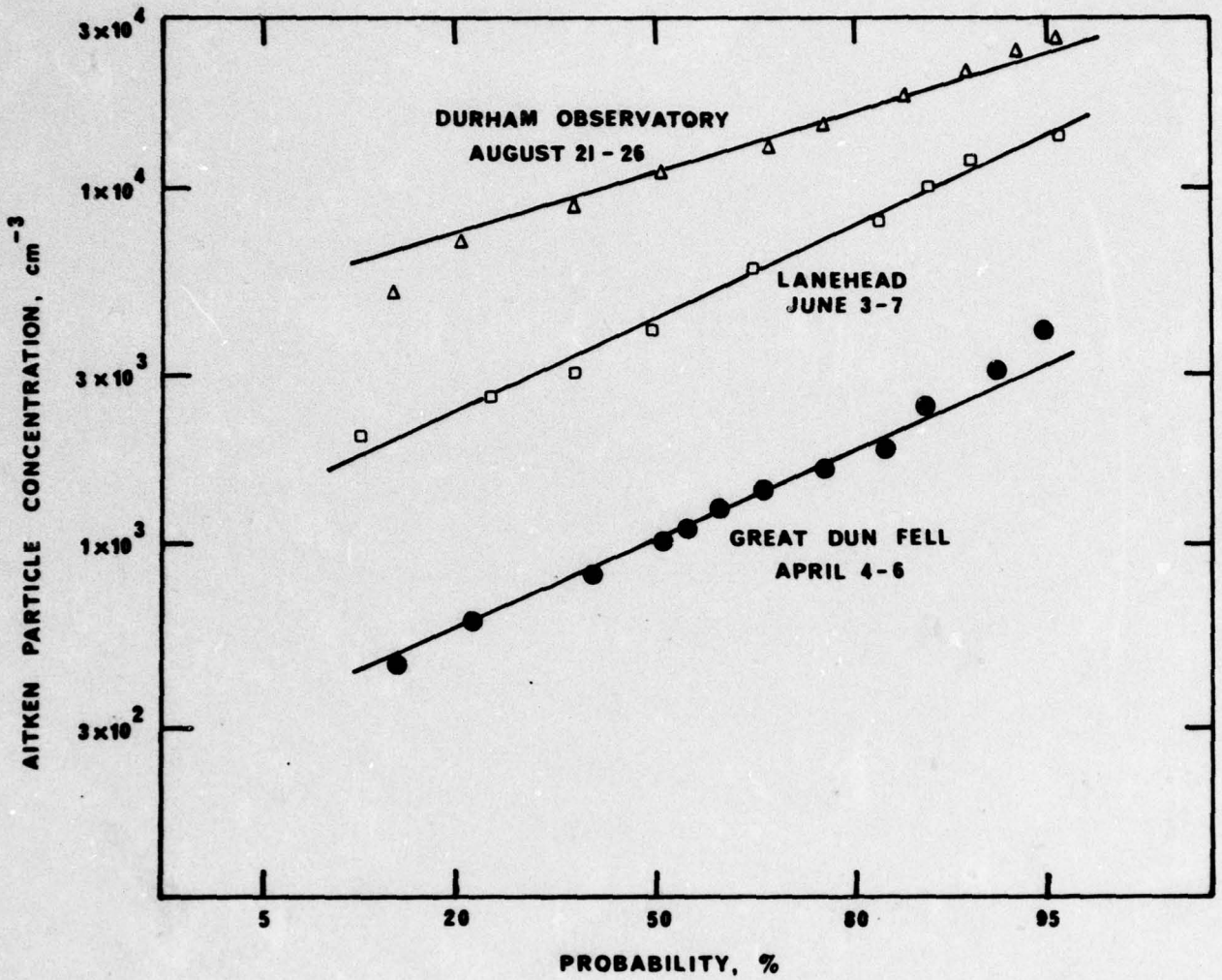
3×10^4
1×10^4
3×10^3
1×10^3
3×10^2
AITKEN PARTICLE CONCENTRATION, cm^-3
DURHAM OBSERVATORY
AUGUST 21 - 26
LANEHEAD
JUNE 3-7
GREAT DUN FELL
APRIL 4-6
5
20
50
80
95
PROBABILITY, %

FIGURE 2.3

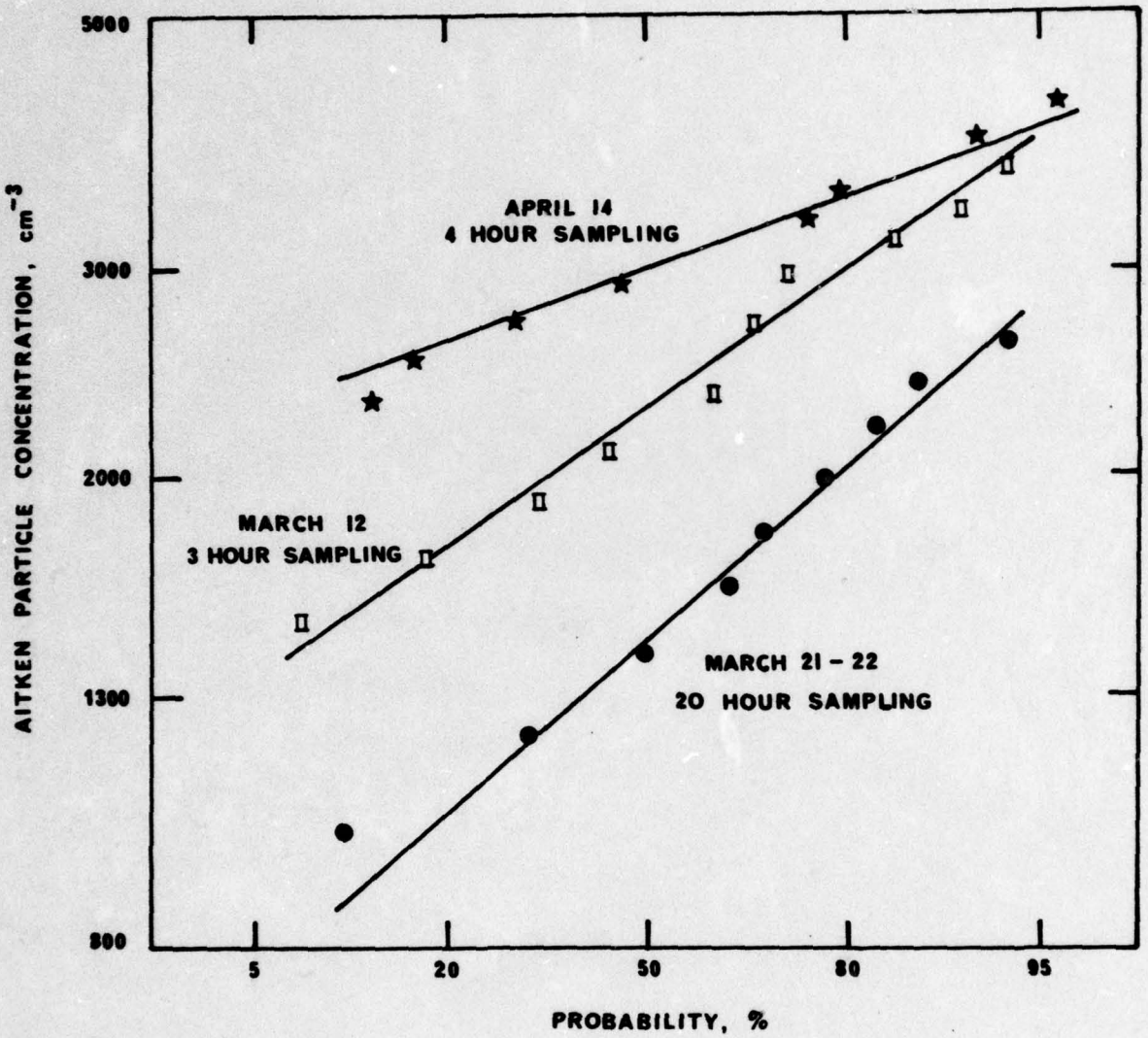
5000
3000
2000
1300
800
AITKEN PARTICLE CONCENTRATION, cm⁻³
APRIL 14
4 HOUR SAMPLING
MARCH 12
3 HOUR SAMPLING
MARCH 21 - 22
20 HOUR SAMPLING
5
20
50
80
95
PROBABILITY, %

FIGURE 2.4

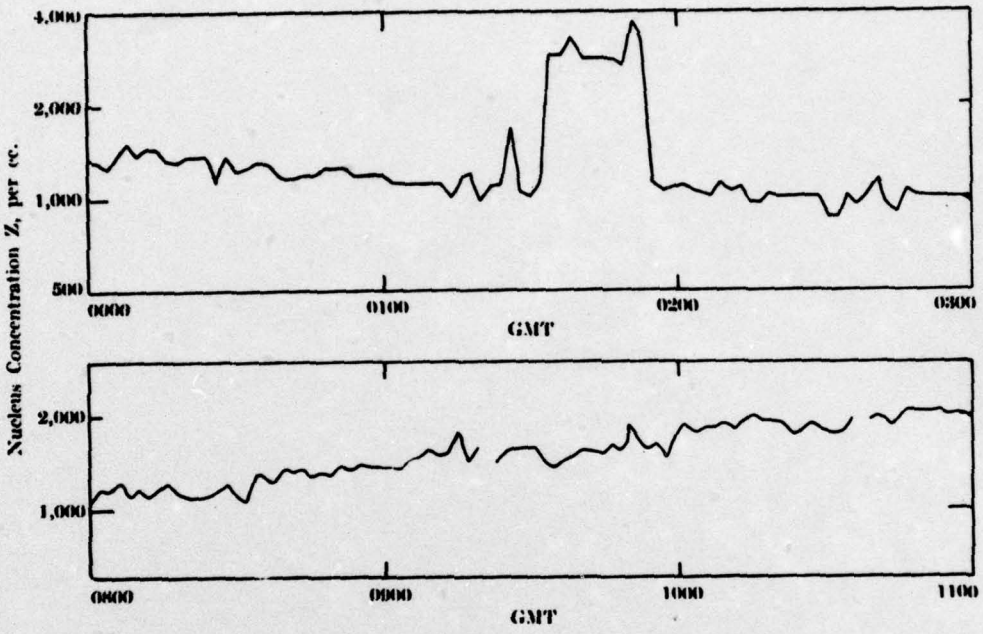

Short term fluctuations in the nucleus concentration.
Upper curve: 0000 — 0300 GMT
Lower Curve: 0800 — 1100 GMT

FIG. 2.5

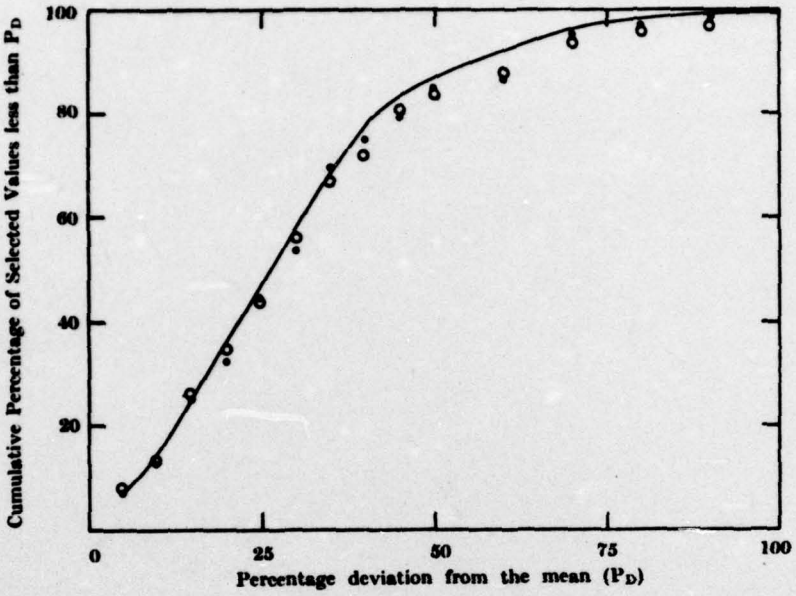

A cumulative percentage plot of observations of nuclei concentrations less than selected values of the percentage deviation from the arithmetic mean.

Solid line : measurements for a 2 minute sampling interval.
○ : measurements for a 10 minute sampling interval.
● : measurements for a 20 minute sampling interval.

FIG. 2.6

DURHAM OBSERVATORY, MARKED X, IN RELATION TO MAJOR INDUSTRIAL SITES AND TOWNS

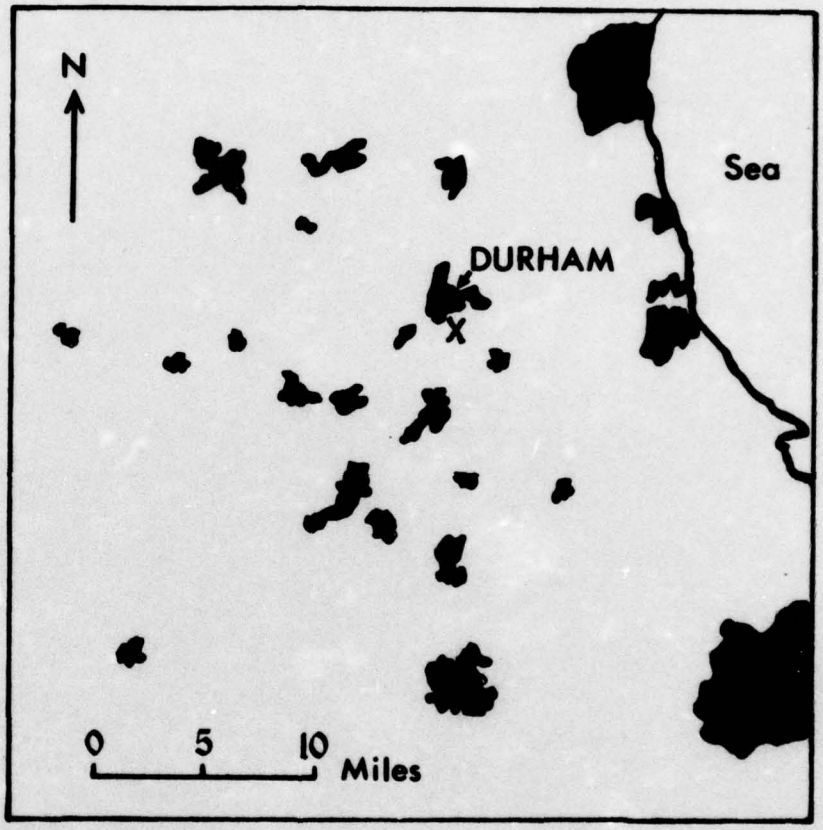

FIGURE 2.7

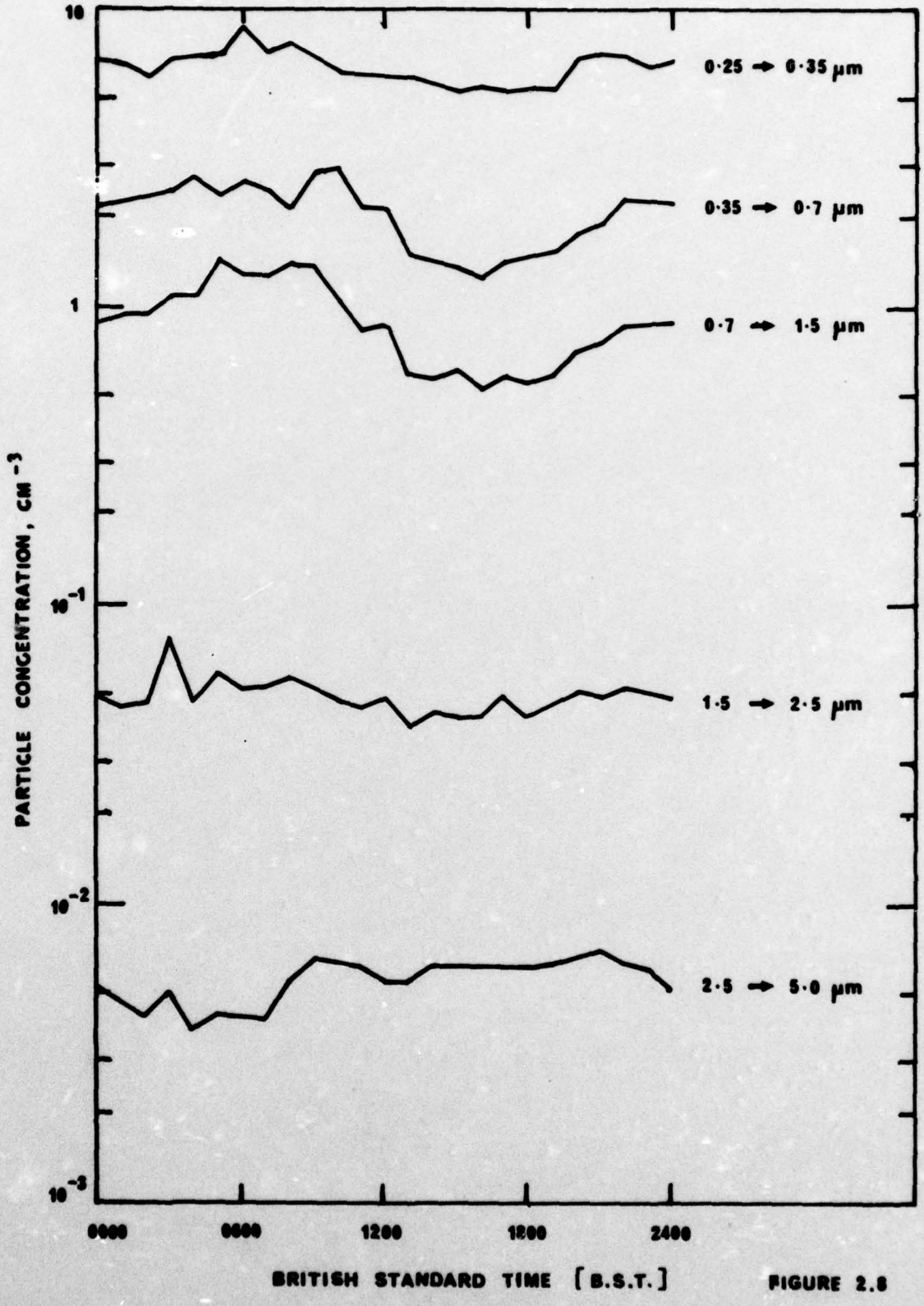
10
1
10^{-1}
10^{-2}
10^{-3}
PARTICLE CONCENTRATION, CM^{-3}
0·25 → 0·35 μm
0·35 → 0·7 μm
0·7 → 1·5 μm
1·5 → 2·5 μm
2·5 → 5·0 μm
0000
0600
1200
1800
2400
BRITISH STANDARD TIME [B.S.T.]

FIGURE 2.8

FIGURE 2.9

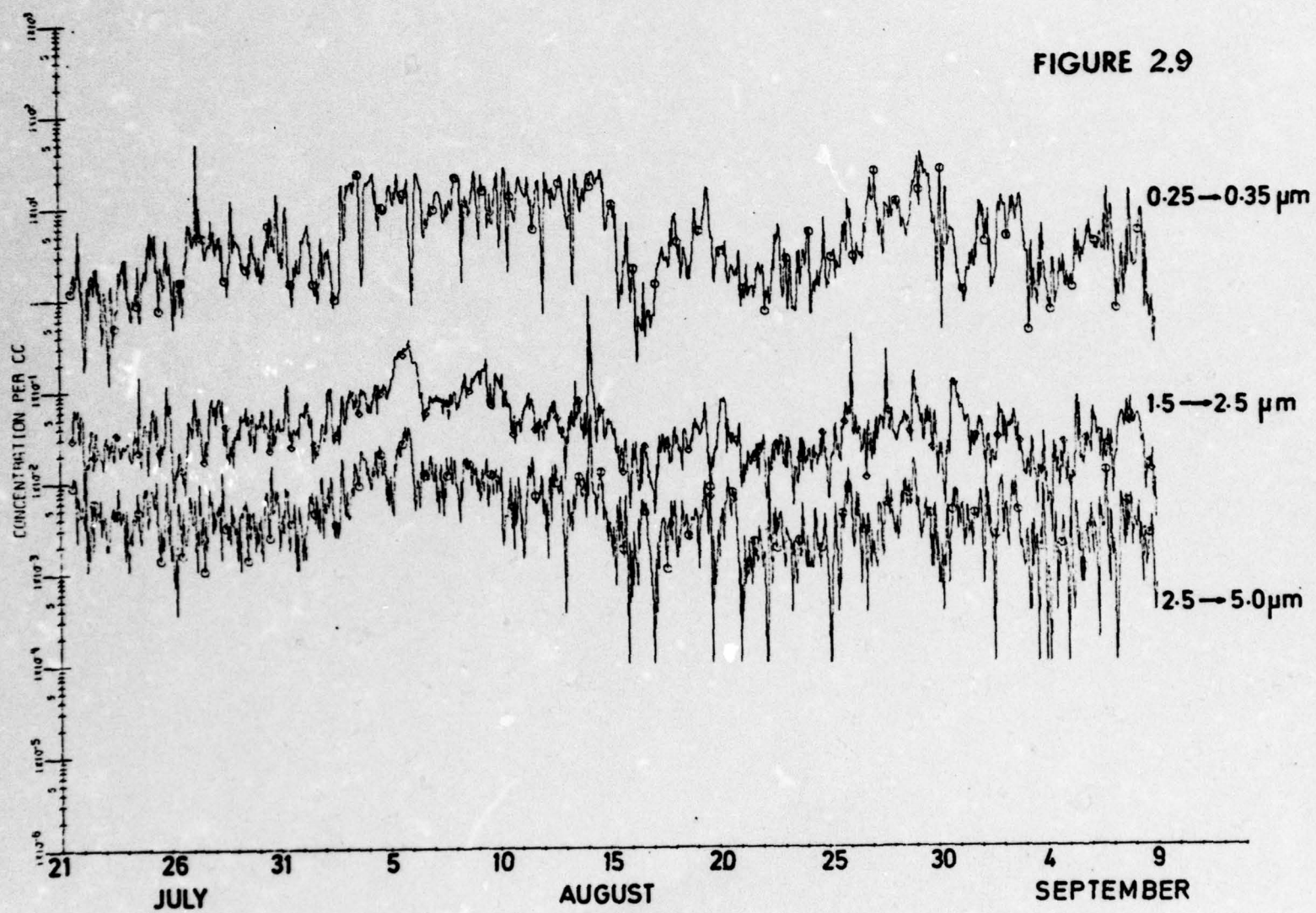
CONCENTRATION PER CC
0·25—0·35 μm
1·5—2·5 μm
2·5—5·0μm
21
26
31
5
10
15
20
25
30
4
9
JULY
AUGUST
SEPTEMBER

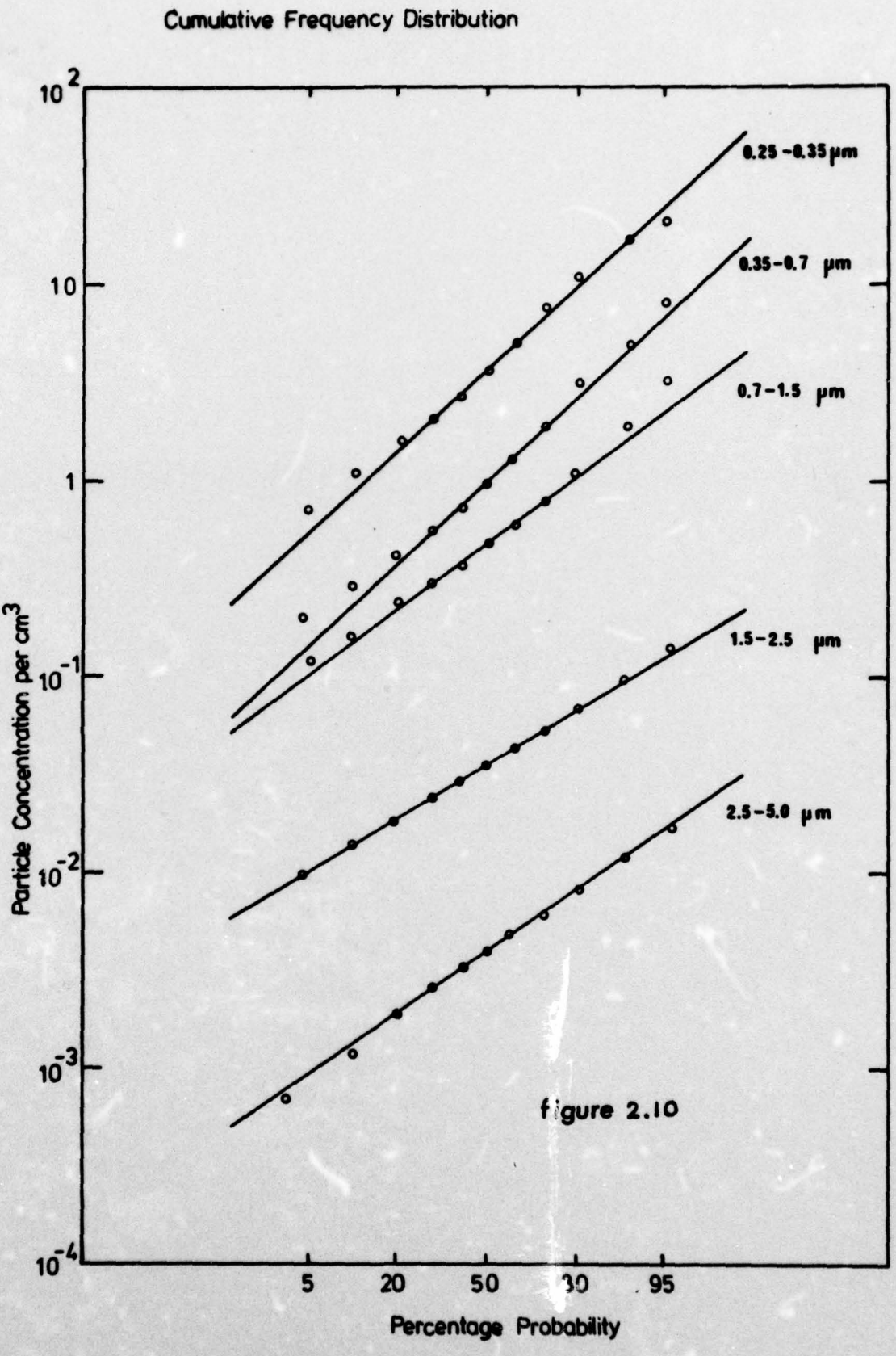
Cumulative Frequency Distribution
10^2
10
1
10^{-1}
10^{-2}
10^{-3}
10^{-4}
Particle Concentration per cm^3
0.25 - 0.35 μm
0.35 - 0.7 μm
0.7 - 1.5 μm
1.5 - 2.5 μm
2.5 - 5.0 μm
5
20
50
80
95
Percentage Probability

figure 2.10

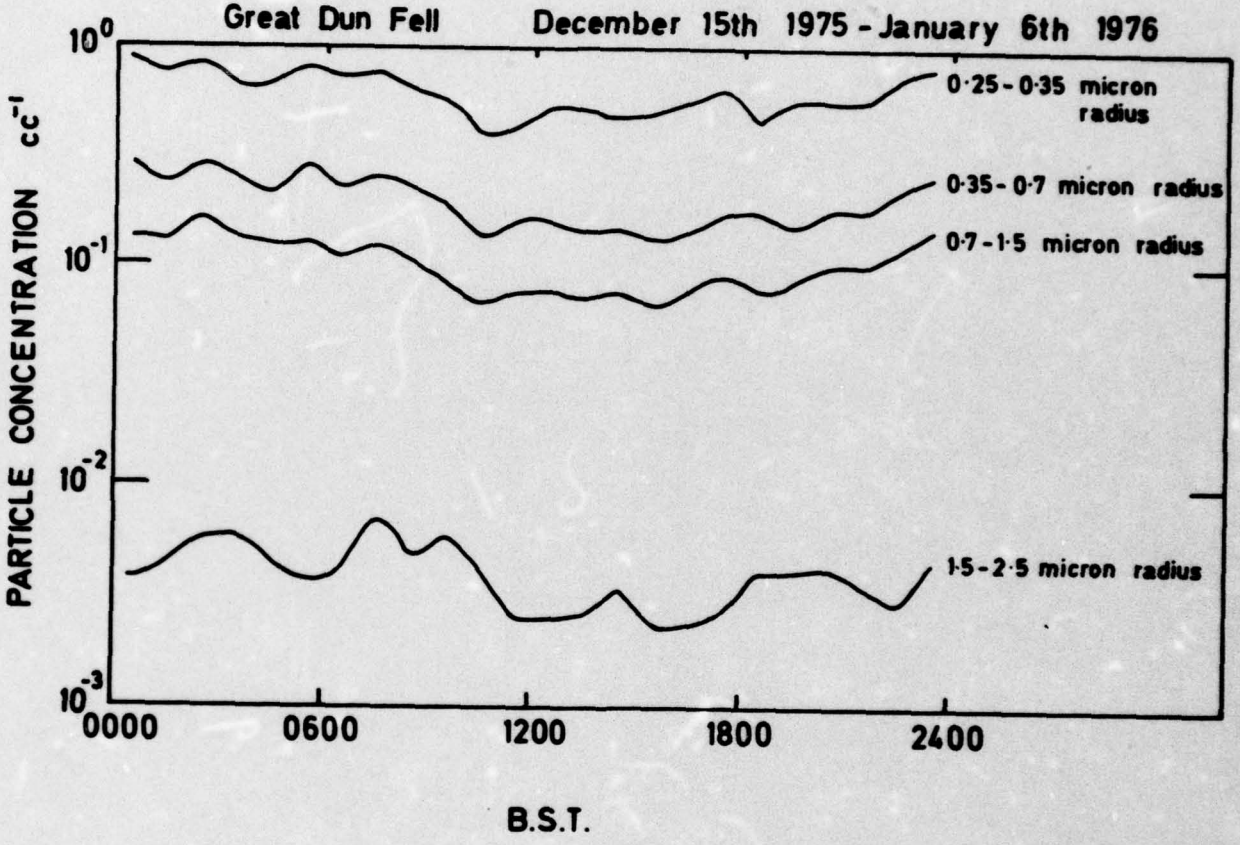
Great Dun Fell
December 15th 1975 - January 6th 1976
PARTICLE CONCENTRATION cc⁻¹
10⁰
10⁻¹
10⁻²
10⁻³
0·25 - 0·35 micron radius
0·35 - 0·7 micron radius
0·7 - 1·5 micron radius
1·5 - 2·5 micron radius
0000
0600
1200
1800
2400
B.S.T.

FIGURE 2.11

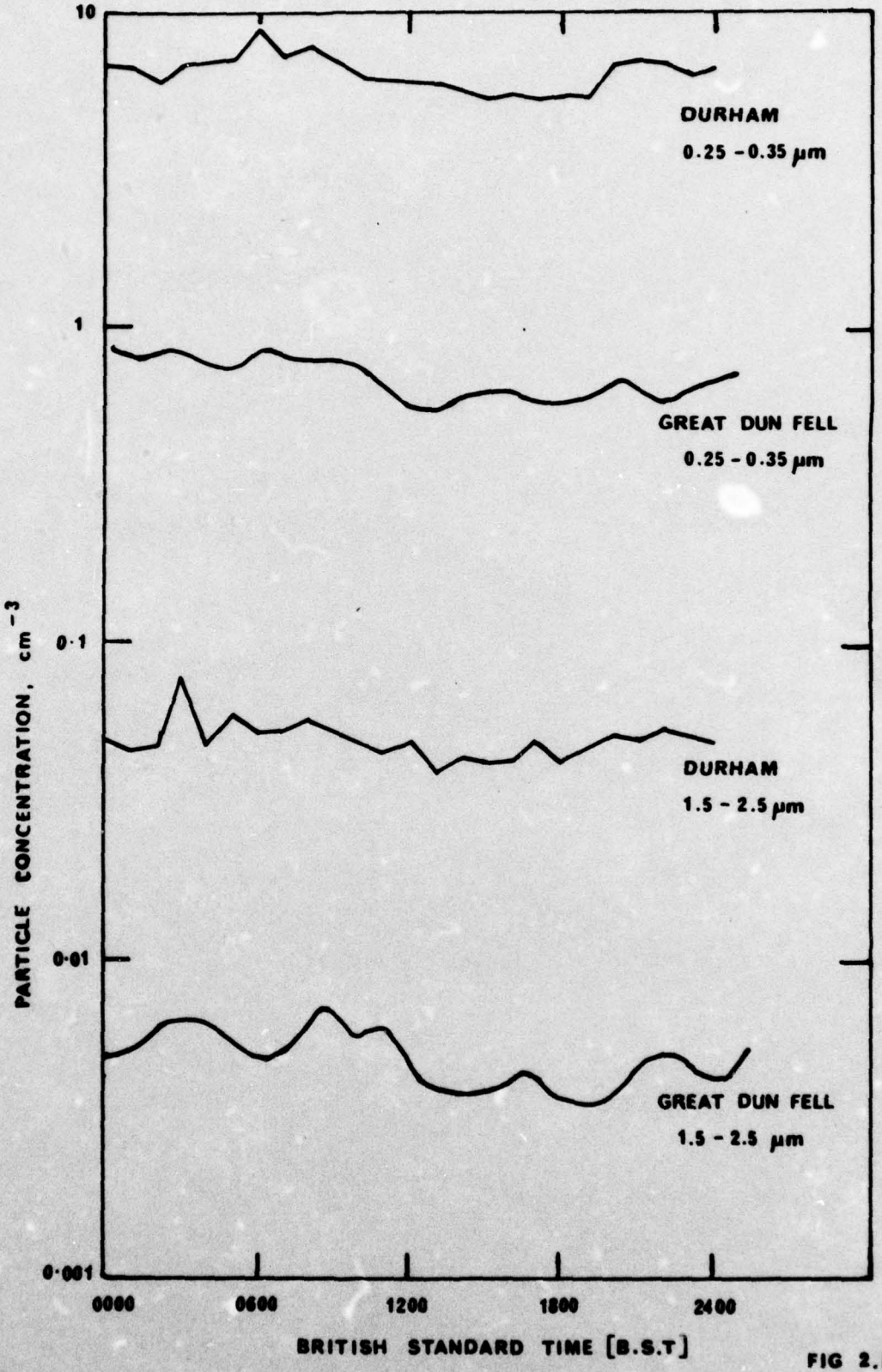
10
1
0·1
0·01
0·001
PARTICLE CONCENTRATION, cm⁻³
DURHAM
0.25 - 0.35 μm
GREAT DUN FELL
0.25 - 0.35 μm
DURHAM
1.5 - 2.5 μm
GREAT DUN FELL
1.5 - 2.5 μm
0000
0600
1200
1800
2400
BRITISH STANDARD TIME [B.S.T]

FIG 2.12

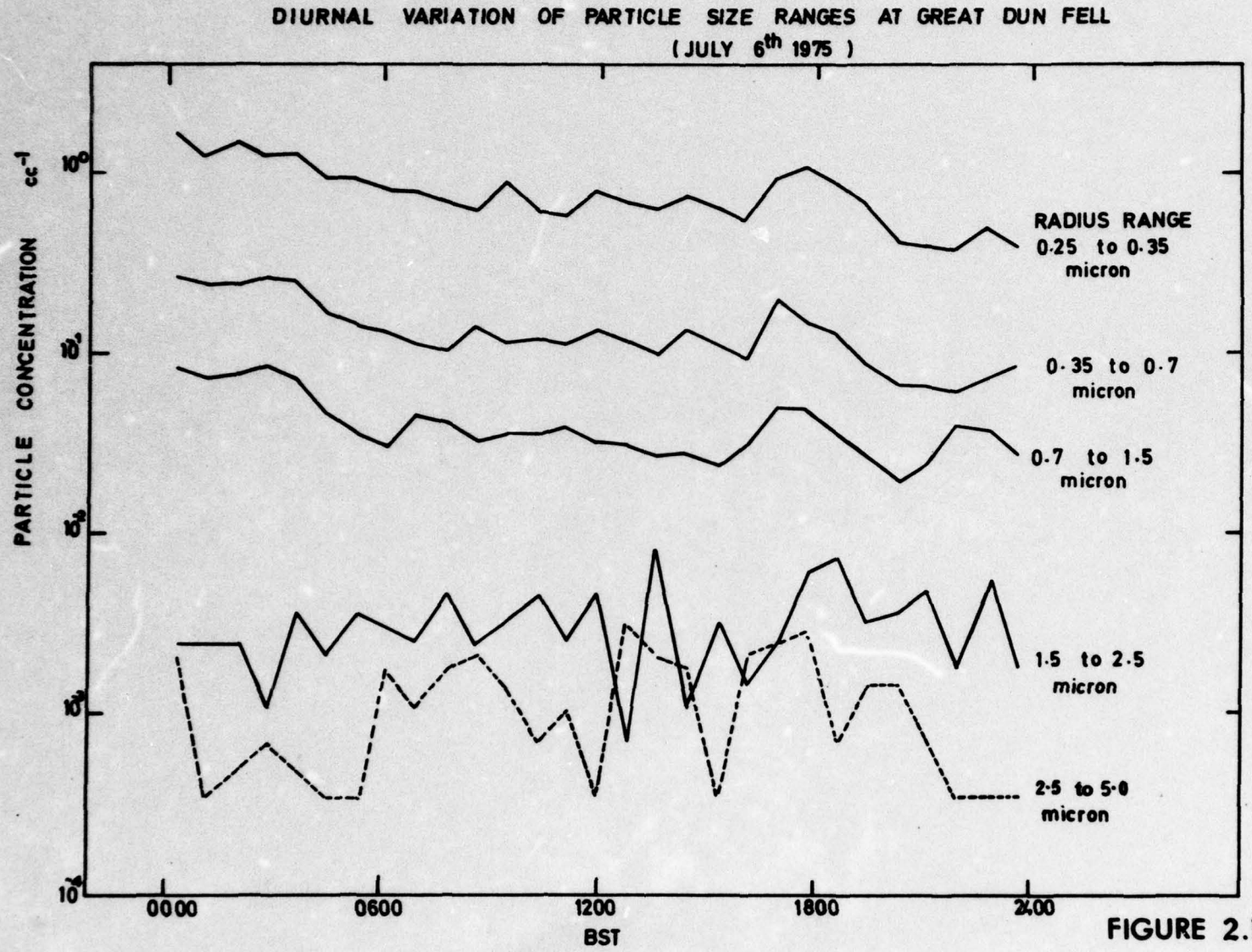
DIURNAL VARIATION OF PARTICLE SIZE RANGES AT GREAT DUN FELL
(JULY 6th 1975)
PARTICLE CONCENTRATION cc-1
RADIUS RANGE
0·25 to 0·35 micron
0·35 to 0·7 micron
0·7 to 1·5 micron
1·5 to 2·5 micron
2·5 to 5·0 micron
0000
0600
1200
1800
2400
BST

FIGURE 2.13

FIG. 2.14

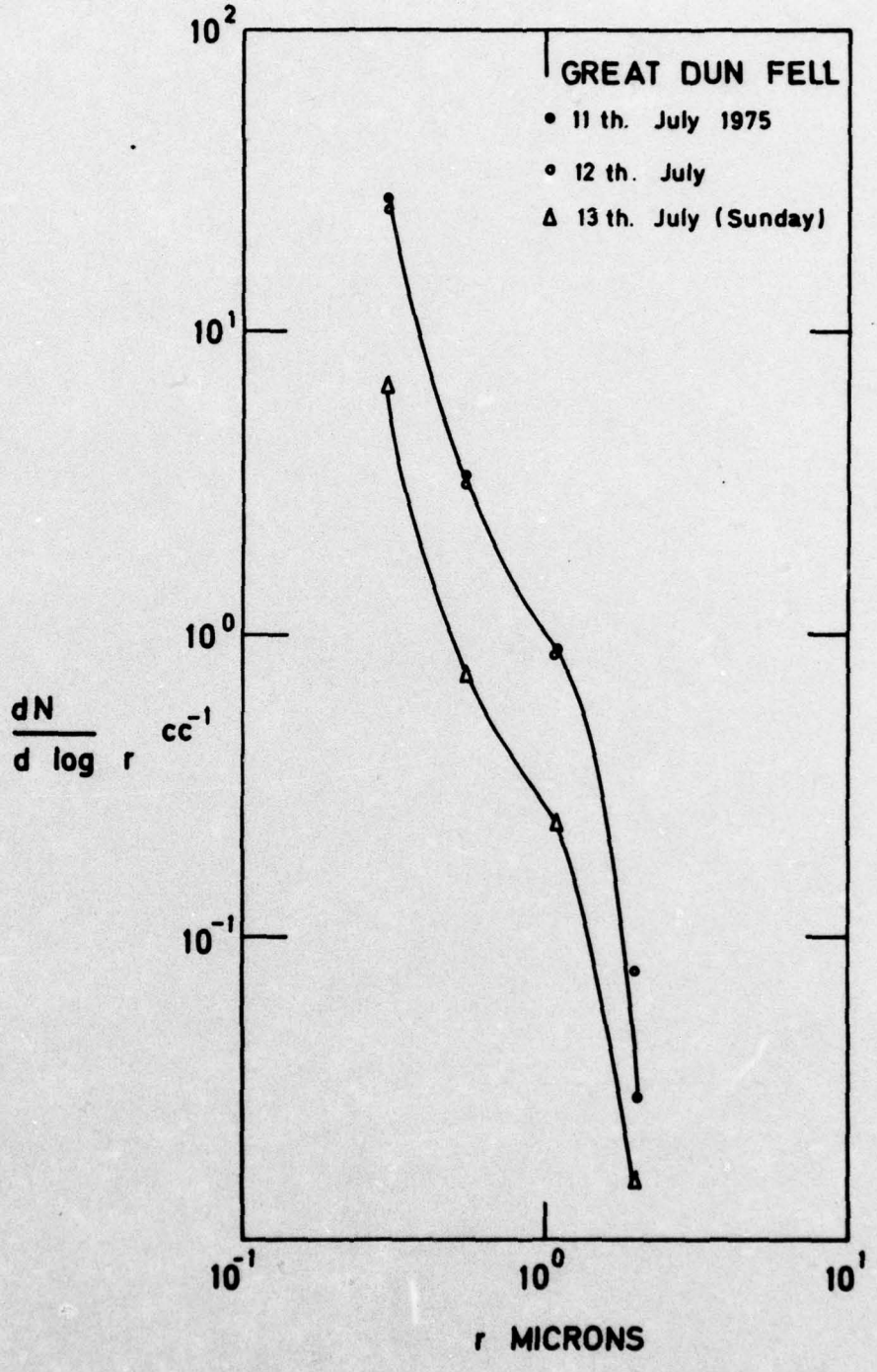
GREAT DUN FELL
• 11 th. July 1975
○ 12 th. July
Δ 13 th. July (Sunday)
10^2
10^1
10^0
10^{-1}
$\frac{dN}{d \log r}$ cc^{-1}
10^{-1}
10^0
10^1
r MICRONS

DURHAM OBSERVATORY. MEAN VALUES OVER 25 DAYS. (21st. JULY — 13th. AUGUST) 1975.

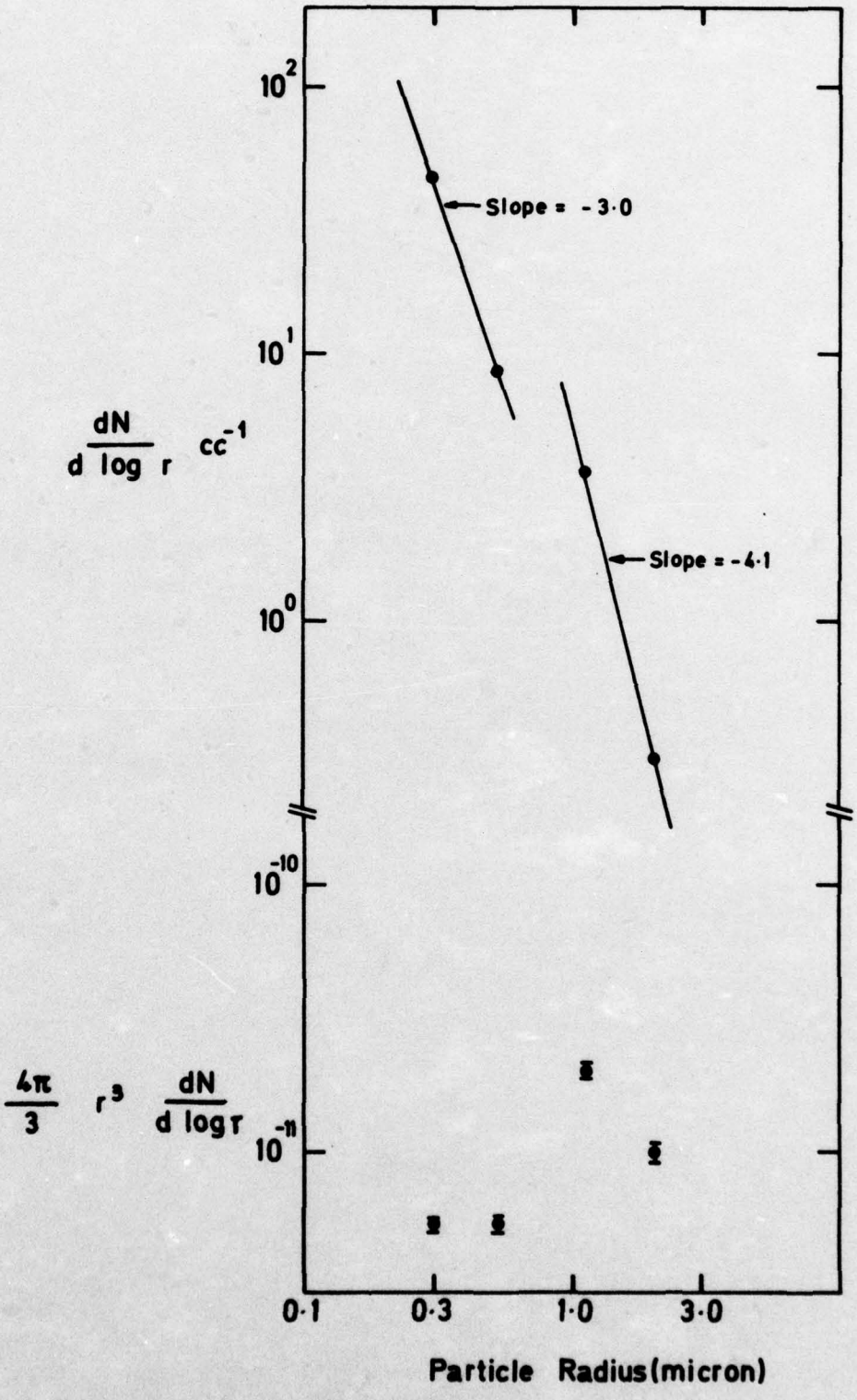

FIG. 2.15

FIG. 2.16

MEAN VALUES OF dN/d log r OVER PERIOD 11 th. MAY – 26 th. MAY 1975 INCLUSIVE, AT PHYSICS DEPARTMENT SITE.

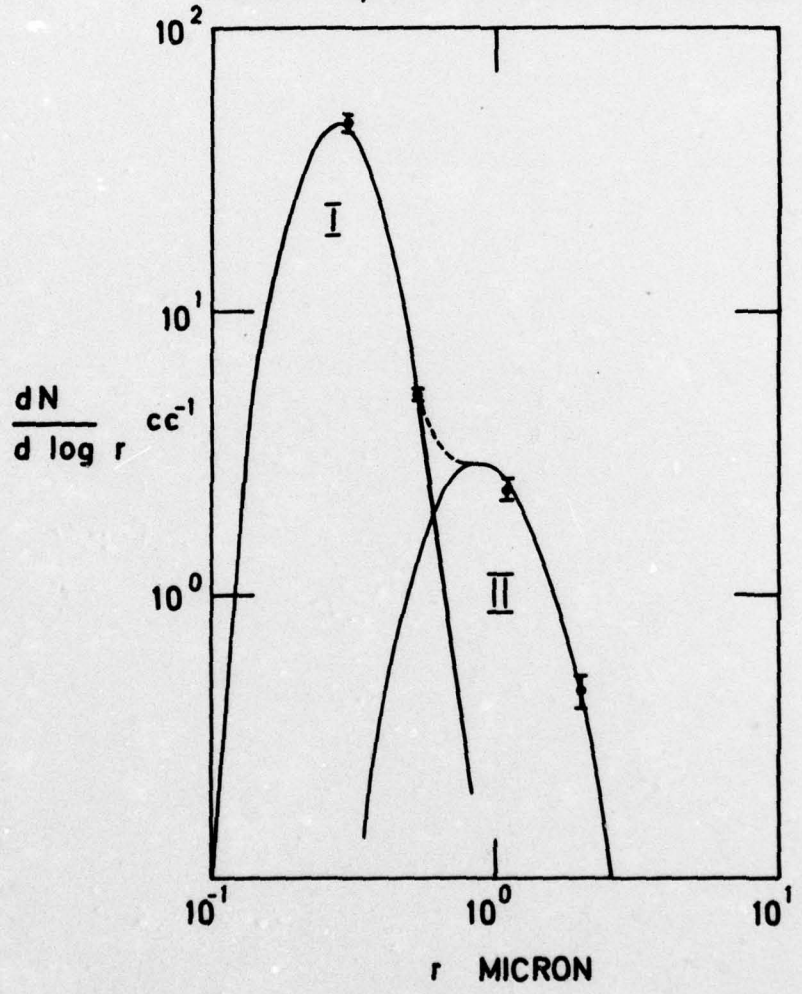

I $\bar{V}g = 1{\cdot}35$, $r_m = 0{\cdot}28$ micron, N cc^{-1} (corrected) = 5·92

II $\bar{V}g = 1{\cdot}5$, $r_m = 0{\cdot}88$ micron, N cc^{-1} (corrected) = 1·23

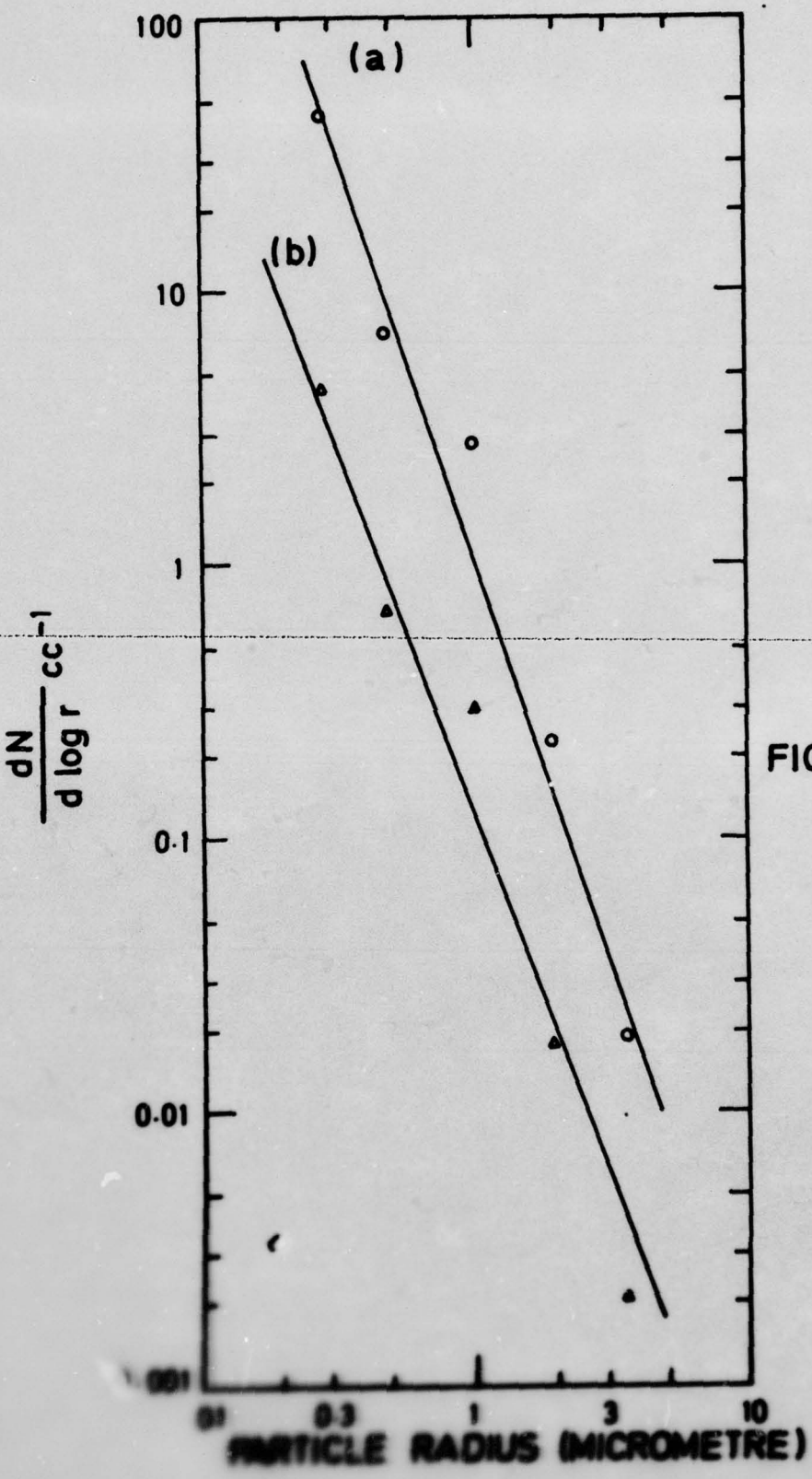
100
10
1
0·1
0·01
(a)
(b)
$\frac{dN}{d \log r}$ cc^{-1}
0·3
1
3
10
PARTICLE RADIUS (MICROMETRE)

FIG. 2.17

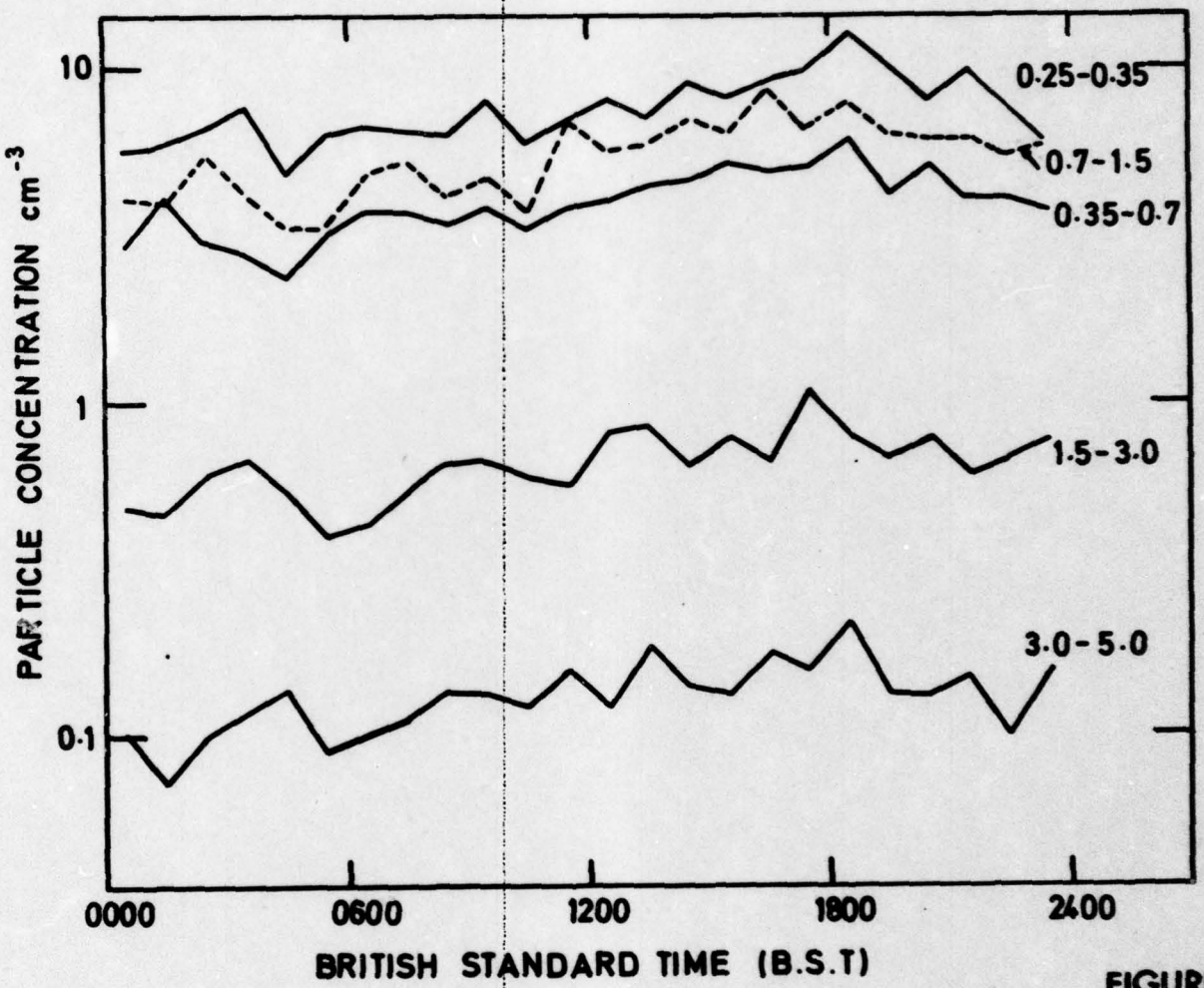
10
1
0·1
PARTICLE CONCENTRATION cm⁻³
0·25-0·35
0·7-1·5
0·35-0·7
1·5-3·0
3·0-5·0
0000
0600
1200
1800
2400
BRITISH STANDARD TIME (B.S.T)

FIGURE 2.18

FIGURE 2.19

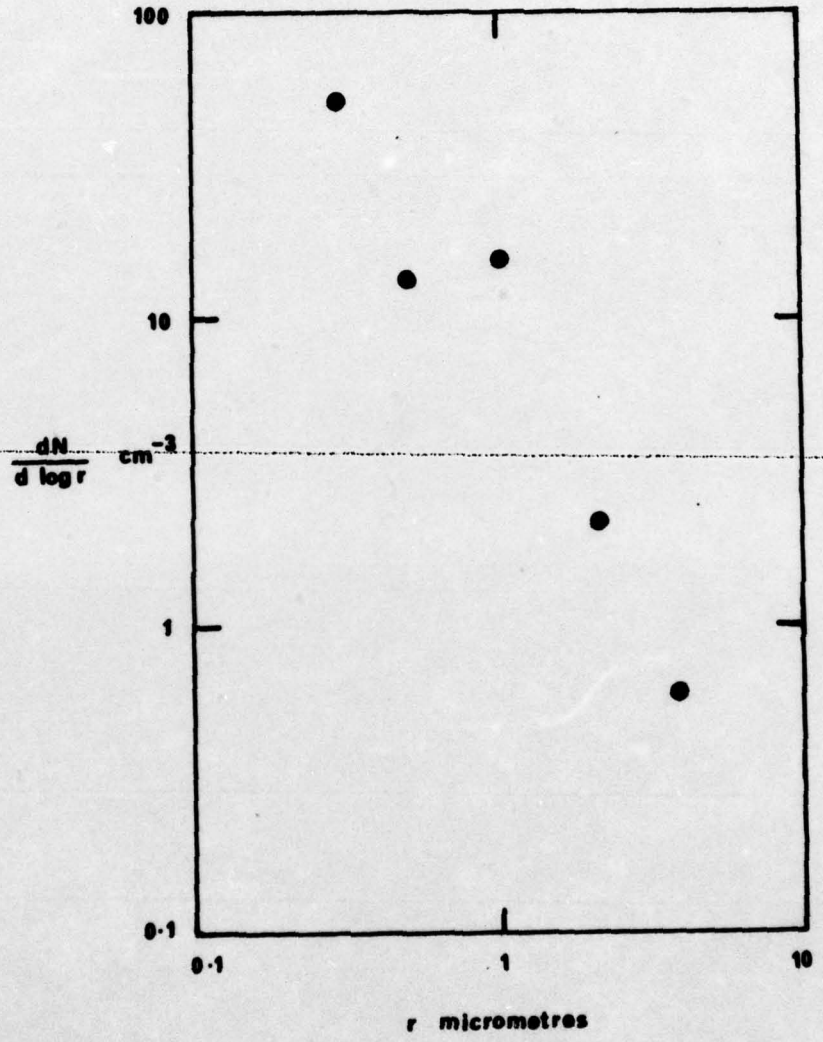

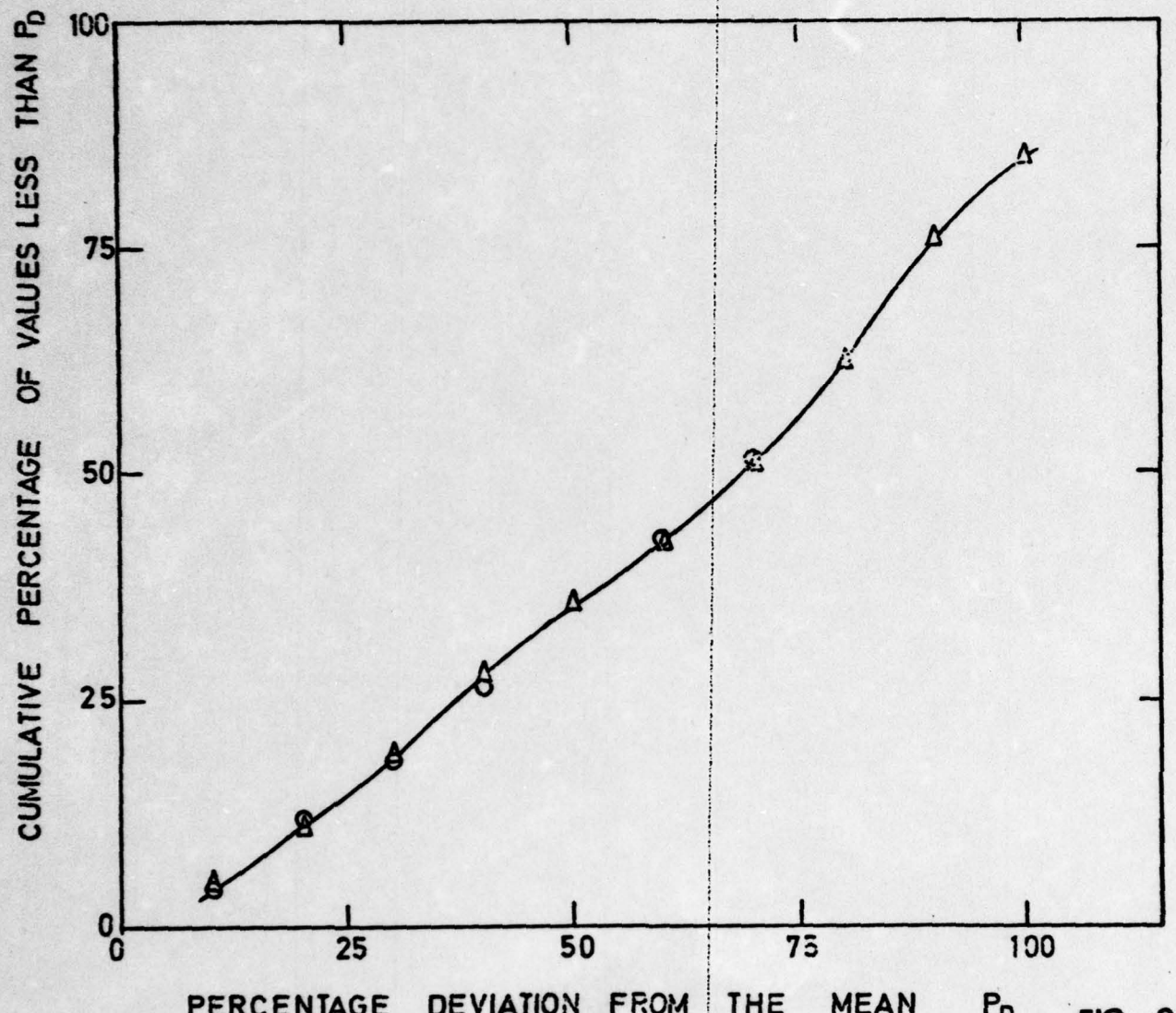
CUMULATIVE PERCENTAGE OF VALUES LESS THAN P_D
100
75
50
25
0
0
25
50
75
100
PERCENTAGE DEVIATION FROM THE MEAN P_D

FIG. 2.20

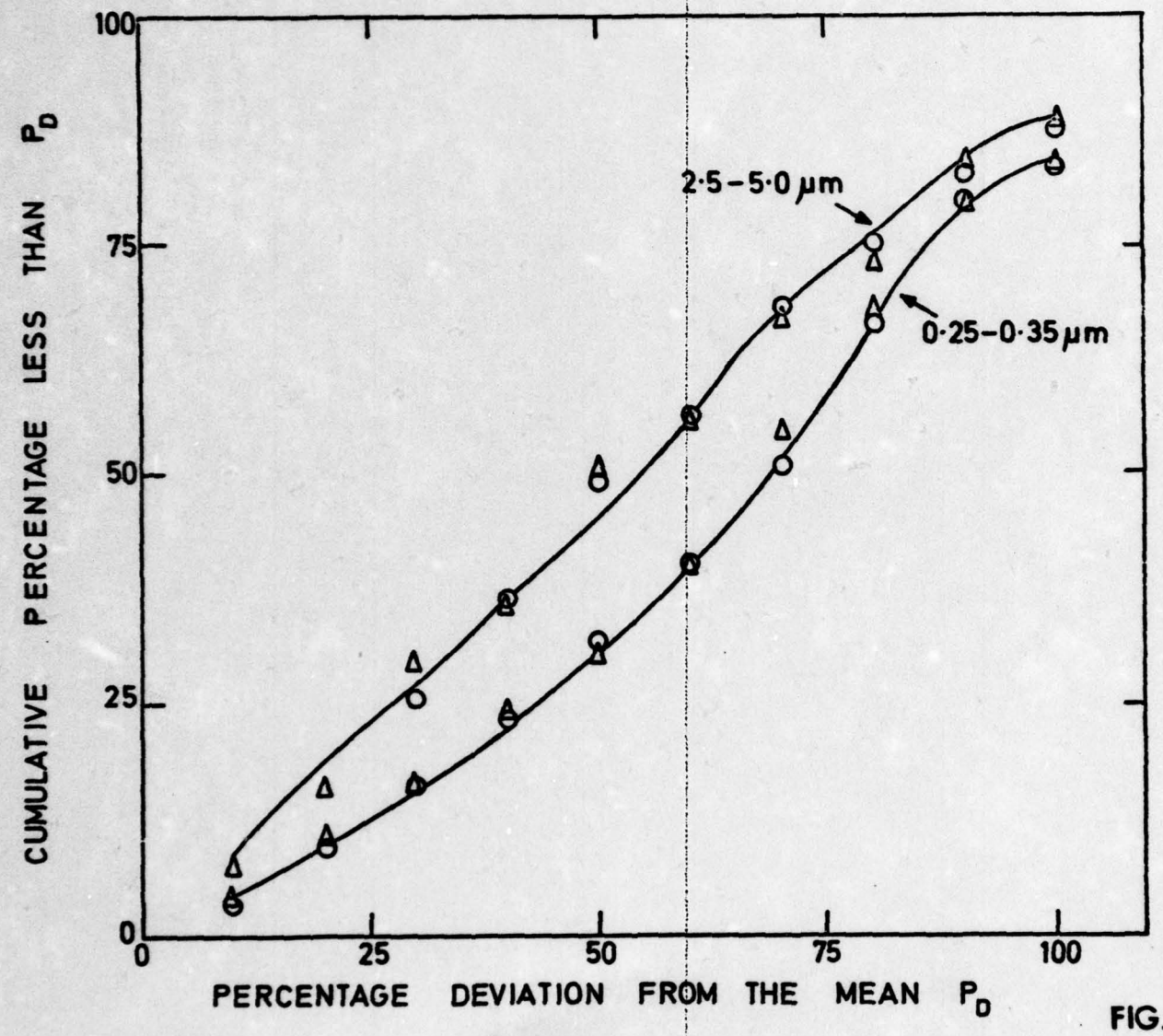
100
75
50
25
0
0
25
50
75
100
CUMULATIVE PERCENTAGE LESS THAN P_D
PERCENTAGE DEVIATION FROM THE MEAN P_D
2·5–5·0 μm
0·25–0·35 μm

FIG. 2.21

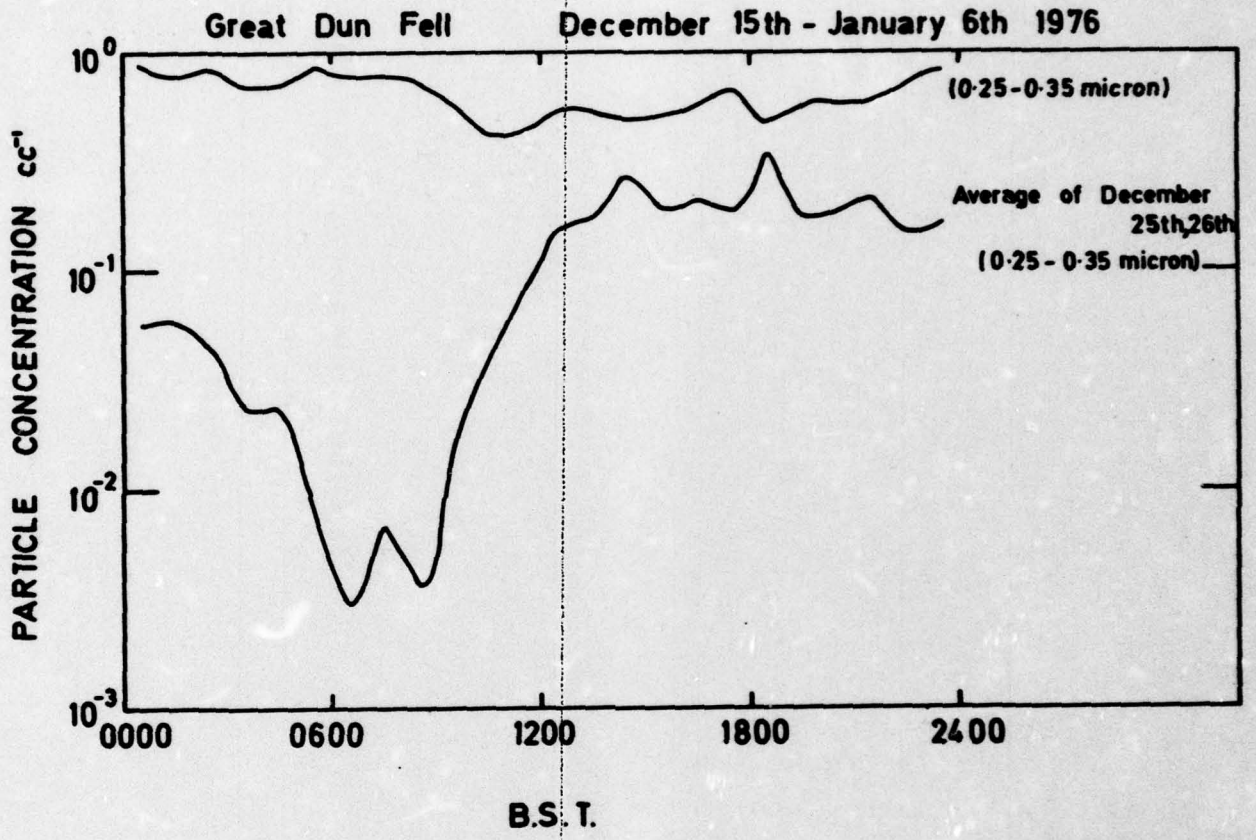
Great Dun Fell
December 15th - January 6th 1976
PARTICLE CONCENTRATION cc⁻¹
10⁰
10⁻¹
10⁻²
10⁻³
(0·25-0·35 micron)
Average of December 25th,26th
(0·25-0·35 micron)
0000
0600
1200
1800
2400
B.S.T.

FIGURE 2.22

WINDSPEED (KNOTS)
0.00
2.00
4.00
6.00
8.00
10.00
12.00
14.00
16.00
18.00
20.00
CONCENTRATION PER CC. (0.5-0.7)

FIG. 2.23

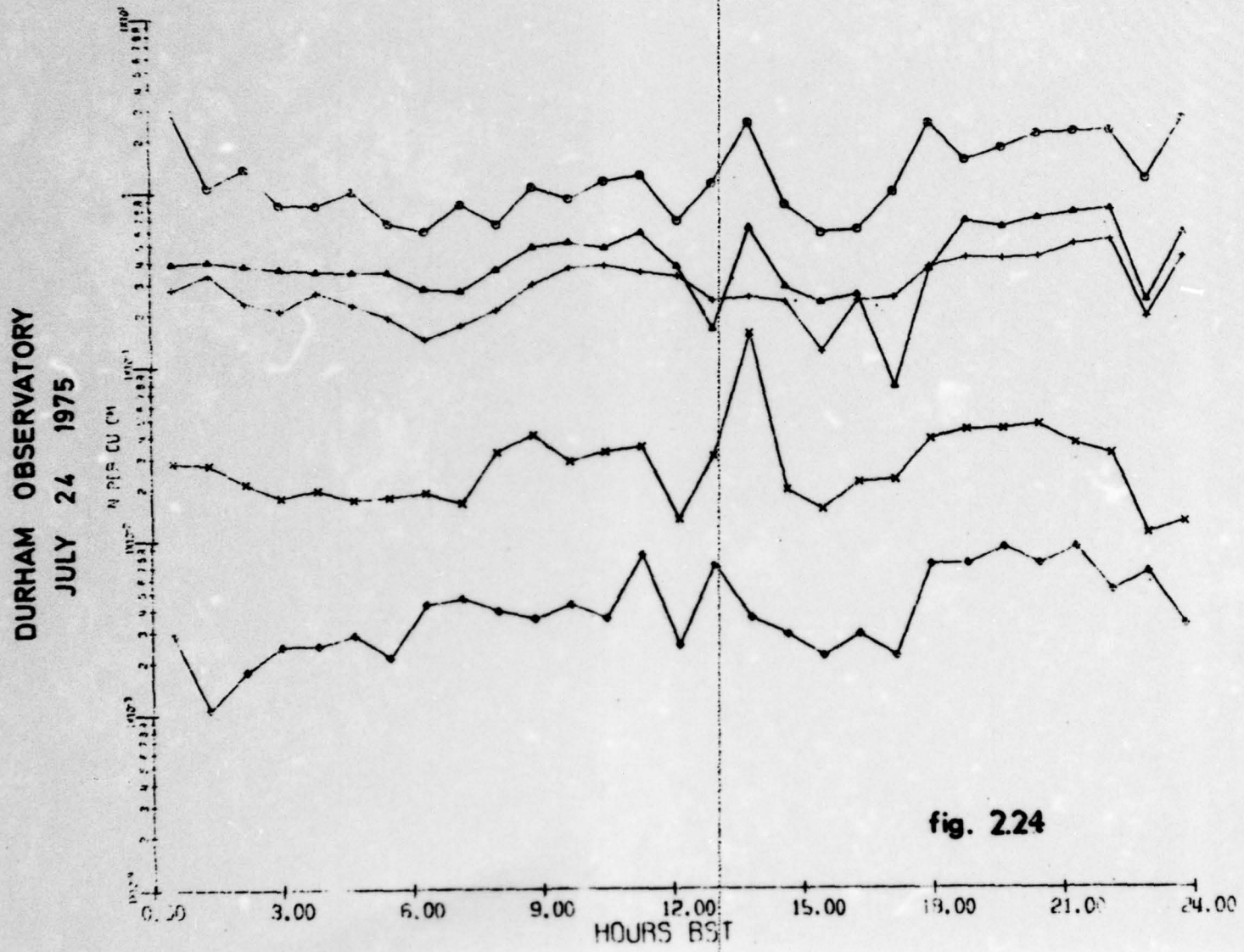
DURHAM OBSERVATORY
JULY 24 1975
3.00
6.00
9.00
12.00
15.00
18.00
21.00
24.00
HOURS BST

fig. 2.24

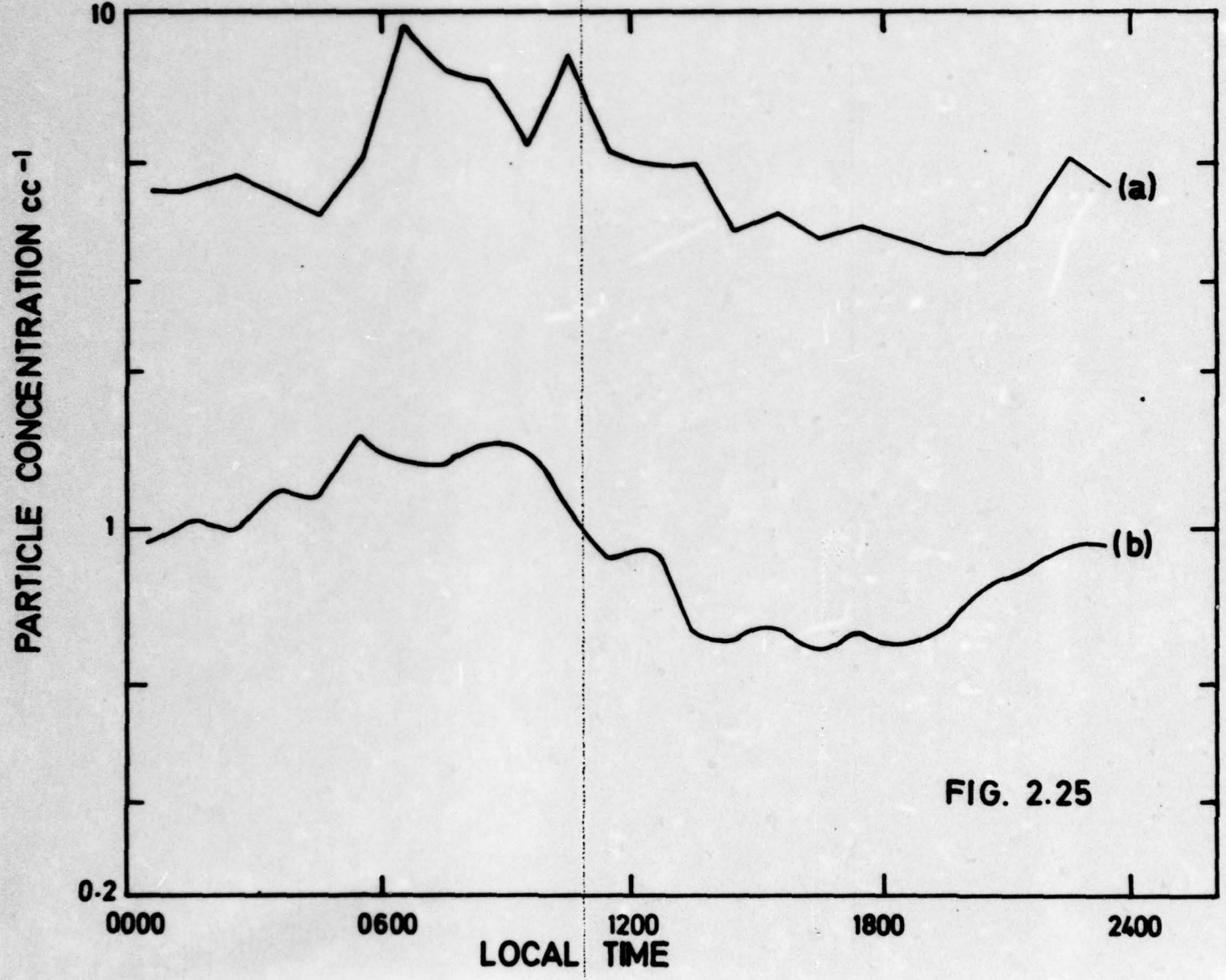
10
1
0·2
PARTICLE CONCENTRATION cc⁻¹
(a)
(b)
0000
0600
1200
1800
2400
LOCAL TIME

FIG. 2.25

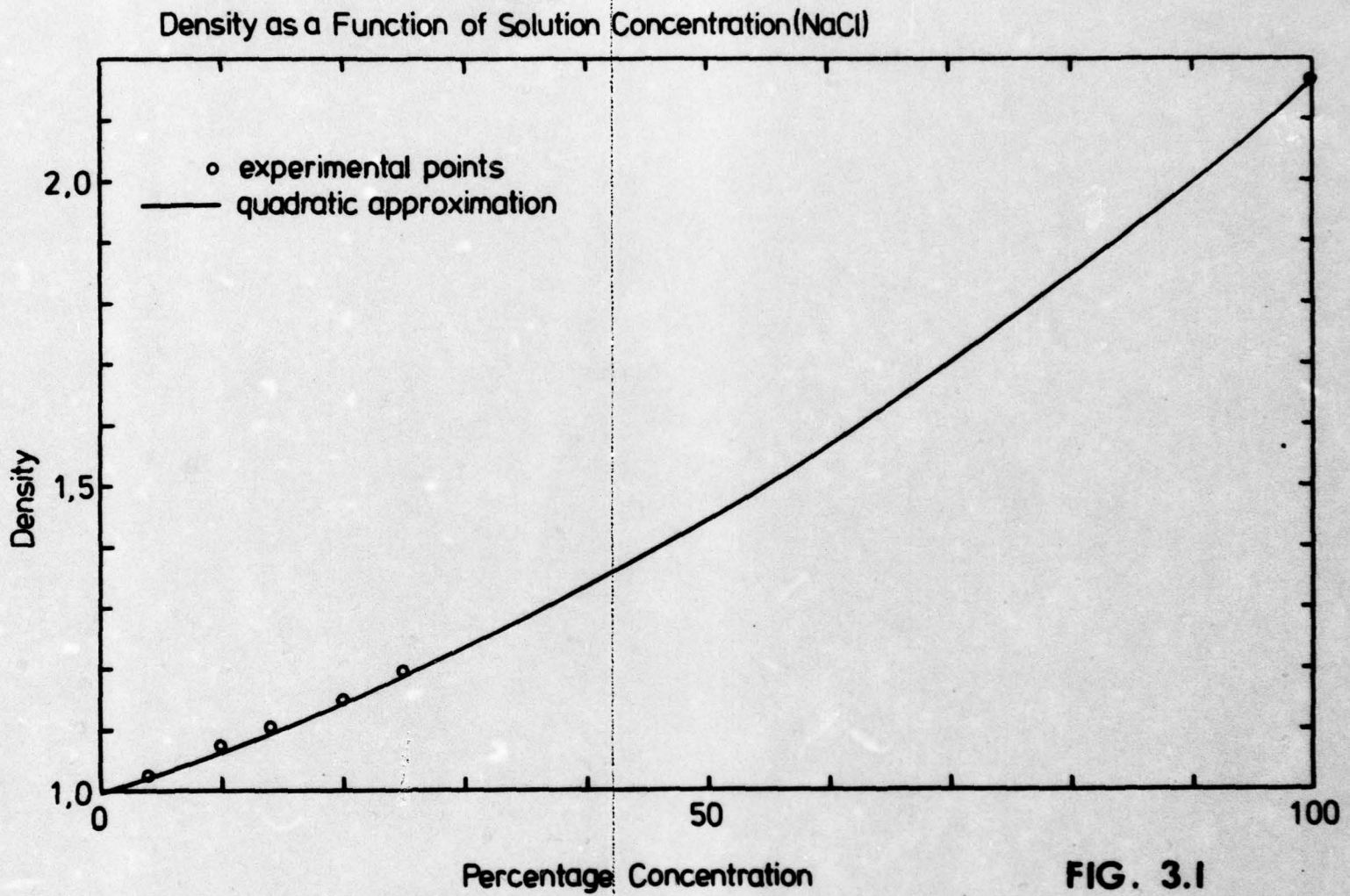
Density as a Function of Solution Concentration (NaCl)
o experimental points
quadratic approximation
2,0
1,5
1,0
Density
0
50
100
Percentage Concentration

FIG. 3.1

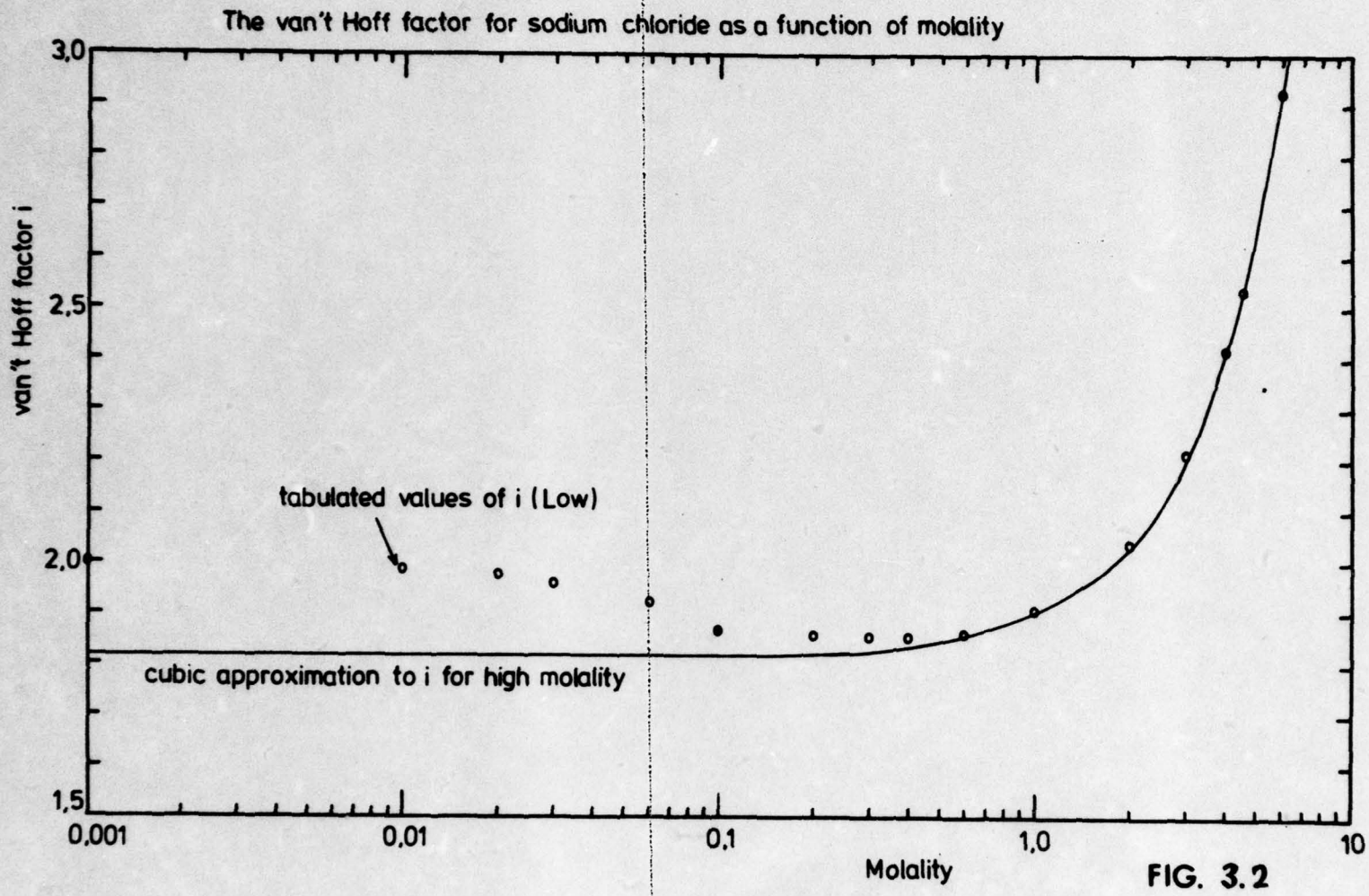
The van't Hoff factor for sodium chloride as a function of molality
van't Hoff factor i
3,0
2,5
2,0
1,5
tabulated values of i (Low)
cubic approximation to i for high molality
0,001
0,01
0,1
1,0
10
Molality

FIG. 3.2

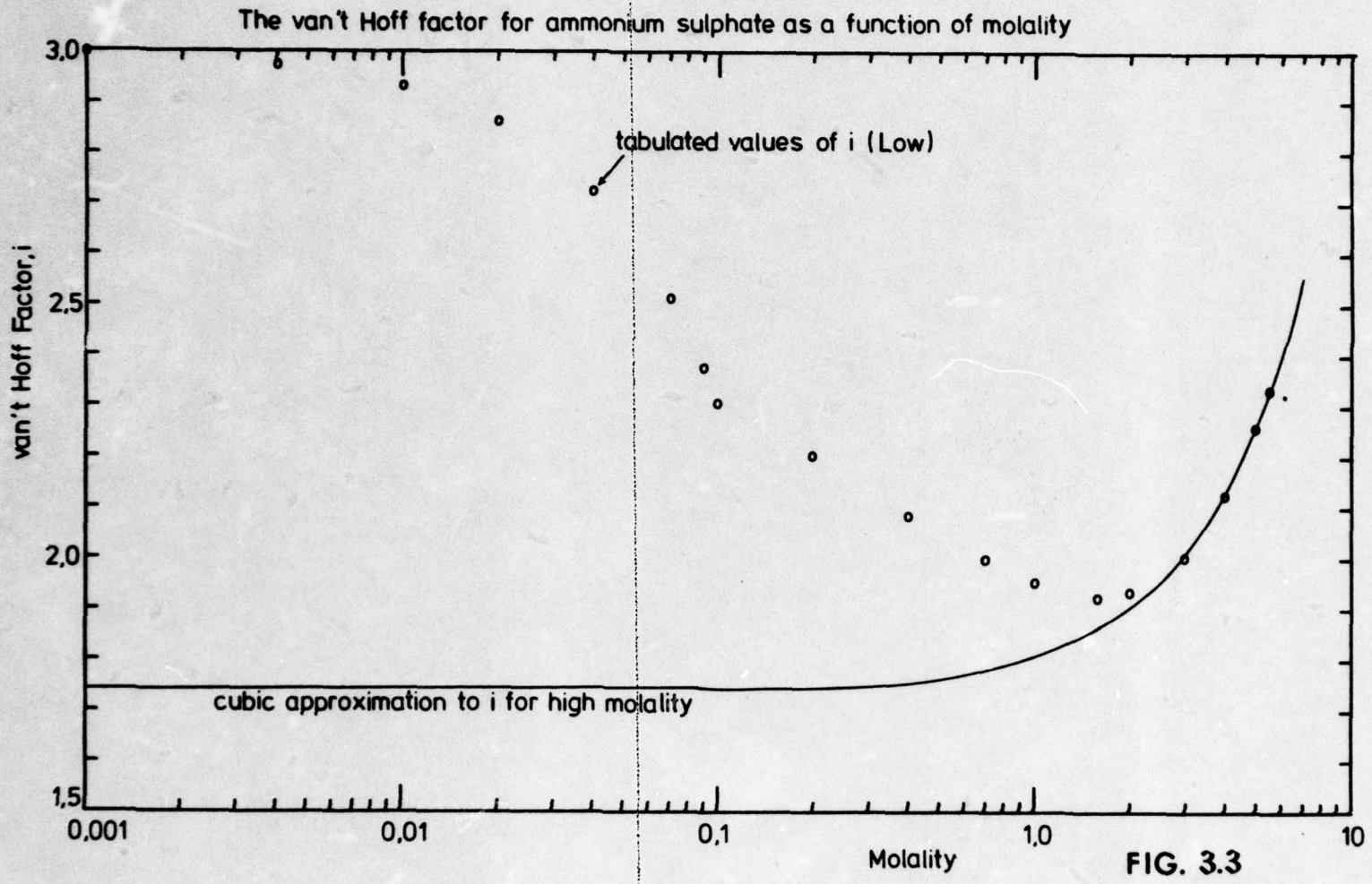
The van't Hoff factor for ammonium sulphate as a function of molality
3,0
2,5
2,0
1,5
van't Hoff Factor, i
tabulated values of i (Low)
cubic approximation to i for high molality
0,001
0,01
0,1
1,0
10
Molality

FIG. 3.3

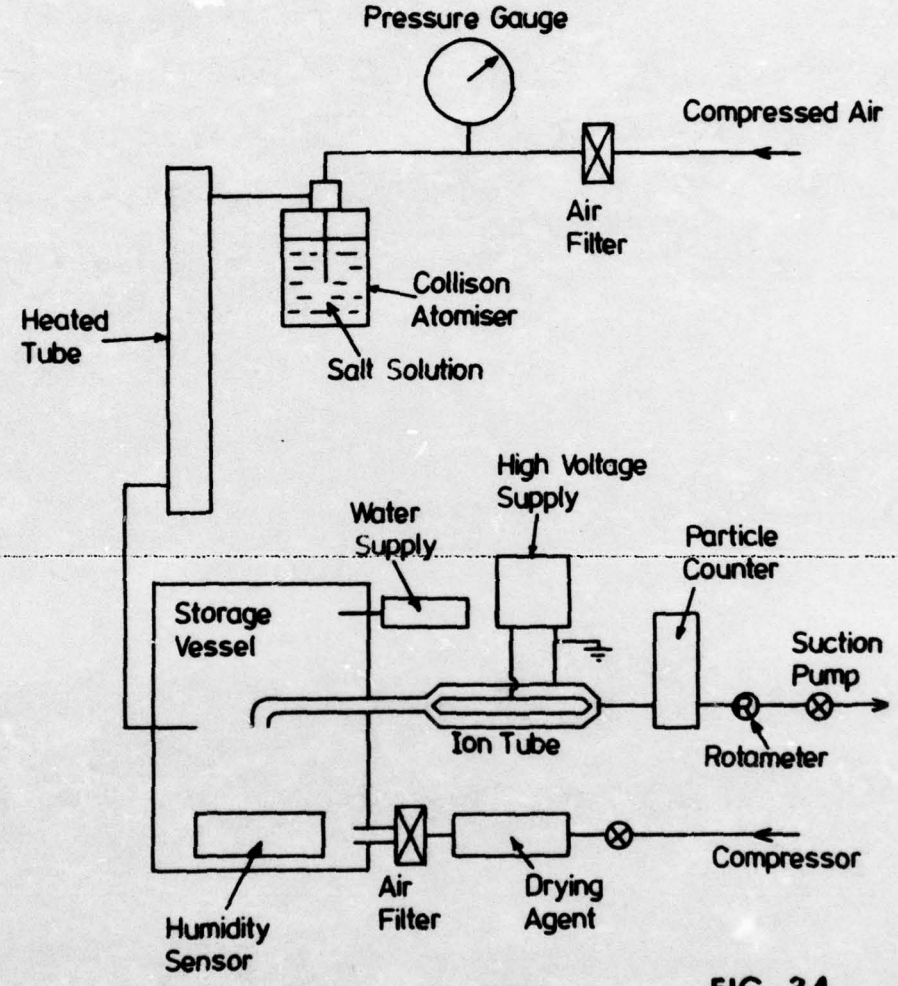
Pressure Gauge
Compressed Air
Air Filter
Collison Atomiser
Heated Tube
Salt Solution
High Voltage Supply
Water Supply
Particle Counter
Storage Vessel
Suction Pump
Ion Tube
Rotameter
Compressor
Air Filter
Drying Agent
Humidity Sensor

FIG. 3.4

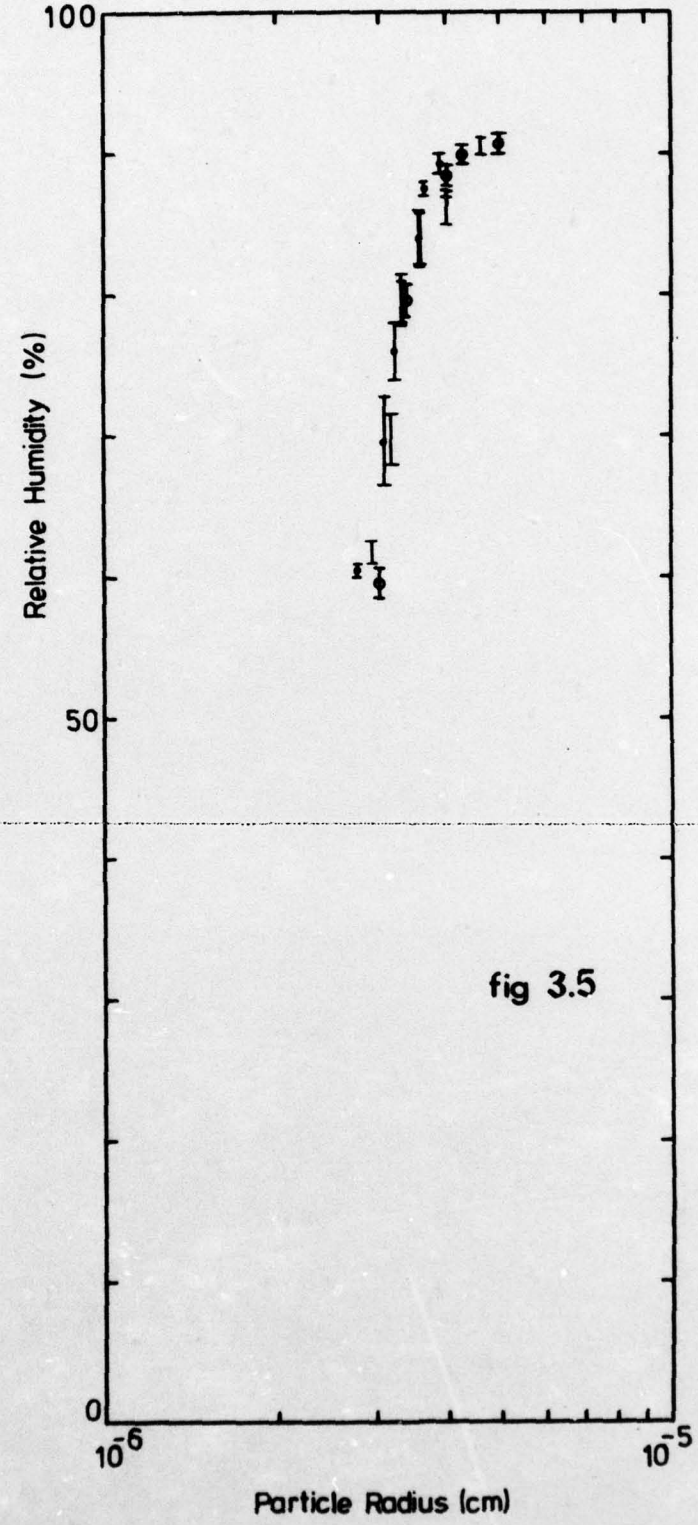

fig 3.5

AD-A036 088 DURHAM UNIV (ENGLAND) DEPT OF PHYSICS F/G 4/1
PHYSICAL CHARACTERISTICS OF THE NATURAL ATMOSPHERIC AEROSOL.(U)
OCT 76 S G JENNINGS DAJA37-75-C-1913
UNCLASSIFIED NL

2 OF 2
AD A036088

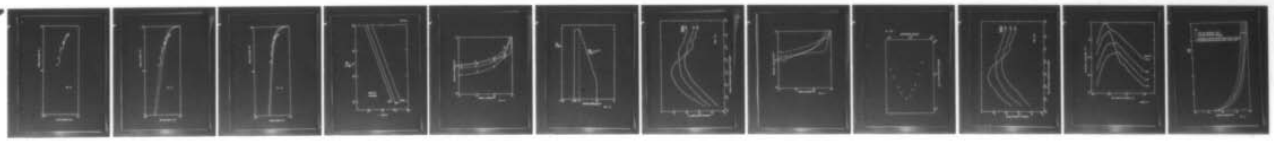

END

DATE FILMED
3-77

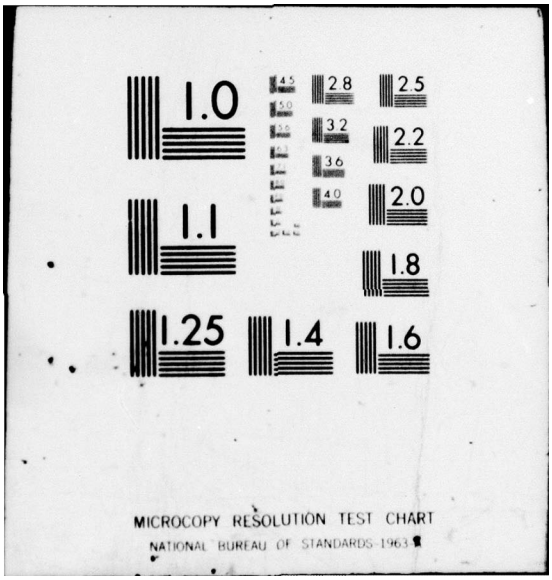
1.0
1.1
1.25
1.4
1.6
1.8
2.0
2.2
2.5
2.8
3.2
3.6
4.0
MICROCOPY RESOLUTION TEST CHART
NATIONAL BUREAU OF STANDARDS-1963-A

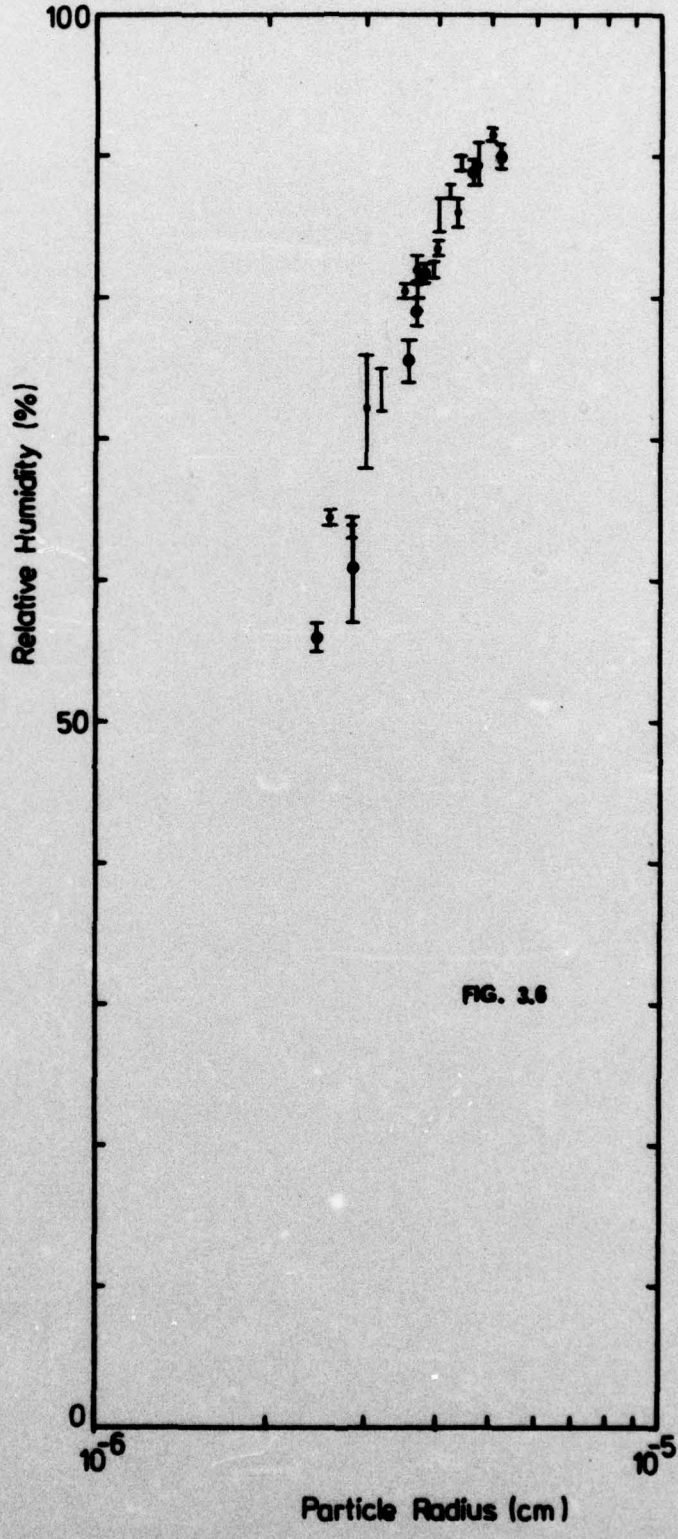

FIG. 3.6

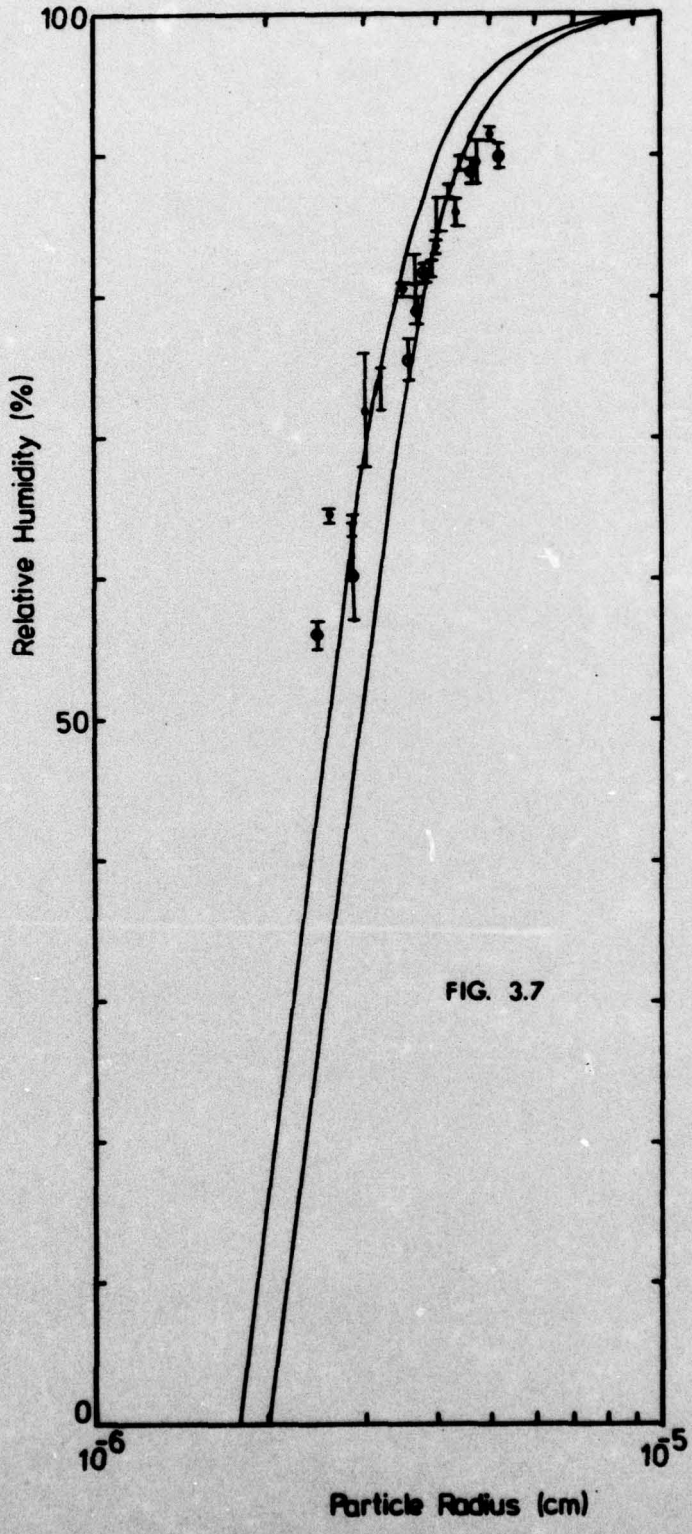

FIG. 3.7

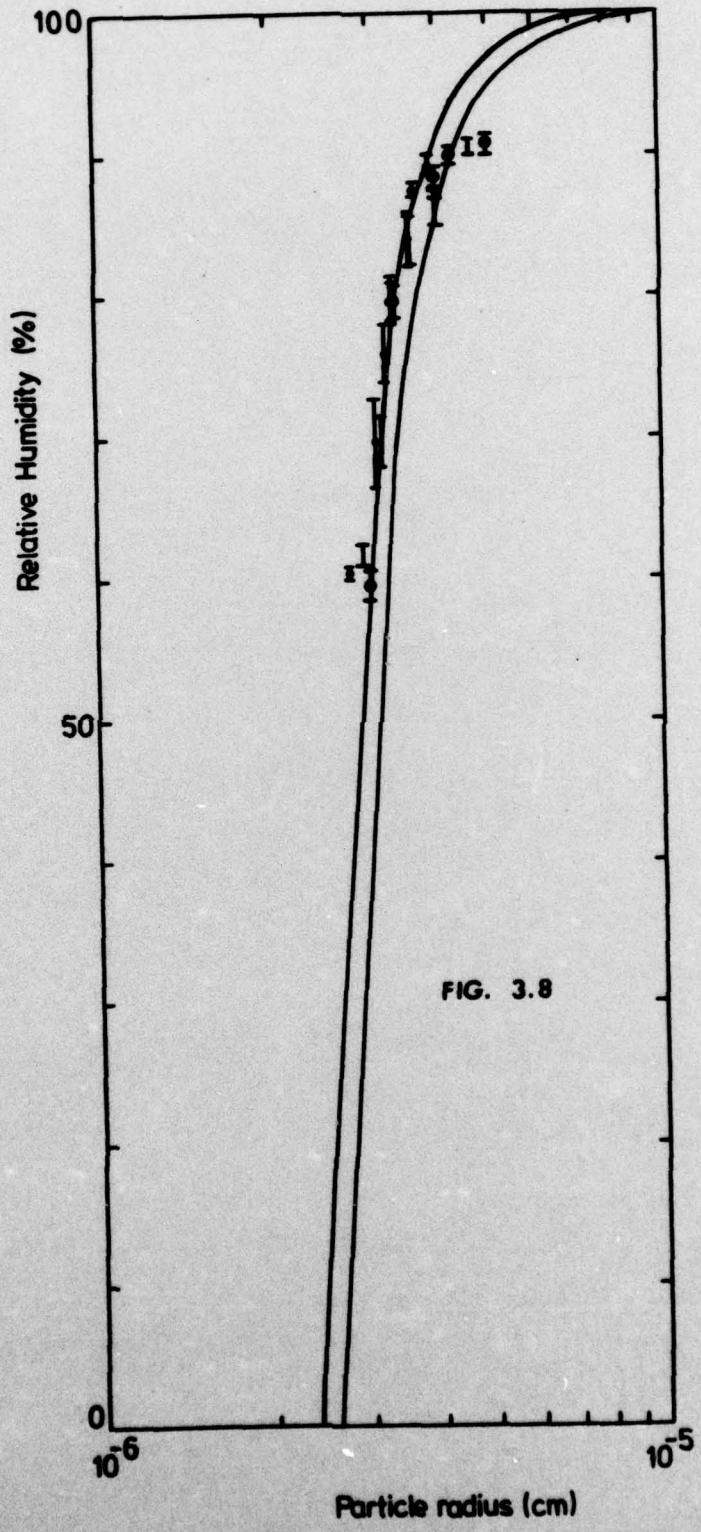

FIG. 3.8

FIG. 4.1

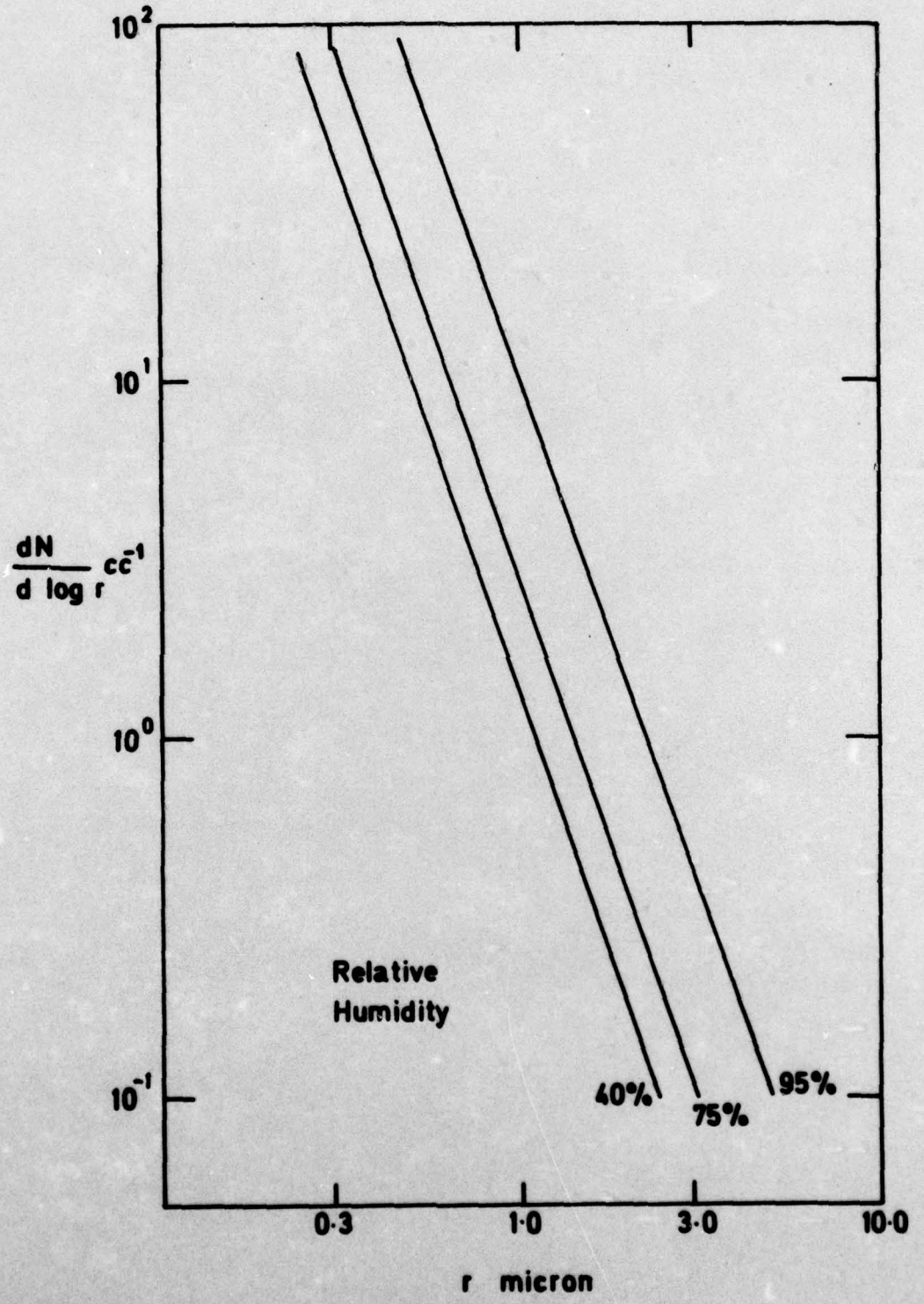
10^2
10^1
10^0
10^{-1}
$\frac{dN}{d \log r}$ cc^{-1}
Relative Humidity
40%
75%
95%
0·3
1·0
3·0
10·0
r micron

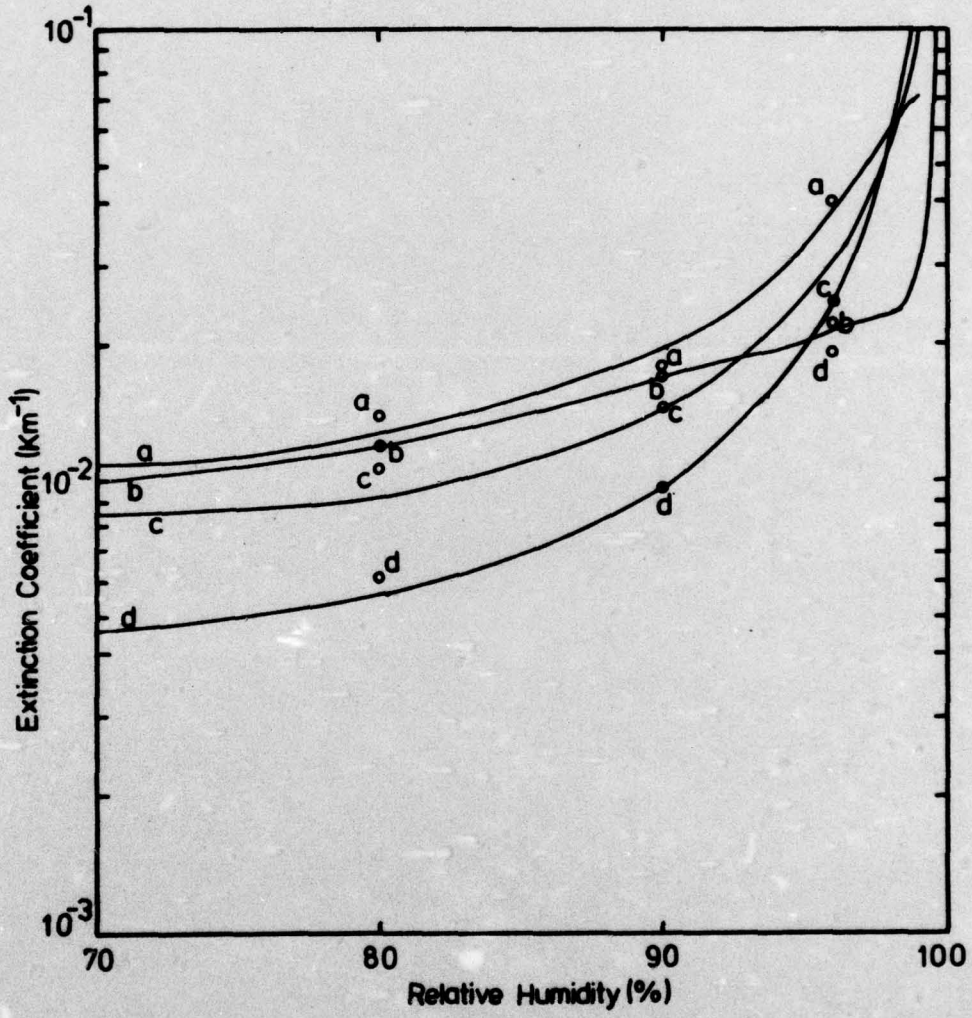
10^{-1}
10^{-2}
10^{-3}
Extinction Coefficient (Km^{-1})
70
80
90
100
Relative Humidity (%)
a
b
c
d

FIG. 4.2

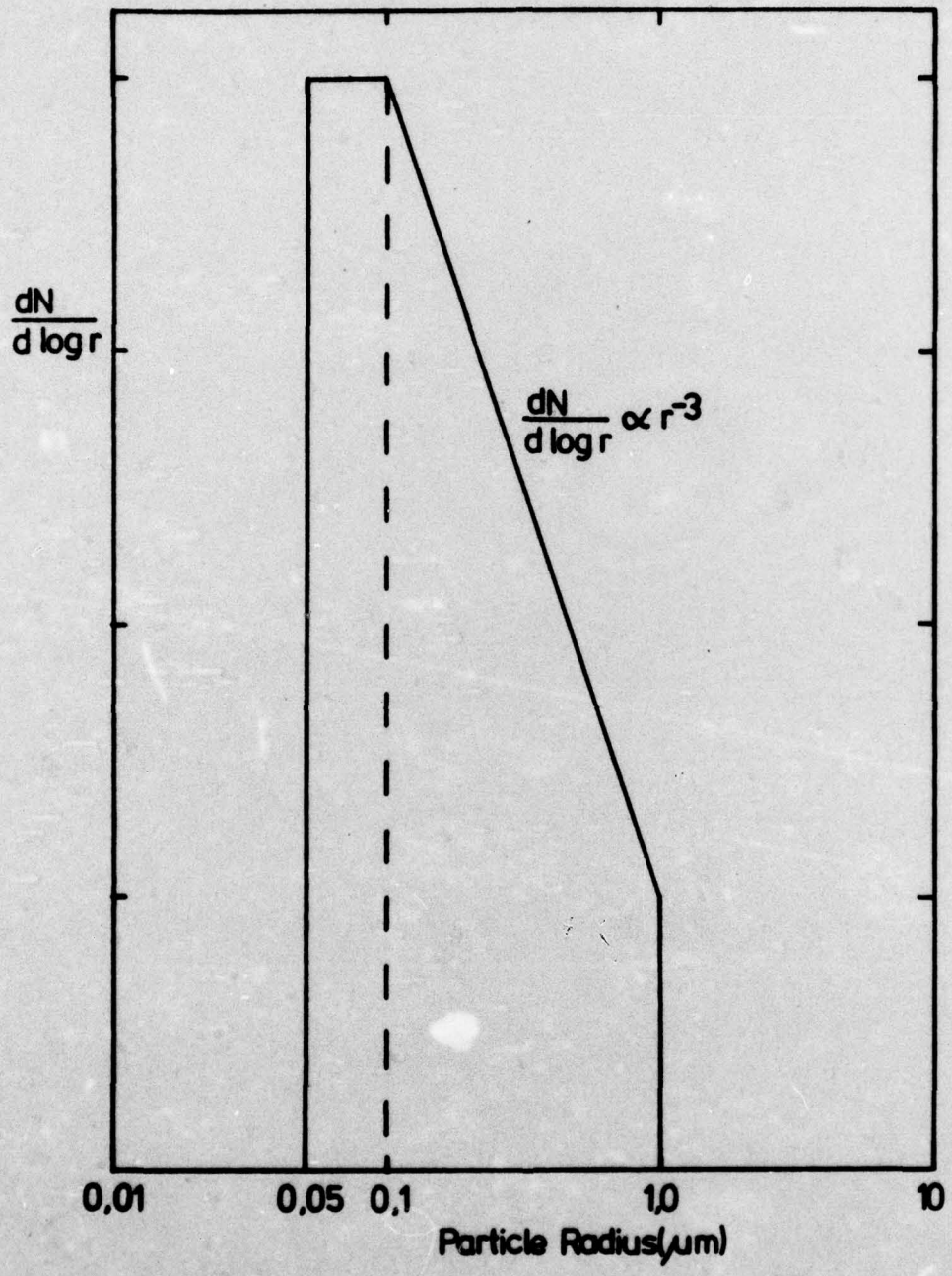

FIG. 4.3

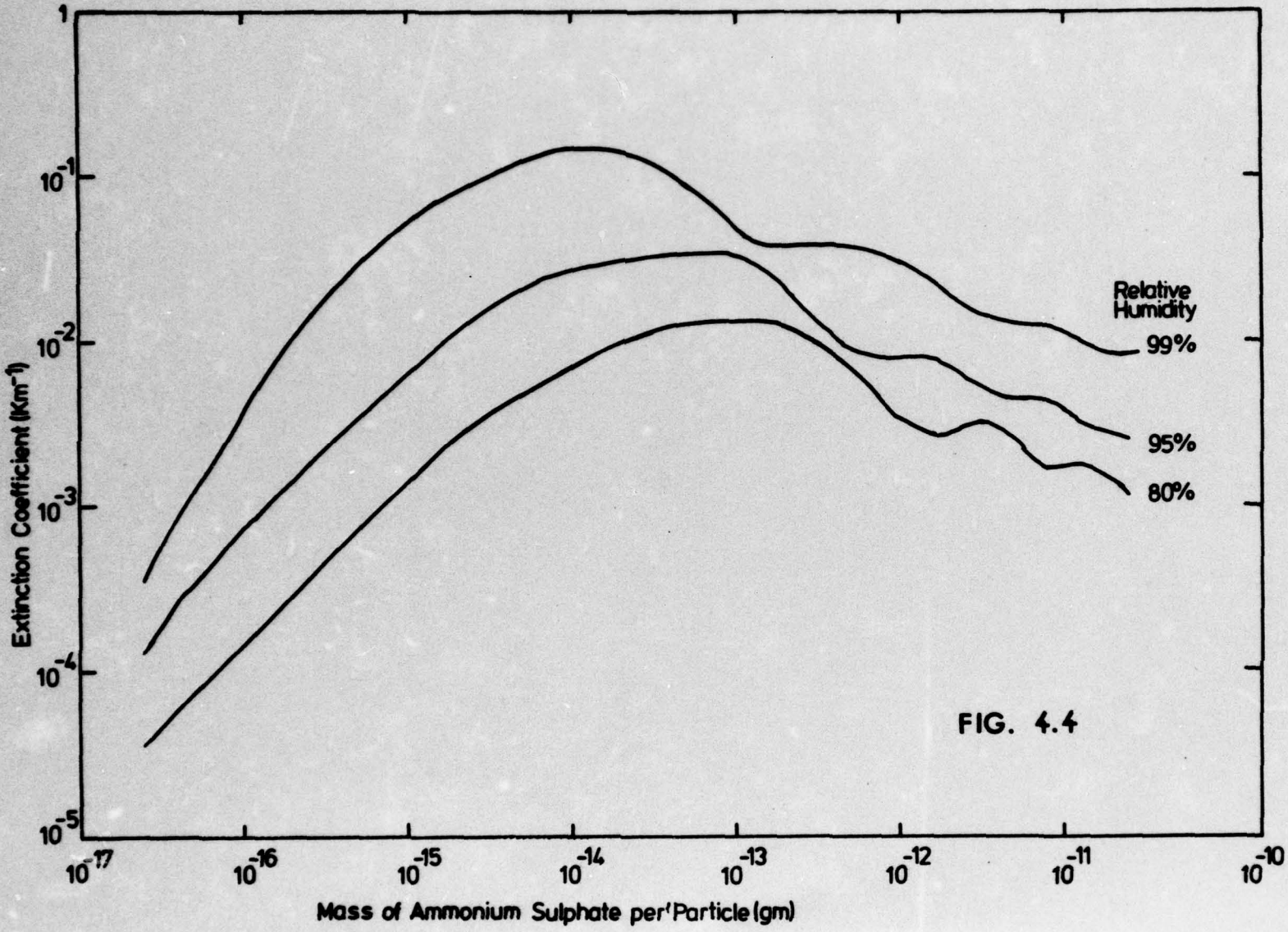
1
10^{-1}
10^{-2}
10^{-3}
10^{-4}
10^{-5}
Extinction Coefficient (Km^{-1})
Relative Humidity
99%
95%
80%
10^{-17}
10^{-16}
10^{-15}
10^{-14}
10^{-13}
10^{-12}
10^{-11}
10^{-10}
Mass of Ammonium Sulphate per Particle (gm)

FIG. 4.4

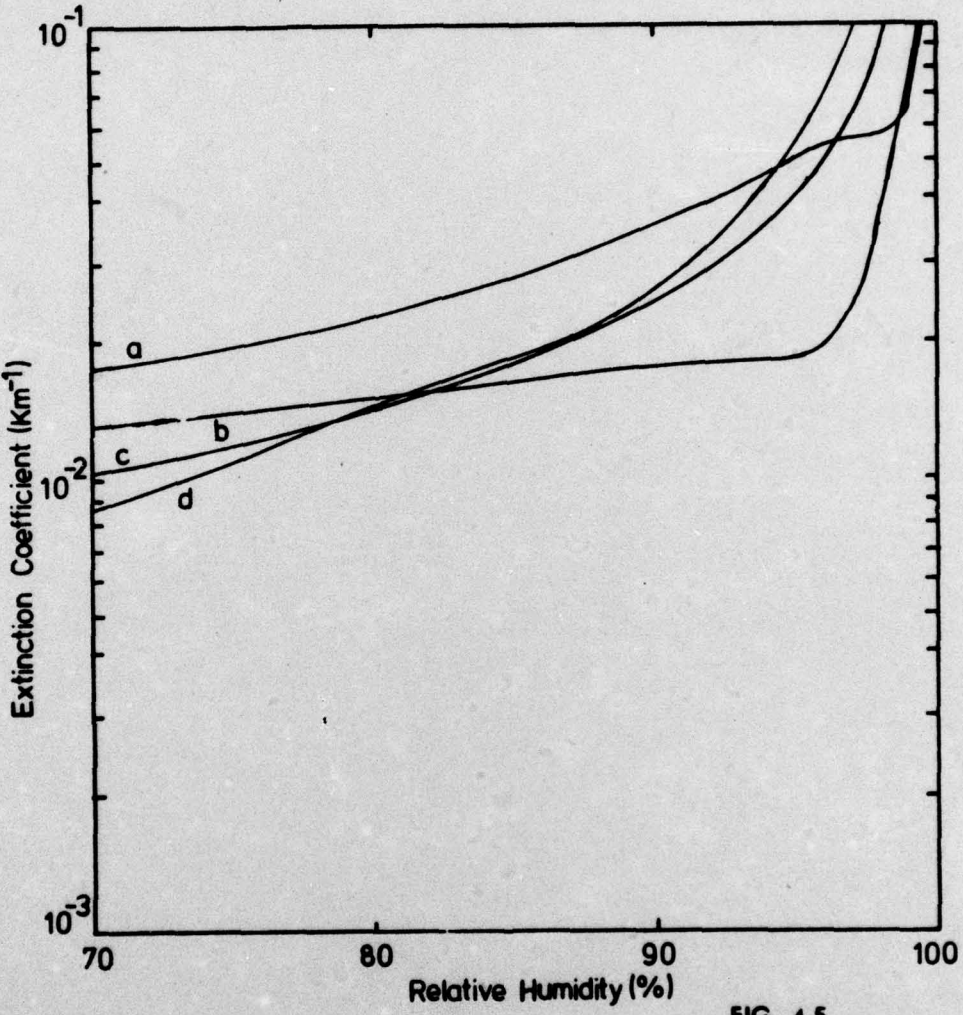
10^{-1}
10^{-2}
10^{-3}
Extinction Coefficient (Km^{-1})
a
b
c
d
70
80
90
100
Relative Humidity (%)

FIG. 4.5

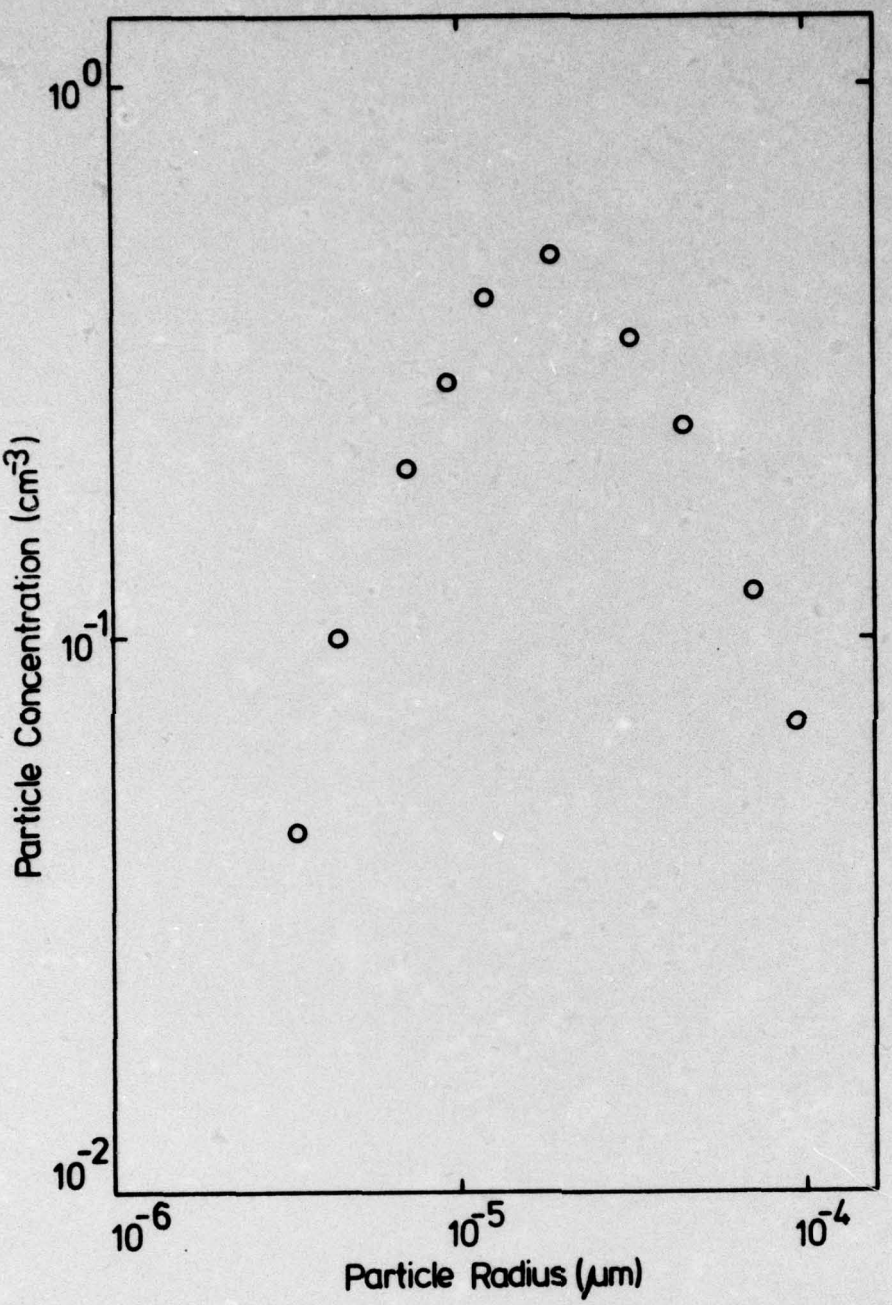
10^0
10^{-1}
10^{-2}
Particle Concentration (cm^3)
10^{-6}
10^{-5}
10^{-4}
Particle Radius (μm)

FIG. 4.6

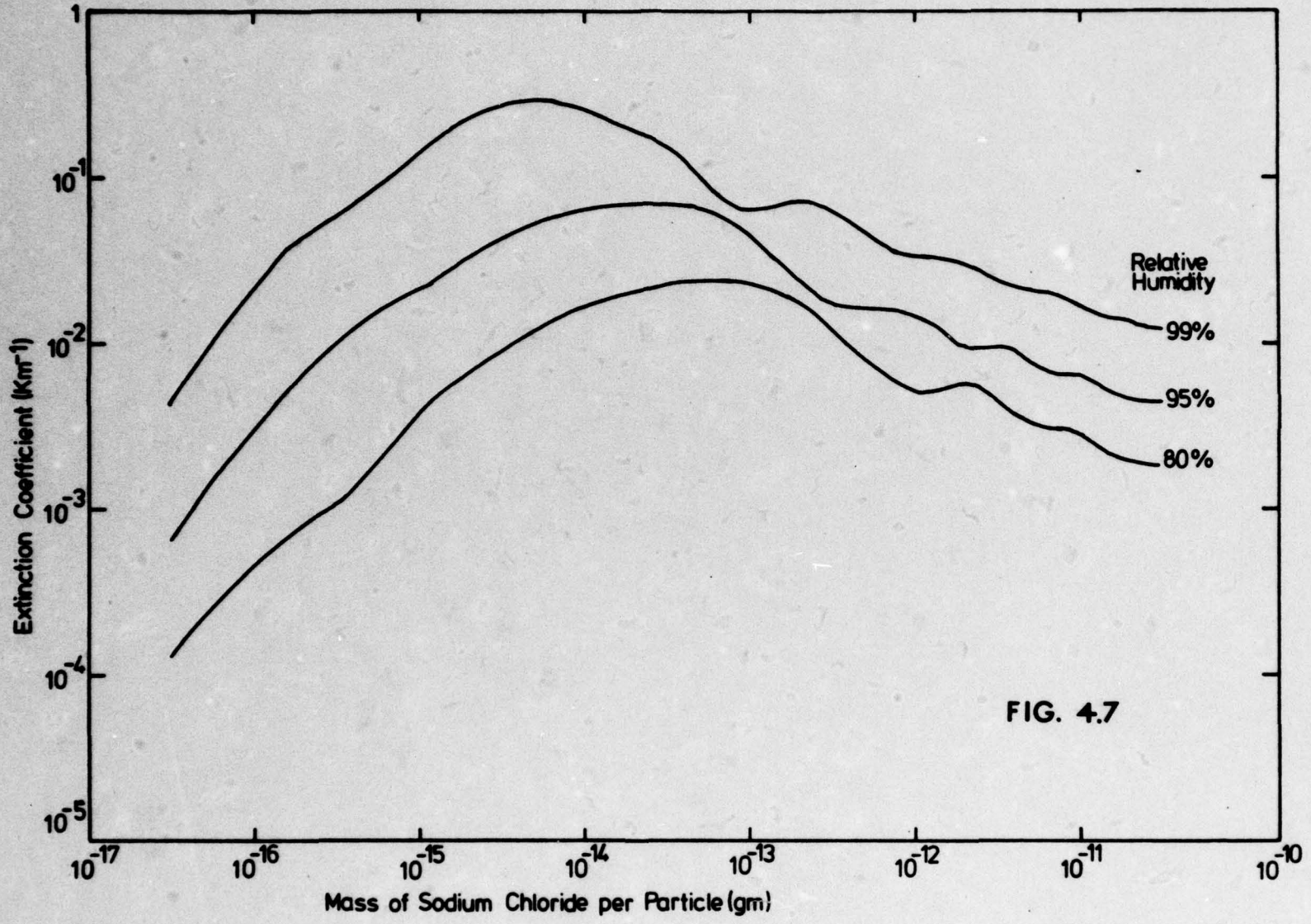
1
10^{-1}
10^{-2}
10^{-3}
10^{-4}
10^{-5}
Extinction Coefficient (Km^{-1})
Relative Humidity
99%
95%
80%
10^{-17}
10^{-16}
10^{-15}
10^{-14}
10^{-13}
10^{-12}
10^{-11}
10^{-10}
Mass of Sodium Chloride per Particle (gm)

FIG. 4.7

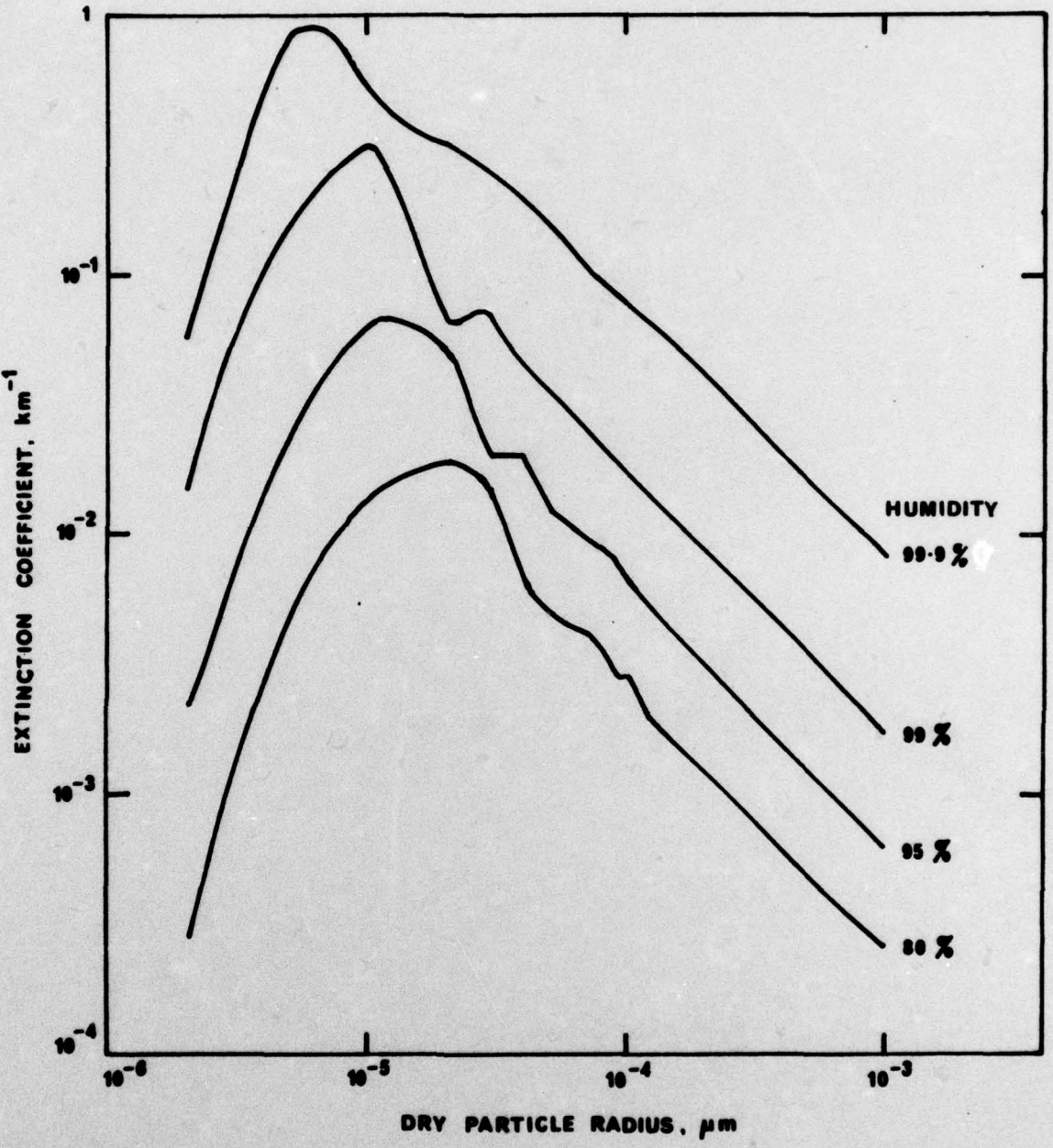
1
10^{-1}
10^{-2}
10^{-3}
10^{-4}
EXTINCTION COEFFICIENT, km^{-1}
HUMIDITY
99·9 %
99 %
95 %
80 %
10^{-6}
10^{-5}
10^{-4}
10^{-3}
DRY PARTICLE RADIUS, μm

FIGURE 4.8

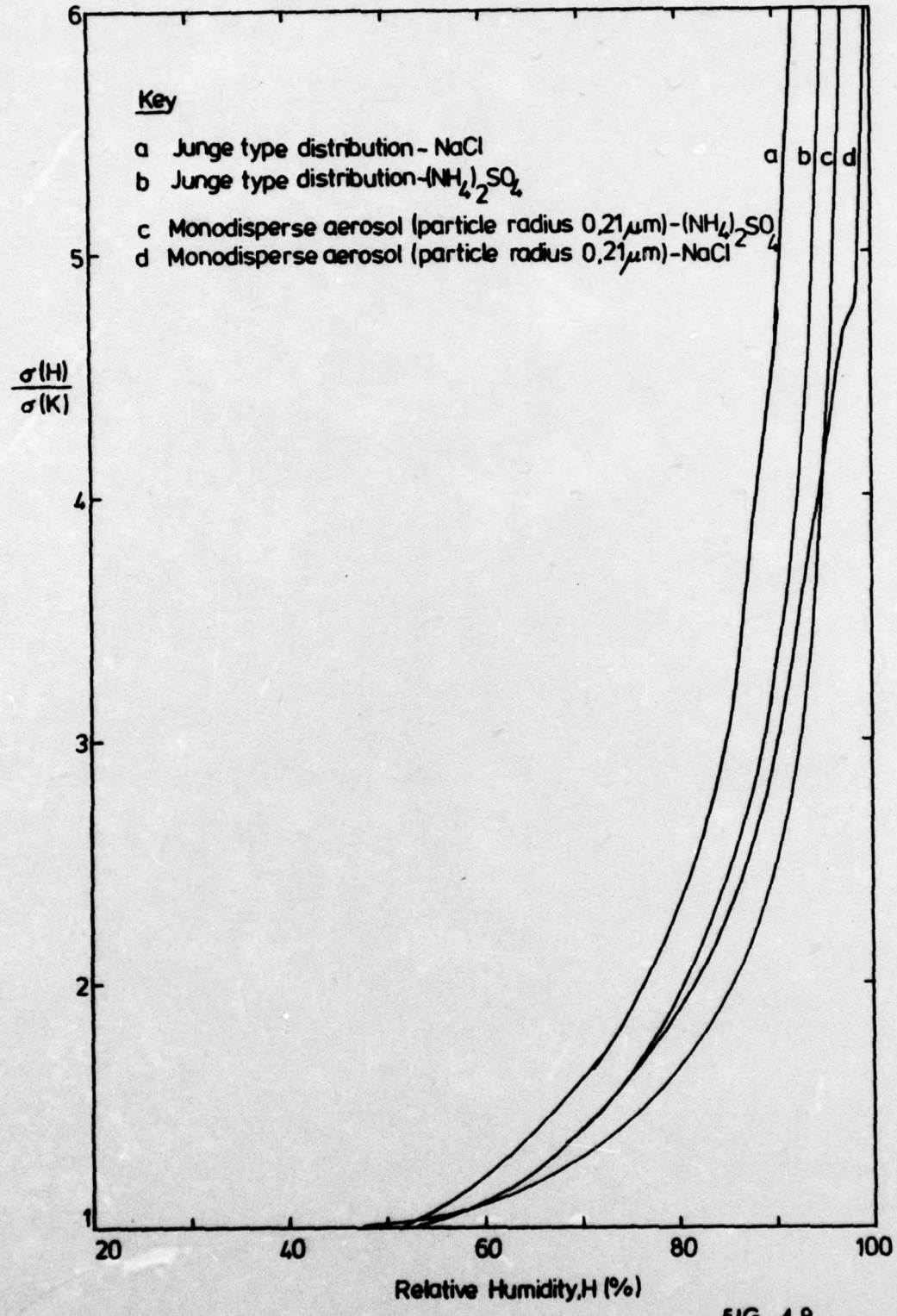
Key
a Junge type distribution - NaCl
b Junge type distribution - $(NH_4)_2SO_4$
c Monodisperse aerosol (particle radius 0,21 μm) - $(NH_4)_2SO_4$
d Monodisperse aerosol (particle radius 0,21 μm) - NaCl
a b c d
$\frac{\sigma(H)}{\sigma(K)}$
6
5
4
3
2
1
20
40
60
80
100
Relative Humidity, H (%)

FIG. 4.9

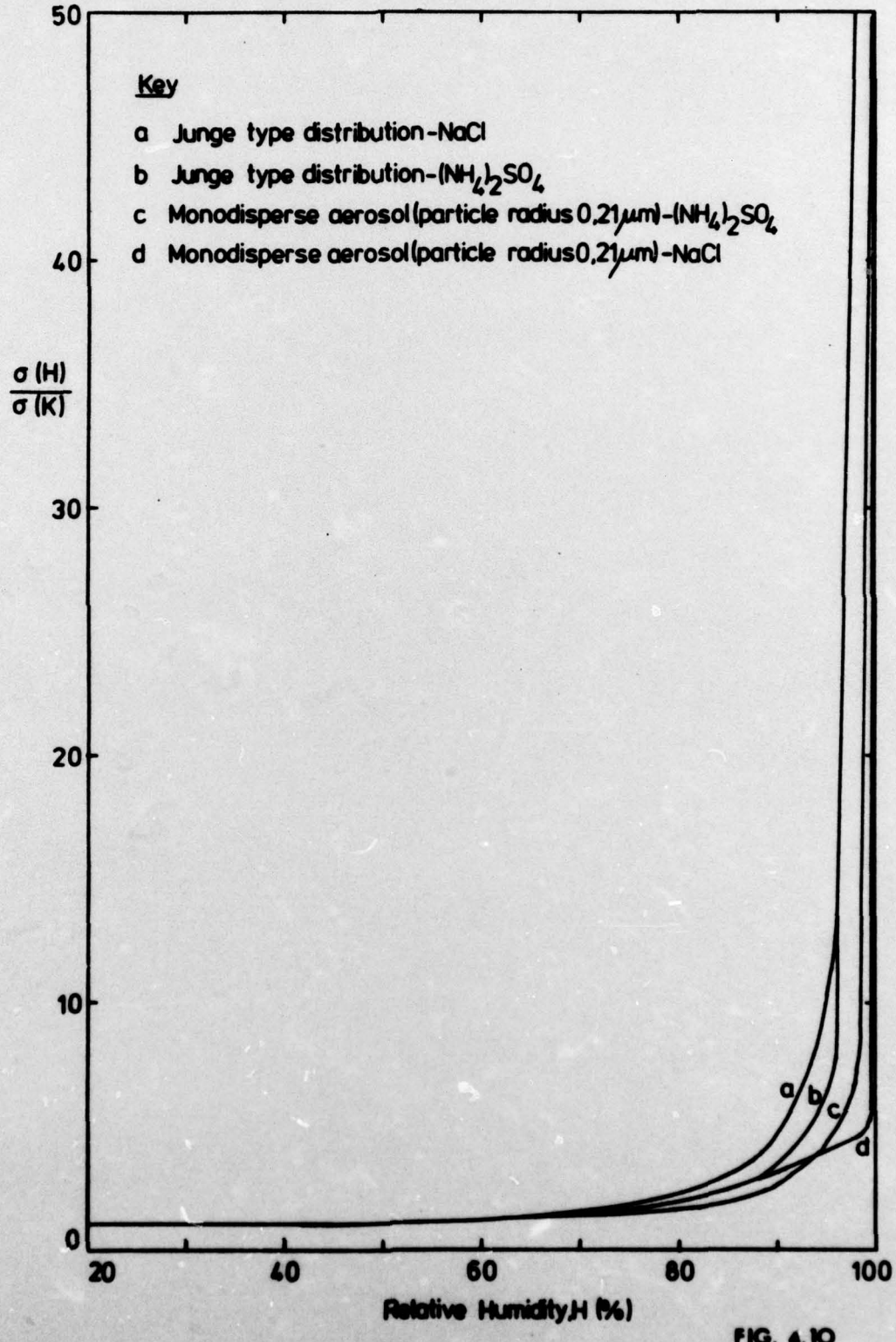
Key
a Junge type distribution-NaCl
b Junge type distribution-$(NH_4)_2SO_4$
c Monodisperse aerosol (particle radius 0.21 μm)-$(NH_4)_2SO_4$
d Monodisperse aerosol (particle radius 0.21 μm)-NaCl
$\frac{\sigma(H)}{\sigma(K)}$
50
40
30
20
10
0
20
40
60
80
100
Relative Humidity, H (%)
a
b
c
d

FIG. 4.10